Validating the genetic alterations in cutaneous T-cell lymphoma: unraveling the role of SOCS1 and HNRNPK through genetically engineered mouse models

Luo, Y.

Validating the Genetic Alterations in Cutaneous T-cell Lymphoma:

Unraveling the Role of SOCS1 and HNRNPK through Genetically Engineered Mouse Models

Yixin Luo

2024

The research described in this thesis was performed at the department of Dermatology, Leiden University Medical Center, the Netherlands.

ISBN: 978-90-7401-319-2
Uitgever: Tensen Scientific
Lay-out: Yixin Luo
Cover design: Yixin Luo
Thesis printing: PRINTSUPPORT4U

Validating the Genetic Alterations in Cutaneous T-cell Lymphoma:

Unraveling the Role of *SOCS1* and *HNRNPK* through Genetically Engineered Mouse Models

Proefschrift

ter verkrijging van
de graad van doctor aan de Universiteit Leiden,
op gezag van rector magnificus prof.dr.ir. H. Bijl,
volgens besluit van het college voor promoties
te verdedigen op dinsdag 12 november 2024
klokke 11:30 uur

door

Yixin Luo

geboren te Henan, China
in 1990

Promotors:

Prof. dr. M. H. Vermeer

Co-promotor:

Dr. C. P. Tensen

Dr. F. R. de Gruijl

Leden promotiecommissie:

Prof. dr. R. van Doorn

Prof. dr. T. van Hall

Prof. dr. M. W. Bekkenk (AMC)

Prof. dr. P. W. B. Derksen (UMC Utrecht)

Prof. dr. K. E. de Visser (NKI)

Contents

Chapter 1	General introduction	10
Chapter 2	*In vivo* modelling of Cutaneous T-cell lymphoma: The role of *SOCS1*	36
Chapter 3	*Socs1*-knockout in skin-resident CD4 T cells in a protracted contact-allergic reaction results in an autonomous skin inflammation with features of early-stage mycosis fungoides	62
Chapter 4	A novel knockout mouse model to assess the impact of one-copy loss of *Hnrnpk* in CD4+ T cells in chronically inflamed skin as a prelude to CTCL	84
Chapter 5	Role of *HNRNPK* Deletion in Initiating Cutaneous T-Cell Lymphoma Pathogenesis: An Inducible Knockout Mouse Model	106
Chapter 6	General discussion and future perspective	140
Appendix	Nederlandse Samenvatting List of publications Curriculum vitae Portfolio Acknowledgement	154

1

General introduction

General introduction

This chapter was adapted from “Next top mouse models advancing CTCL research”

“Next top” mouse models advancing CTCL research

Yixin Luo[1], Frank R. de Gruijl[1], Maarten H. Vermeer[1], Cornelis P. Tensen[1]

1.Department of Dermatology, Leiden University Medical Center, Leiden, the Netherlands

Front. Cell Dev. Biol., 10 April 2024. doi: 10.3389/fcell.2024.1372881

Introduction

Cutaneous T-cell lymphoma (CTCL), a rare form of non-Hodgkin lymphoma, accounts for approximately 3% of all lymphoma cases and presents unique challenges in oncological research. Characterized by malignant T-cell accumulation in the skin, often without initial spread beyond this organ, CTCL exemplifies the complexity and variability of rare malignancies (1). CTCL represents a heterogeneous group of disorders, including subtypes such as mycosis fungoides (MF), Sézary syndrome (SS) and CD30+ lymphoproliferative disorders (LPDs). While primarily a skin disease, CTCL can evolve into systemic lymphoma, spreading to lymph nodes and internal organs. As it constitutes approximately 75% of all primary cutaneous lymphomas, understanding CTCL's intricate pathobiology demands comprehensive and detailed research approaches (2). In this regard, *in vivo* mouse models are potentially powerful tools in unraveling the complexities of CTCL's pathogenesis. Such models can lead to the design of well-targeted early-stage treatments, which can then be preclinically tested in these experimentally accessible models.

In this introductory chapter, we thoroughly examine various *in vivo* mouse models currently at the forefront of CTCL research. This includes a focused discussion on the latest developments in transplantation models and genetically engineered mouse models (GEMMs). We will clarify the subtypes of CTCL if the references classify the model clearly. When the model's CTCL subtype is not clear, we will use the term 'CTCL model' broadly to encompass the diverse spectrum of this disease. Each model provides insights into different aspects of the disease, from tumor-host environment interactions and gene functions to drug efficacy validation. These contribute to our deepening understanding of CTCL and aid in the advancement of innovative therapeutic approaches. Here we will categorize and introduce mouse models of CTCL including the next top mouse models, serving as a reference for researchers unfamiliar with mouse experimentation when selecting models for CTCL research.

1. Transplantation Mouse Models in CTCL Research

Transplant models are essential in CTCL research and typically involve transplanting (human) donor cells or tissues into a recipient organism (mice). CTCL transplant models focused on late-stage human cutaneous lymphomas. These 'Xenograft models' involve transplants between different species, requiring immunodeficient mice to receive human CTCL cells or tissues. However, these models lack a fully competent immune system, which is a significant limitation, as it prevents a complete understanding of immune system interactions in CTCL. Additionally, they primarily focus on established tumors, offering limited insight into the early stages of CTCL pathogenesis. This underscores the need

for cautious interpretation of results from these models, especially regarding immune response and early disease development. 'Syngeneic transplant models' use genetically identical mice to avoid graft-host reactions and preserve normal interactions between tumor and immune system, but do not involve genuine human CTCL. These models, detailed in subsequent sections, offer valuable insights into CTCL pathogenesis and treatment response (3).

1.1. Immunodeficient Mouse Models with Transplantation

Immunodeficient mouse models are critical for CTCL research, allowing the study of tumor progression and response to treatments. These models are particularly valuable for precision medicine, enabling individualized testing of medication in the laboratory to circumvent disease heterogeneity. Patient-derived xenograft (PDX) and cell line-derived xenograft (CDX) models, wherein tumor cells from patients or established cell lines from MF, SS and other CTCL subtypes are transplanted into immunodeficient mice, play a key role. Among the cell lines utilized to study CTCL, SeAx, Sez4, SZ4, H9, and Hut78 correspond to SS origins, providing insight into this subtype. Similarly, Myla and HH cell lines reflect advanced MF, while Mac2A and PB2B are indicative of CD30+ LPDs, and MJ and Hut102 lines are associated with Adult T-cell Leukemia/Lymphoma (ATLL), demonstrating the broad spectrum of CTCL manifestations (4) . The recipient mice for the PDX and CDX model, due to targeted genetic modifications that eliminate certain crucial immune functions, do not reject the transplanted cells or samples (5). However, the absence of a fully functional tumor microenvironment and a comprehensive host immune response are notable limitations of these models.

Current CTCL research lacks comprehensive studies comparing engraftment efficiency and metastatic rates in various immunodeficient mouse strains (6-8). Predominantly, NSG, NOG, and NRG mice have been preferred in recent CTCL studies due to their superior engraftment capabilities, particularly effective in researching human acute leukemia and melanoma (9, 10). Under specific pathogen-free conditions, these strains exhibit longer lifespans, enhancing their value in xenotransplantation. The pioneering nude mouse model, despite its historical significance in cancer research, shows lower engraftment success (6).

Other strains like NSB, C.B-17 SCID Beige, and *Rag2 -/- γ -/-* mice, despite shorter lifespans, display impressive engraftment abilities. Each strain offers unique traits that are beneficial for specific research purposes. For instance, NOD SCID mice are crucial in studying the pruritic phenotype of CTCL (11, 12).

Selecting the right immunodeficient mouse strain is critical for CTCL research and depends on study goals, graft nature, and experimental conditions. Thoughtful selection is key to translating preclinical results into clinical applications and advancing CTCL understanding and treatment. Below we outline and compare various immunodeficient mice used in CTCL research (refer to **Tables 1 & 2**).

Table 1. The main features of immunodeficient mouse models for transplantation in CTCL research.

Mouse Strain	Mutated gene	Cell population change	Main Features
NSG (6)	*Prkdc*^{scid} *Il2rg*^{tm1Wjl}	No T cells No B cells No NK cells	Long lifespan: a median survival time of 89 weeks. High engraftment ability.
NOG (7)	*Prkdc*^{scid} *Il2rg*^{tm1Sug}	No T cells No B cells No NK cells	Similar to NSG Long lifespan. High engraftment ability.
NRG (13)	*Rag1*^{tm1Mom} *Il2rg*^{tm1Wjl}	No T cells No B cells No NK cells	Similar to NSG Long lifespan. High engraftment ability.
NSB (9)	*Prkdc*^{scid} *B2m*$^{tm1Unc/J}$	No functional T cells No functional B cells Diminished NK cells No MHC class I No complement factor C5	Short lifespan: the average lifespan 30 weeks. High engraftment ability

Nude nu/nu (14)	*Foxn1*^{nu}	No T cells	Moderate lifespan: 6 months to one year. Low engraftment ability.
NOD SCID (11)	*Prkdc*^{scid} (NOD background)	No functional T cells No functional B cells	Short lifespan: the median survival time: 37 weeks Moderate engraftment ability. Slightly lower than NSG, NOG and NRG
CB 17 SCID (15)	*Prkdc*^{scid} (C.B-17 background)	No T cells No B cells	Moderate lifespan: around one year. Moderate engraftment ability.
CB17 SCID beige (16)	*SCID* beige	No T cells No B cells Defective NK cells	Moderate lifespan High engraftment ability.
Rag2 -/- γc-/- (17)	*Rag2*$^{tm1.1Flv}$ *Il2rg*$^{tm1.1Flv}$	No T cells No B cells No NK cells	Short lifespan: the average lifespan 34 weeks. High engraftment ability.

Table 2. Transplantation methods for immunodeficient mouse models in CTCL research

Mouse Strain	Subcutaneous injection	Intrahepatreal injection	Intrafemoral injection	Intravenous injection	Skin/tumor grafting
NSG (6)	- SS Blood-derived PBMCs: 1× 10^6 (18) - MF lymph node-derived leukocytes: (5-10) × 10^6 cells (19) - PDX mouse tumor-derived: 4 × 10^6 cells (20) - CTCL cell lines: Myla (MF cell line): 0.8 ×10^6 cells, transferred with miR-125b-5p (21) Hut78 (SS cell line) or HH (MF cell line): 1× 10^6 cells, with TOX knockdown with shRNA (22) Hut78 (SS cell line) or Myla (MF cell line): 2.5 × 10^6 cells (23) Hut78 (SS cell line) or HH (MF cell line) : 1× 10^6 cells (24) HH (MF cell line): 2 ×10^6 cells (25) Myla (MF cell line), PB2B (CD30+ LPDs cell line), HH (MF cell line), H9 (SS cell line), Hut78 (SS cell line), SZ4 (SS cell line), MJ (ATLL cell line), or Hut102 (ATLL cell line): 2.5 × 10^6 cells (26) Hut78 (SS cell line), H9 (SS cell line), MJ (ATLL cell line), or HH (MF cell line): 10 × 10^6 cells (19)	-CTCL cell lines: Myla (MF cell line), Hut78 (SS cell line), HH (MF cell line): 5 ×10^6 cells (32)	-SS Blood-derived PBMCs: 1× 10^6 cells (18)	-SS Blood-derived PBMCs: (5 ~ 20) × 10^6 cells (33) -CTCL cell lines: Hut102 (ATLL cell line): 10 ×10^6 cells (34) (35) HH cells were transduced with lentivirus to express click beetle luciferase green and green fluorescent protein and were further transduced to express runcated CD19 (HH-CBG-GFP-t19) (36) HH (MF cell line) (HH-CBR-GFP): 0.4× 10^6 cells (37)	-

	Hut78 (SS cell line) or HH (MF cell line): 5 × 10^6 cells (27) (28) SeAx (SS cell line): 0.4 × 10^6 cells (ear) (29) SeAx (SS cell line): 3 × 10^6 cells (flank) (30) MJ (ATLL cell line): 3.8 * 10^6 cells /sites, transduced with INSL3-shRNA-TRC58, -TRC61: 3.8× 10^6 cells /sites (31)				
NOG (7)	- CTCL cell lines: HH (MF cell line): 10 × 10^6 cells (38) Myla (MF cell line): 0.2 × 10^6 cells ; HH (MF cell line): 2 × 10^6 cells; Hut78 (SS cell line): 4 × 10^6 cells (39) Myla (MF cell line): 1× 10^6 cells (40) Myla (MF cell line) or HH (MF cell line): 0.2 × 10^6 cells, transfected with GFP-miR-150 (41, 42)	-	-	-	-
NRG (13)	- CTCL cell lines: Luciferized Hut78 (SS cell line): 2× 10^6 cells (8)	-	-	-CTCL cell lines: CD38 knockout luciferized H9 (43)	-
NSB (9)	- CTCL cell lines: Myla2059 (MF cell line): 1× 10^6 cells (44) (45) Myla2000 (MF cell line): 1× 10^6 cells (46)	-	-	-	-
Nude nu/nu (14)	- CTCL cell lines: Myla (MF cell line): 10× 10^6 cells (47) HH (MF cell line): 20 × 10^6 cells (48) HH (MF cell line): 10× 10^6 cells (49) (50) HH (MF cell line): 2 × 10^6 cells (51)	-	-	-	- Myla-derived mouse tumor fragments: 5×3 mm subcutaneous (47)

NOD SCID (11)	- CTCL cell lines: Myla (MF cell line): 10× 10^6 cells (52) (53) Hut102(ATLL cell line): 2 ×10^6 cells (54) HH (MF cell line): 20 × 10^6 cells, transduced with the PAK1-sh2-vector (55) HH (MF cell line): 5 × 10^6 cells, transduced with BIN1 - siRN (56) SeAx (SS cell line): 0.2 × 10^6 cells (57)	-	-	- CTCL cell lines: Hut102(ATLL cell line): 10× 10^6 cells, with sublethally irradiated (1.8 Gy) (54)	
CB 17 SCID (15)	- CTCL cell lines: HH (MF cell line): 5× 10^6 cells (58)				- Skin grafting from SS: 4 × 7 × 0.75mm into 4 pieces (15)
CB17 SCID beige (16)	- CTCL cell lines: Hut78(SS cell line) or Myla 2059 (MF cell line): 3 × 10^6 cells (59) HH (MF cell line): 1 × 10^6 cells (60)	-	-	-	-
Rag2 -/- γc-/- (17)	-	- CTCL cell lines: Hut78 (SS cell line) or SeAx (SS cell line): (0.5 - 6) ×10^6 cells (61)	-	- SS Blood-derived PBMCs: (0.5 -1) × 10^6 cells (with irradiation) (62)	

CTCL: cutaneous T cell lymphoma; PBMC: peripheral blood mono-nuclear cell; SS: Sézary syndrome; MF: mycosis fungoides

1.1.1. NSG mouse in CTCL

NSG mouse strain, formally named NOD.Cg-*Prkdc*^{scid} *Il2rg*^{tm1Wjl}, is indispensable for CTCL studies because of its broad immunodeficiency (6). Their unique genetic background amalgamates traits from NOD, SCID(*Prkdc*^{scid}), and gamma mutation (*Il2rg*^{tm1Wjl}), resulting in the absence of functional T cells, B cells, and NK cells. The profound immunodeficiency of NSG mice positions them as an exemplary recipient for development of intrahepatic xenograft models of CTCL, facilitating the evaluation of tumorigenicity and therapeutic responses. The maintenance of NSG mice requires stringent pathogen-free conditions due to their lack of immune defenses, which has implications for the management and costs of these studies. Despite this, the NSG model's inability to mount an adaptive immune response offers an excellent recipient.

With the aid of this model, researchers have progressively unveiled tumor-driving pathways and corresponding treatment of CTCL, e.g. the cMyc/miR-125b-5p signaling axis (21), *TOX* genes (22), Mucin 1 (23), and the potential therapeutic effects of gallium maltolate in inhibiting tumor growth (24). Furthermore, the NSG mouse model has demonstrated its utility in the rapid assessment of CTCL (32), and in subsequently testing novel therapeutic modalities, in particular employing demethylating agents in conjunction with mucin 1 inhibitors (25). These studies not only underscore the importance of CTCL heterogeneity but also highlight the therapeutic potential of coordinated treatments involving PI3Kalpha/delta and HDAC (18, 19, 26), kinase inhibitors with TAK1 (27, 29), the synergistic combination of Bcl-2 and NFκB inhibitors (30) and the effectiveness of a bispecific IL2-CCR4 immunotoxin (34). Recent advancements include the superior performance of CCR4-IL2 immunotoxin (35), RT39 peptide therapy (33), novel drug NT1721 (28), JAK3-INSL3 fusion transcripts (31), anti-CCR4 CAR T cells (36), universal CD2 CAR-T therapy (37) and the antibody-drug conjugate SGN-CD70A (20) have further expanded the therapeutic research landscape for CTCL.

1.1.2. NOG mouse in CTCL

The NOG mouse model, formally designated as NOD.Cg-*Prkdc*^{scid} *Il2rg*^{tm1Sug}, stands out in CTCL research for its pronounced immunodeficiency, miming severe combined immunodeficiency (SCID) in humans (63). IN close similarity to NSG, this strain is void of functional B and T lymphocytes due to the *Prkdc*^{scid} mutation and lacks natural killer (NK) cells due to the *IL-2Rγ*^{null} mutation, making them an ideal platform for human cell engraftment (38). In researching the effects of microRNAs on CTCL, the NOG model has revealed the tumor-suppressive role of microRNA-16, while IL-22 may facilitate tumor

metastasis (39, 40). Furthermore, miR-150 has demonstrated potential in inhibiting tumor metastasis (41) and histone deacetylase inhibitors targeting miR-150 and CCR6, such as Vorinostat, have presented new strategies for the treatment of advanced CTCL (42).

1.1.3. NRG mouse in CTCL

The official name for the NRG mouse model is NOD.Cg-*Rag1*^{tm1Mom} *Il2rg*^{tm1Wjl}. Due to the knockout of the *Rag1* and *Il2rg* genes, this mouse model lacks mature T, B, and NK cells (13).

The studies using NRG mice for CTCL research found that the combined use of chlorpromazine and romidepsin displayed significant antitumor activity (8), and the expression of CD38 is associated with the progression of CTCL, suggesting that CD38 may play a significant role in the immunopathogenesis of CTCL and could potentially become a new target for therapeutic intervention (43).

1.1.4. NSB mouse in CTCL

The NSB mouse model with the official name NOD.Cg-*Prkdc*^{scid}*B2m*$^{tmUnc/J}$, distinct in their immunodeficiency due to a *B2m*^{tm1Unc} mutation affecting MHC class I expression, lack CD8+ T cells and exhibit impaired NK cell function (64). This characteristic enables the strain to support the engraftment of malignant T cells such as Myla2059, providing a robust model for the study of late-stage CTCL, especially MF, dissemination and treatment (44). Additionally, the secretion of molecules such as galectin-1 and -3 by malignant T cells has been associated with the disruption of skin architecture and the proliferation of keratinocytes in CTCL (45, 46).

Distinct from the NOG and NSG strains, which suffer from impaired NK cell function due to mutations in the *IL2R* gamma chain, the deficit in this strain arises from the impact of the *B2m* mutation on MHC class I expression, marking its unique role in the study of CTCL models

1.1.5. Nude (nu/nu) mouse in CTCL

The “nude” (nu/nu) mouse model, which lacks a mature thymus due to a *Foxn1* gene mutation, resulting in underdeveloped T cells (14), has become a critical model for evaluating CTCL therapies, especially in terms of treatment responses for MF patient-derived skin lesions. These mice with transplants of MF have shown enhanced effects of combination therapies, like PUVA and mogamulizumab, a monoclonal antibody targeting CCR4, compared to monotherapies (47, 48). Further studies using “nude” mice have been conducted to test the effectiveness of Vorinostat and the HIF-1α inhibitor Echinomycin,

unveiling their potential in combating CTCL (49, 65). The dual PI3K/mTOR inhibitor PF-502 has also been shown to prolong survival in “nude” mice, suggesting its potential as a promising therapeutic for CTCL (50). And metabolic analysis of CTCL model mice has led to the discovery of fluctuations in L-glutamate and adenosine monophosphate levels, which could contribute to understanding CTCL the dynamics of biomarkers (51).

1.1.6. NOD SCID mouse in CTCL

The NOD SCID mouse model, formally designated as the NOD. CB17-*Prkdc*^{scid} strain, is valuable in CTCL research as recipient mice due to its lack of mature T and B cells, making it suitable not only for studying pruritus—a hallmark symptom of CTCL (12) —but also for investigating tumor growth, early symptoms, and the role of gender in disease mechanisms (52, 53). Employing the NOD SCID mice for the CTCL model, LW-213 has shown notable therapeutic potential, inhibiting the growth of CTCL-associated xenograft tumors and improving survival rates (54). Additionally, this model has been used to validate the role of PAK1 in CTCL cell proliferation and the therapeutic potential of its inhibitors (55), as well as to study the role of BIN1 in disease progression through its regulation of c-FLIP affected Fas/FasL-mediated apoptosis (56). Moreover, the combined application of retinoic acid and histone deacetylase inhibitors has demonstrated antitumor effects (57).

1.1.7. CB17 SCID mouse in CTCL

The CB17 SCID mouse model, originating from the C.B-17 strain, bears a *Prkdc*^{SCID} gene mutation that results in a profound deficiency in adaptive immunity by impairing T and B lymphocytes (66). This strain, as recipient mouse of CTCL from SS patient-derived skin, provides valuable insights into the pathology and can aid in developing new therapeutic strategies (15). Recent research has demonstrated that the combined use of Brentuximab Vedotin (BV) with doxorubicin exhibits significant tumor suppression in the HH cell tumor model in CB17SCID mice, further confirming the potential of this drug combination in the treatment of T-cell lymphomas (58).

1.1.8. CB17 SCID Beige mouse in CTCL

The CB-17 SCID beige mouse model, due to the combined *SCID* and *beige* mutations, possesses an extensive range of immunodeficiencies, including the absence of T cells, B cells, and compromised NK cell function, providing a more comprehensive immunodeficient model than the CB17 SCID defect only (16). As a recipient, these mice excel in tumor studies due to their increased tumor growth rates compared to less immunodeficient nude mice, ideal for aggressive tumor research contrasting slower-progressing SS tumors (59). In CTCL research, these mice, together with the EL4 mouse T-cell

lymphoma model, have aided in discovering that the expression of galectin-9 on tumor cells is inversely proportional to CD8+ T cell infiltration in the skins of EL4 mouse model and serum levels of galectin-9 correlate with disease severity. However, the anti-tumor effect of exogenous high-dose galectin-9 administration demonstrated anti-tumor effects in CTCL, underscore its significance as a potential therapeutic target (60).

1.1.9. Rag2 -/- mouse in CTCL

The Rag2-/- mouse model carries a mutation that disables the *Rag2* gene, essential for T and B lymphocyte development through V(D)J recombination. This mutation results in a complete absence of mature T and B cells, creating a foundational model for immunodeficiency studies (67). While not a primary model for CTCL itself, Rag2-/- mice serve as recipients in specific studies, such as those involving subcutaneous injections of modified CD4+ T cells from Myc+ Cdkn2a -/- mice, to explore the mechanisms of cutaneous hypersensitivity and the immunological roles of IL-7 and IL-15 (68). An enhanced version of this model, the Rag 2-/- γc-/- mice, lack functional T, B, and NK cells due to the knockout of both the Rag2 and the interleukin-2 receptor gamma chain gene (Il2rg or γc), which affects cytokine receptor production. This strain is suitable for xenotransplantation studies on SS, in particular it sustains long-term systemic repopulation with injected SS cell lines or primary cells without immune rejection (61).

The SRG15 mouse, an advanced version of the Rag 2-/- model, combines *Rag2-/- , γc-/-* mutations and humanized IL15 and human signal regulatory protein alpha (SIRPA) mutations (69). These 'humanized' mice are engineered to express human IL-15, accommodating the growth of SS tissue samples more effectively than traditional immunodeficient models. Integrating of human *IL-15* and *SIRPα* genes in the SRG15 mice enables them to support human NK and T cells, making them excellent tools for studying human immune cell behaviors (62).

1.2. Non-immunodeficient Mouse Models with Syngeneic Transplantation

Syngeneic transplantation models, wherein syngeneic lymphomas are introduced into the skin of mice, serve as valuable tools for investigating tumor behavior and host-tumor interactions. These models allow for studying tumor dynamics within a genetically consistent background, offering insights into the tumor's interaction with a native immune system. However, it is crucial to acknowledge that these models have limitations in representing the human immune system and the diverse variants of the disease. Specifically, they lack the complexity and heterogeneity inherent in human CTCLs. Such differences are crucial for researchers to consider, ensuring that the distinct differences

between model and human disease are accounted for in research conclusions and clinical applications.

1.2.1. MBL2 mouse model in CTCL

The Mannose-Binding Lectin 2 (MBL2) mouse model, utilizing C57BL/6 mice as a syngeneic platform, creates an auto transplantation model for CTCL by injecting MBL2 lymphoma cells and inducing inflammation with DNFB. Although not based on genuine CTCLs, this model effectively simulates the impact of inflammation observed in CTCL and highlights the potential of anti-inflammatory treatments such as the PARP-1 inhibitor talazoparib and IL-10 suppression in controlling tumor growth (70-72). Further research has confirmed the efficacy of CD47 blockade agents and CCR2 inhibitors in slowing tumor growth and modulating the tumor microenvironment (73, 74). The discovery that rapamycin inhibits tumor growth by highlighting its impact on the metabolism of lymphoma cells, particularly reducing the reliance on aerobic glycolysis, offers a new avenue for metabolic intervention in treating CTCL (75).

1.2.2. EL4 mouse T-cell lymphoma model

The EL4 mouse model uses a T-cell lymphoma cell line derived from C57BL/6 mice and serves as a syngeneic transplant model for CTCL by virtue of inoculation in the skin with an impact on matching immune system. Studies utilizing this model in CTCL-related research have shown that bexarotene demonstrates immunomodulatory potential by reducing levels of CCL22 (76). Moreover, combining mogamulizumab with PUVA therapy shows enhanced therapeutic effects (77). This model has also demonstrated a possible role for CXCL11 in anti-CTCL treatment (78), revealed the role of TSLP in promoting a Th2-dominant tumor environment (79), and identified galectin-9 as a potential new therapeutic target for CTCL (80). Additionally, the EL4 model has elucidated the role of IL9 and its regulatory factors in MF (80), as well as the importance of PlGF in promoting lymphoma cell growth and disease progression in CTCL (81).

1.2.3. Murine bone marrow transplantation model

The bone marrow transplantation model for CTCL, examining the *JAK3*^{A572V} mutation, provides insights into lymphocyte development and the mutation's role in T-cell proliferation and survival. This model reflects the pathological traits of aggressive lymphoproliferative disorders, including CTCL, with manifestations such as skin involvement in human CTCL. Findings indicate the *JAK3*^{A572V} mutation's capacity to induce a transplantable, diverse CTCL-like disease, exacerbated by trisomy 21, which may result in fatal leukemia from CTCL phenotypes (82, 83). Bone marrow transplantation models

are relatively complex to operate and require high-standard experimental equipment and environments, which limits the application of the model.

2. Non-Skin Target Genetically Engineered Mouse Models (GEMMs) in CTCL Research: carcinogenesis from a to z.

Genetically Engineered Mouse Models (GEMMs) offer a physiologically relevant platform to study human CTCL by introducing specific gene modifications (84). Genomic analysis has identified a number of genes as potential therapeutic targets in CTCL (85). Given that mice share about 85% genetic similarity with humans (86, 87), GEMMs facilitate understanding the role of specific genetic modifications in CTCL development. These models enable the study of natural cancer progression and interaction with the immune system from the onset (88). However, non-skin target GEMMs primarily simulate systemic CTCL pathogenesis and often do not originate from skin-homing CD4+ T cells, the main origin of CTCL genesis, limiting their applicability to skin-centric CTCL features.

2.1. Knockout Mouse Models in CTCL Research: Starting from systemic tumorigenesis.

Knockout mouse models are prevalent in CTCL research, enabling the study of gene function by gene deletion, particularly in the core cell type implicated in CTCL, CD4+ T cells (89). The CD4*CreER*^{T2} transgenic mouse model exemplifies this, where Cre is controlled by the CD4 promoter and gene editing thus selectively targets CD4+ T cells. The Cre/lox system used here allows for temporal and cell-specific gene inactivation via tamoxifen-activated *CreER*^{T2} recombinase. Such inducible knockouts are tools for dissecting gene roles in CD4+ T cells, providing insights into their complex functions in immunity and disease progression. Although, they may predominantly manifest skin symptoms similar to CTCL, they originate from systemic T cell disorders, aligning more with secondary CTCL types (90). It highlights the need for careful consideration when extrapolating findings from these models to primary CTCL.

2.1.1. *R26STAT3C*$^{stopfl/+}$ *CD4Cre* Mouse Model

The *R26STAT3C*$^{stopfl/+}$ *CD4Cre* mouse model is utilized to assess the consequences of persistently active STAT3 in CD4+ T cells. These mice are genetically engineered to have a modified *STAT3C* gene at the *ROSA26* locus (91), which is continuously expressed in CD4 cells due to removing a stop sequence flanked by loxP sites through the CreLoxP system. This persistent activation of STAT3 simulates skin abnormalities akin to those seen in CTCL. Research by Fanok et al. using this model revealed that dysregulated cytokine signaling, particularly aberrations in the IL-2 receptor signaling pathway and the JAK-STAT signaling

pathway, as well as imbalances in microenvironmental factors, like the skin microbiome, may promote the onset and progression of CTCL (92).

2.1.2. *CD4CreER^{T2}Satb1$^{fl/fl}$ Rosa26$^{N1\text{-}ICD}$* Mouse Model

The *CD4CreER^{T2}Satb1$^{fl/fl}$Rosa26$^{N1\text{-}ID}$* mouse model is designed to study the role of SATB1 protein by deletion and Notch1 by overexpression (intracellular domain N1-ICD) in CD4+ T cells (not only those residing in the skin). This model mirrors advanced - CTCL pathogenesis. *SATB1* loss leads to increased chemokine receptors including CCR4, affecting T-cell migration with the transformation of CD8+ T cells into CD4+ CD8+ double-positive T cells and more infiltration of CD3+ T cells in the skin of the mice, and CTCL progression. Moreover, with exhibiting CD8 and CD11b co-expression and symptoms like splenomegaly and lymphadenopathy, it is a valuable tool for exploring late-stage CTCL's advancement and treatment (93).

2.2. Transgenic Mouse Models in CTCL Research

Transgenic mouse models are created by inserting exogenous DNA into the mouse genome, which allows for precise manipulation of gene expression to assess gene function and its impact during a disease (94). In CTCL research, these models are crucial for exploring genes associated with the disease, providing a window on the mechanisms of CTCL onset and progression.

2.2.1. IL-15 Overexpression Mouse Model

The IL-15 overexpression mouse model uses transgenic technology to introduce an exogenous *IL-15* gene into the mouse genome, leading to its overexpression and causing the mice to develop a CTCL-like disease similar to the human condition. IL-15 is a cytokine involved in the maturation of lymphocytes (95, 96). This model mirrors the high levels of IL-15 found in CTCL patients and allows for the observation of clinical symptoms and disease progression *in vivo*, aiding in the understanding of the role of IL-15 in the pathogenesis of CTCL (97, 98). It helps identify potential therapeutic targets, including the regulation of Zeb1 and exploring inhibitors of HDAC and miR-214 (97, 99). The highlighted negative regulatory relationship between miR-29b and BRD4 opens up new avenues for preventing the progression of CTCL (100).

It is important to note that while the IL-15 overexpression mouse model provides valuable insights into the role of IL-15 in CTCL, it cannot explain the mechanisms by which IL-15 overexpression occurs in patients. Therefore, further studies are needed to understand this fully and develop effective treatments.

Based on the latest advances in CTCL research, we aim to create autochthonous mouse models that can effectively replicate the disease's initial skin-based progression (1). These models are designed to modify genes in skin-homing CD4+ T cells and local inflammation, closely mimicking the natural development of CTCL. They significantly enhance our understanding of the origins of early-stage CTCL and show promise in designing early intervention measures.

The scope of this thesis

This thesis starts with an overview in **Chapter 1**, introducing the application of *in vivo* mouse models in the study of CTCL. These mouse models are crucial for deciphering the pathogenesis of the disease and testing potential treatment methods. My Ph.D. pursuit aims to establish Skin-Targeted Genetically Engineered Mouse Models (GEMMs) using gene alterations found in patient tumors through high-throughput sequencing, which might be the key factors to trigger CTCL. These models are intended to investigate the pathogenic role of these genes in the early stages of CTCL. Insights from these works are expected to contribute to the advancement of CTCL research and personalized treatment strategies.

In **Chapter 2**, we first obtained GEMM mice capable of specific *Socs1* knockout in skin-homing CD4+ T cells through breeding. We explored optimal conditions for tamoxifen administration outside the skin. Subsequently, an eight-week experiment using GEMM mice demonstrated that a single copy loss of *Socs1*, combined with persistent inflammation, was insufficient to initiate an early-stage mycosis fungoides-like phenotype within these mice in eight weeks.

To further confirm the causal role of *Socs1* allele loss in the development of MF, **Chapter 3** involves a larger group size (8-9) for stronger statistical power and extends the duration of the experiment. The experimentally induced contact allergic reaction continued for 20 weeks. Ten weeks after stopping the contact allergic challenge, we found that local *Socs1* mono-allelic loss in CD4+ T cells in chronically inflamed skin leads to autonomous skin inflammation with early MF characteristics.

Chapter 4 introduces a novel conditional knockout mouse model with *Hnrnpk* mono-allelic deletion in CD4+ T cells in the skin. Repeated contact allergic challenges were performed to maintain prolonged skin inflammation for 20 weeks, followed by a 20-week period without further treatment. This model mimics key features of early CTCL, including chronic skin inflammation, CD3+ CD4+ cell infiltration, and minimal disturbance in peripheral blood. It offers an experimental pathway to study complex microenvironments and immune

responses, enabling in-depth research into the function of *HNRNPK*, especially regarding de novo development against CTCL.

In **Chapter 5**, we utilized the novel strain of homozygous and heterozygous mice developed in **Chapter 4** to elucidate the role of *Hnrnpk* as an initiating factor when deleted in skin-homing CD4+ T cells, combined with repeated exposure to OXA. We further investigated the role of *Hnrnpk* deletion as an initiating factor in the pathogenesis of CTCL in skin-resident CD4+ T cells.

Chapter 6 presents a comprehensive overview of the data gathered in this study, along with an exploration of both clinical and research implications associated with this thesis.

References

1. Willemze R, Cerroni L, Kempf W, et al. The 2018 update of the WHO-EORTC classification for primary cutaneous lymphomas [published correction appears in Blood. 2019 Sep 26;134(13):1112]. Blood. 2019;133(16):1703-1714. doi:10.1182/blood-2018-11-881268

2. Tensen CP, Quint KD, Vermeer MH. Genetic and epigenetic insights into cutaneous T-cell lymphoma. Blood. 2022;139(1):15-33. doi:10.1182/blood.2019004256

3. Voskoglou-Nomikos T, Pater JL, Seymour L. Clinical predictive value of the in vitro cell line, human xenograft, and mouse allograft preclinical cancer models. Clin Cancer Res. 2003;9(11):4227-4239.

4. Gill RPK, Gantchev J, Martínez Villarreal A, et al. Understanding Cell Lines, Patient-Derived Xenograft and Genetically Engineered Mouse Models Used to Study Cutaneous T-Cell Lymphoma. Cells. 2022;11(4):593. Published 2022 Feb 9. doi:10.3390/cells11040593

5. Mosier DE. Immunodeficient mice xenografted with human lymphoid cells: new models for in vivo studies of human immunobiology and infectious diseases. J Clin Immunol. 1990;10(4):185-191. doi:10.1007/BF00918650

6. Shultz LD, Lyons BL, Burzenski LM, et al. Human lymphoid and myeloid cell development in NOD/LtSz-scid IL2R gamma null mice engrafted with mobilized human hemopoietic stem cells. J Immunol. 2005;174(10):6477-6489. doi:10.4049/jimmunol.174.10.6477

7. Yamashita Y, Sato T, Noishiki K, et al. Data on long-term survival of the NOD/Shi-scid IL-2Rγnull (NOG) mouse in two facilities. J Toxicol Sci. 2021;46(10):453-469. doi:10.2131/jts.46.453

8. Cortes JR, Patrone CC, Quinn SA, et al. Jak-STAT Inhibition Mediates Romidepsin and Mechlorethamine Synergism in Cutaneous T-Cell Lymphoma. J Invest Dermatol. 2021;141(12):2908-2920.e7. doi:10.1016/j.jid.2021.04.023

9. Agliano A, Martin-Padura I, Mancuso P, et al. Human acute leukemia cells injected in NOD/LtSz-scid/IL-2Rgamma null mice generate a faster and more efficient disease compared to other NOD/scid-related strains. Int J Cancer. 2008;123(9):2222-2227. doi:10.1002/ijc.23772

10. Carreno BM, Garbow JR, Kolar GR, et al. Immunodeficient mouse strains display marked variability in growth of human melanoma lung metastases. Clin Cancer Res. 2009;15(10):3277-3286. doi:10.1158/1078-0432.CCR-08-2502

11. Brehm MA, Shultz LD, Luban J, Greiner DL. Overcoming current limitations in humanized mouse research. J Infect Dis. 2013;208 Suppl 2(Suppl 2):S125-S130. doi:10.1093/infdis/jit319

12. Prochazka M, Gaskins HR, Shultz LD, Leiter EH. The nonobese diabetic scid mouse: model for spontaneous thymomagenesis associated with immunodeficiency. Proc Natl Acad Sci U S A. 1992;89(8):3290-3294. doi:10.1073/pnas.89.8.3290

13. Pearson T, Shultz LD, Miller D, et al. Non-obese diabetic-recombination activating gene-1 (NOD-Rag1 null) interleukin (IL)-2 receptor common gamma chain (IL2r gamma null) null mice: a radioresistant model for human lymphohaematopoietic engraftment. Clin Exp Immunol. 2008;154(2):270-284. doi:10.1111/j.1365-2249.2008.03753.x

14. Kaushik A, Kelsoe G, Jaton JC. The nude mutation results in impaired primary antibody repertoire. Eur J Immunol. 1995;25(2):631-634. doi:10.1002/eji.1830250249

15. Charley MR, Tharp M, Locker J, et al. Establishment of a human cutaneous T-cell lymphoma in C.B-17 SCID mice. J Invest Dermatol. 1990;94(3):381-384. doi:10.1111/1523-1747.ep12874500
16. Shibata S, Asano T, Ogura A, et al. SCID-bg mice as xenograft recipients. Lab Anim. 1997;31(2):163-168. doi:10.1258/002367797780600107
17. Chicha L, Tussiwand R, Traggiai E, et al. Human adaptive immune system Rag2-/-gamma(c)-/- mice. Ann N Y Acad Sci. 2005;1044:236-243. doi:10.1196/annals.1349.029
18. Manfè V, Biskup E, Willumsgaard A, et al. cMyc/miR-125b-5p signalling determines sensitivity to bortezomib in preclinical model of cutaneous T-cell lymphomas. PLoS One. 2013;8(3):e59390. doi:10.1371/journal.pone.0059390
19. Huang Y, Su MW, Jiang X, Zhou Y. Evidence of an oncogenic role of aberrant TOX activation in cutaneous T-cell lymphoma. Blood. 2015;125(9):1435-1443. doi:10.1182/blood-2014-05-571778
20. Jain S, Stroopinsky D, Yin L, et al. Mucin 1 is a potential therapeutic target in cutaneous T-cell lymphoma. Blood. 2015;126(3):354-362. doi:10.1182/blood-2015-02-628149
21. Wu X, Wang TW, Lessmann GM, et al. Gallium maltolate inhibits human cutaneous T-cell lymphoma tumor development in mice. J Invest Dermatol. 2015;135(3):877-884. doi:10.1038/jid.2014.476
22. Andrique L, Poglio S, Prochazkova-Carlotti M, et al. Intrahepatic Xenograft of Cutaneous T-Cell Lymphoma Cell Lines: A Useful Model for Rapid Biological and Therapeutic Evaluation. Am J Pathol. 2016;186(7):1775-1785. doi:10.1016/j.ajpath.2016.03.012.
23. Jain S, Washington A, Leaf RK, et al. Decitabine Priming Enhances Mucin 1 Inhibition Mediated Disruption of Redox Homeostasis in Cutaneous T-Cell Lymphoma. Mol Cancer Ther. 2017;16(10):2304-2314. doi:10.1158/1535-7163.MCT-17-0060.
24. Netchiporouk E, Gantchev J, Tsang M, et al. Analysis of CTCL cell lines reveals important differences between mycosis fungoides/Sézary syndrome vs. HTLV-1+ leukemic cell lines. Oncotarget. 2017;8(56):95981-95998. Published 2017 Oct 7. doi:10.18632/oncotarget.21619
25. Poglio S, Prochazkova-Carlotti M, Cherrier F, et al. Xenograft and cell culture models of Sézary syndrome reveal cell of origin diversity and subclonal heterogeneity. Leukemia. 2021;35(6):1696-1709. doi:10.1038/s41375-020-01068-2
26. Wu CH, Yang CY, Wang L, et al. Cutaneous T-Cell Lymphoma PDX Drug Screening Platform Identifies Cooperation between Inhibitions of PI3Kα/δ and HDAC. J Invest Dermatol. 2021;141(2):364-373. doi:10.1016/j.jid.2020.05.110
27. Zhang XH, Nam S, Wu J, et al. Multi-Kinase Inhibitor with Anti-p38γ Activity in Cutaneous T-Cell Lymphoma. J Invest Dermatol. 2018;138(11):2377-2387. doi:10.1016/j.jid.2018.04.030
28. Gallardo F, Bertran J, López-Arribillaga E, et al. Novel phosphorylated TAK1 species with functional impact on NF-κB and β-catenin signaling in human Cutaneous T-cell lymphoma. Leukemia. 2018;32(10):2211-2223. doi:10.1038/s41375-018-0066-4
29. Froehlich TC, Müller-Decker K, Braun JD, et al. Combined inhibition of Bcl-2 and NFκB synergistically induces cell death in cutaneous T-cell lymphoma. Blood. 2019;134(5):445-455. doi:10.1182/blood.2019001545
30. Wang H, Wang Z, Zhang H, et al. Bispecific human IL2-CCR4 immunotoxin targets human cutaneous T-cell lymphoma. Mol Oncol. 2020;14(5):991-1000. doi:10.1002/1878-0261.12653

31. Wang Z, Ma J, Zhang H, et al. CCR4-IL2 bispecific immunotoxin is more effective than brentuximab for targeted therapy of cutaneous T-cell lymphoma in a mouse CTCL model. FEBS Open Bio. 2023;13(7):1309-1319. doi:10.1002/2211-5463.13625

32. Habault J, Thonnart N, Ram-Wolff C, et al. Validation of AAC-11-Derived Peptide Anti-Tumor Activity in a Single Graft Sézary Patient-Derived Xenograft Mouse Model. Cells. 2022;11(19):2933. Published 2022 Sep 20. doi:10.3390/cells11192933

33. Lin M, Kowolik CM, Xie J, Yadav S, Overman LE, Horne DA. Potent Anticancer Effects of Epidithiodiketopiperazine NT1721 in Cutaneous T Cell Lymphoma [published correction appears in Cancers (Basel). 2021 Dec 07;13(24):]. Cancers (Basel). 2021;13(13):3367. Published 2021 Jul 5. doi:10.3390/cancers13133367

34. Velatooru LR, Hu CH, Bijani P, et al. New JAK3-INSL3 Fusion Transcript-An Oncogenic Event in Cutaneous T-Cell Lymphoma. Cells. 2023;12(19):2381. Published 2023 Sep 29. doi:10.3390/cells12192381

35. Watanabe K, Gomez AM, Kuramitsu S, et al. Identifying highly active anti-CCR4 CAR T cells for the treatment of T-cell lymphoma. Blood Adv. 2023;7(14):3416-3430. doi:10.1182/bloodadvances.2022008327.

36. Xiang J, Devenport JM, Carter AJ, et al. An “off-the-shelf” CD2 universal CAR-T therapy for T-cell malignancies. Leukemia. 2023;37(12):2448-2456. doi:10.1038/s41375-023-02039-z

37. Wu CH, Wang L, Yang CY, et al. Targeting CD70 in cutaneous T-cell lymphoma using an antibody-drug conjugate in patient-derived xenograft models. Blood Adv. 2022;6(7):2290-2302. doi:10.1182/bloodadvances.2021005714

38. Ohbo K, Suda T, Hashiyama M, et al. Modulation of hematopoiesis in mice with a truncated mutant of the interleukin-2 receptor gamma chain. Blood. 1996;87(3):956-967.

39. Ito A, Ishida T, Yano H, et al. Defucosylated anti-CCR4 monoclonal antibody exercises potent ADCC-mediated antitumor effect in the novel tumor-bearing humanized NOD/Shi-scid, IL-2Rgamma(null) mouse model. Cancer Immunol Immunother. 2009;58(8):1195-1206. doi:10.1007/s00262-008-0632-0

40. Kitadate A, Ikeda S, Teshima K, et al. MicroRNA-16 mediates the regulation of a senescence-apoptosis switch in cutaneous T-cell and other non-Hodgkin lymphomas. Oncogene. 2016;35(28):3692-3704. doi:10.1038/onc.2015.435

41. Matsuda Y, Ikeda S, Abe F, et al. Downregulation of miR-26 promotes invasion and metastasis via targeting interleukin-22 in cutaneous T-cell lymphoma. Cancer Sci. 2022;113(4):1208-1219. doi:10.1111/cas.15296

42. Ito M, Teshima K, Ikeda S, et al. MicroRNA-150 inhibits tumor invasion and metastasis by targeting the chemokine receptor CCR6, in advanced cutaneous T-cell lymphoma. Blood. 2014;123(10):1499-1511. doi:10.1182/blood-2013-09-527739

43. Abe F, Kitadate A, Ikeda S, et al. Histone deacetylase inhibitors inhibit metastasis by restoring a tumor suppressive microRNA-150 in advanced cutaneous T-cell lymphoma. Oncotarget. 2017;8(5):7572-7585. doi:10.18632/oncotarget.13810

44. Isabelle C, McConnell K, Boles AE, et al., Therapeutic Potential and Role of CD38 in Cutaneous T-Cell Lymphoma Pathogenesis. Blood, 2022. 140(Supplement 1): p. 9216-9218. doi:10.1182/blood-2022-170550

45. Christianson SW, Greiner DL, Hesselton RA, et al. Enhanced human CD4+ T cell engraftment in beta2-microglobulin-deficient NOD-scid mice. J Immunol. 1997;158(8):3578-3586.
46. Krejsgaard T, Kopp K, Ralfkiaer E, et al. A novel xenograft model of cutaneous T-cell lymphoma. Exp Dermatol. 2010;19(12):1096-1102. doi:10.1111/j.1600-0625.2010.01138.x
47. Pedersen IH, Willerslev-Olsen A, Vetter-Kauczok C, et al. Vascular endothelial growth factor receptor-3 expression in mycosis fungoides. Leuk Lymphoma. 2013;54(4):819-826. doi:10.3109/10428194.2012.726720
48. Thode C, Woetmann A, Wandall HH, et al. Malignant T cells secrete galectins and induce epidermal hyperproliferation and disorganized stratification in a skin model of cutaneous T-cell lymphoma. J Invest Dermatol. 2015;135(1):238-246. doi:10.1038/jid.2014.284
49. Thaler S, Burger AM, Schulz T, et al. Establishment of a mouse xenograft model for mycosis fungoides. Exp Dermatol. 2004;13(7):406-412. doi:10.1111/j.0906-6705.2004.00201.x
50. Nakahashi K, Nihira K, Suzuki M, Ishii T, Masuda K, Mori K. A novel mouse model of cutaneous T-cell lymphoma revealed the combined effect of mogamulizumab with psoralen and ultraviolet a therapy. Exp Dermatol. 2022;31(11):1693-1698. doi:10.1111/exd.14641
51. Xia C, He Z, Cai Y, Liang S. Vorinostat upregulates MICA via the PI3K/Akt pathway to enhance the ability of natural killer cells to kill tumor cells. Eur J Pharmacol. 2020;875:173057. doi:10.1016/j.ejphar.2020.173057
52. Wang B, Li K, Wang H, Shen X, Zheng J. Systemic chemotherapy promotes HIF-1α-mediated glycolysis and IL-17F pathways in cutaneous T-cell lymphoma. Exp Dermatol. 2020;29(10):987-992. doi:10.1111/exd.14133
53. Bresin A, Cristofoletti C, Caprini E, et al. Preclinical Evidence for Targeting PI3K/mTOR Signaling with Dual-Inhibitors as a Therapeutic Strategy against Cutaneous T-Cell Lymphoma. J Invest Dermatol. 2020;140(5):1045-1053.e6. doi:10.1016/j.jid.2019.08.454
54. Le Y, Shen X, Kang H, et al. Accelerated, untargeted metabolomics analysis of cutaneous T-cell lymphoma reveals metabolic shifts in plasma and tumor adjacent skins of xenograft mice [published correction appears in J Mass Spectrom. 2018 Aug;53(8):739]. J Mass Spectrom. 2018;53(2):172-182. doi:10.1002/jms.4048
55. Chen O, He Q, Han Q, et al. Mechanisms and treatments of neuropathic itch in a mouse model of lymphoma. J Clin Invest. 2023;133(4):e160807. Published 2023 Feb 15. doi:10.1172/JCI160807
56. Furutani K, Chen O, McGinnis A, et al. Novel proresolving lipid mediator mimetic 3-oxa-PD1n-3 docosapentaenoic acid reduces acute and chronic itch by modulating excitatory and inhibitory synaptic transmission and astroglial secretion of lipocalin-2 in mice. Pain. 2023;164(6):1340-1354. doi:10.1097/j.pain.0000000000002824
57. Yu XX, Zhu MY, Wang JR, et al. LW-213 induces cell apoptosis in human cutaneous T-cell lymphomas by activating PERK-eIF2α-ATF4-CHOP axis. Acta Pharmacol Sin. 2021;42(2):290-300. doi:10.1038/s41401-020-0466-7
58. Wang Y, Gu X, Li W, Zhang Q, Zhang C. PAK1 overexpression promotes cell proliferation in cutaneous T cell lymphoma via suppression of PUMA and p21. J Dermatol Sci. 2018;90(1):60-67. doi:10.1016/j.jdermsci.2017.11.019

59. Esmailzadeh S, Huang Y, Su MW, Zhou Y, Jiang X. BIN1 tumor suppressor regulates Fas/Fas ligand-mediated apoptosis through c-FLIP in cutaneous T-cell lymphoma. Leukemia. 2015;29(6):1402-1413. doi:10.1038/leu.2015.9

60. Kato Y, Egusa C, Maeda T, Tsuboi R. Combination of retinoid and histone deacetylase inhibitor produced an anti-tumor effect in cutaneous T-cell lymphoma by restoring tumor suppressor gene, retinoic acid receptorβ2, via histone acetylation. J Dermatol Sci. 2016;81(1):17-25. doi:10.1016/j.jdermsci.2015.10.016

61. Cattan AR, Douglas E. The C.B.17 scid mouse strain as a model for human disseminated leukaemia and myeloma in vivo. Leuk Res. 1994;18(7):513-522. doi:10.1016/0145-2126(94)90089-2

62. Tonozuka Y, Tanaka H, Nomura K, Sakaguchi K, Soeda J, Kakimoto Y. The combination of brentuximab vedotin and chidamide synergistically suppresses the proliferation of T-cell lymphoma cells through the enhancement of apoptosis. Cancer Chemother Pharmacol. 2024;93(2):137-149. doi:10.1007/s00280-023-04609-5

63. Doebbeling U. A mouse model for the Sézary syndrome. J Exp Clin Cancer Res. 2010;29(1):11. Published 2010 Feb 11. doi:10.1186/1756-9966-29-11

64. Nakajima R, Miyagaki T, Kamijo H, et al. Possible therapeutic applicability of galectin-9 in cutaneous T-cell lymphoma. J Dermatol Sci. 2019;96(3):134-142. doi:10.1016/j.jdermsci.2019.09.004

65. Hao Z, Rajewsky K. Homeostasis of peripheral B cells in the absence of B cell influx from the bone marrow. J Exp Med. 2001;194(8):1151-1164. doi:10.1084/jem.194.8.1151

66. Adachi T, Kobayashi T, Sugihara E, et al. Hair follicle-derived IL-7 and IL-15 mediate skin-resident memory T cell homeostasis and lymphoma. Nat Med. 2015;21(11):1272-1279. doi:10.1038/nm.3962

67. van der Fits L, Rebel HG, Out-Luiting JJ, et al. A novel mouse model for Sézary syndrome using xenotransplantation of Sézary cells into immunodeficient RAG2(-/-) γc(-/-) mice. Exp Dermatol. 2012;21(9):706-709. doi:10.1111/j.1600-0625.2012.01556.x

68. Herndler-Brandstetter D, Shan L, Yao Y, et al. Humanized mouse model supports development, function, and tissue residency of human natural killer cells. Proc Natl Acad Sci U S A. 2017;114(45):E9626-E9634. doi:10.1073/pnas.1705301114

69. Gao J, Ren S, Choonoo G, et al. Microenvironment-dependent growth of Sezary cells in humanized IL-15 mice. Dis Model Mech. 2023;16(10):dmm050190. doi:10.1242/dmm.050190

70. Wu X, Sells RE, Hwang ST. Upregulation of inflammatory cytokines and oncogenic signal pathways preceding tumor formation in a murine model of T-cell lymphoma in skin. J Invest Dermatol. 2011;131(8):1727-1734. doi:10.1038/jid.2011.89

71. Kruglov O, Wu X, Hwang ST, Akilov OE. The synergistic proapoptotic effect of PARP-1 and HDAC inhibition in cutaneous T-cell lymphoma is mediated via Blimp-1. Blood Adv. 2020;4(19):4788-4797. doi:10.1182/bloodadvances.2020002049

72. Wu X, Schulte BC, Zhou Y, et al. Depletion of M2-like tumor-associated macrophages delays cutaneous T-cell lymphoma development in vivo. J Invest Dermatol. 2014;134(11):2814-2822. doi:10.1038/jid.2014.206

73. Kruglov O, Johnson LDS, Minic A, et al. The pivotal role of cytotoxic NK cells in mediating the therapeutic effect of anti-CD47 therapy in mycosis fungoides. Cancer Immunol Immunother. 2022;71(4):919-932. doi:10.1007/s00262-021-03051-x

74. Wu X, Singh R, Hsu DK, et al. A Small Molecule CCR2 Antagonist Depletes Tumor Macrophages and Synergizes with Anti-PD-1 in a Murine Model of Cutaneous T-Cell Lymphoma (CTCL). J Invest Dermatol. 2020;140(7):1390-1400.e4. doi:10.1016/j.jid.2019.11.018

75. Kittipongdaja W, Wu X, Garner J, et al. Rapamycin Suppresses Tumor Growth and Alters the Metabolic Phenotype in T-Cell Lymphoma. J Invest Dermatol. 2015;135(9):2301-2308. doi:10.1038/jid.2015.153

76. Tanita K, Fujimura T, Sato Y, et al. Bexarotene Reduces Production of CCL22 From Tumor-Associated Macrophages in Cutaneous T-Cell Lymphoma. Front Oncol. 2019;9:907. Published 2019 Sep 20. doi:10.3389/fonc.2019.00907

77. Ohuchi K, Fujimura T, Kambayashi Y, et al. Successful treatment of mogamulizumab-resistant mycosis fungoides with mogamulizumab plus etoposide combined therapy: Investigation of the immunomodulatory effects of etoposide on the tumor microenvironment. Dermatol Ther. 2020;33(4):e13487. doi:10.1111/dth.13487

78. Hensbergen PJ, Wijnands PG, Schreurs MW, Scheper RJ, Willemze R, Tensen CP. The CXCR3 targeting chemokine CXCL11 has potent antitumor activity in vivo involving attraction of CD8+ T lymphocytes but not inhibition of angiogenesis. J Immunother. 2005;28(4):343-351. doi:10.1097/01.cji.0000165355.26795.27

79. Takahashi N, Sugaya M, Suga H, et al. Thymic Stromal Chemokine TSLP Acts through Th2 Cytokine Production to Induce Cutaneous T-cell Lymphoma. Cancer Res. 2016;76(21):6241-6252. doi:10.1158/0008-5472.CAN-16-0992

80. Vieyra-Garcia PA, Wei T, Naym DG, et al. STAT3/5-Dependent IL9 Overexpression Contributes to Neoplastic Cell Survival in Mycosis Fungoides. Clin Cancer Res. 2016;22(13):3328-3339. doi:10.1158/1078-0432.CCR-15-1784

81. Miyagaki T, Sugaya M, Oka T, et al. Placental Growth Factor and Vascular Endothelial Growth Factor Together Regulate Tumour Progression via Increased Vasculature in Cutaneous T-cell Lymphoma. Acta Derm Venereol. 2017;97(5):586-592. doi:10.2340/00015555-2623

82. Cornejo MG, Kharas MG, Werneck MB, et al. Constitutive JAK3 activation induces lymphoproliferative syndromes in murine bone marrow transplantation models. Blood. 2009;113(12):2746-2754. doi:10.1182/blood-2008-06-164368

83. Rivera-Munoz P, Laurent AP, Siret A, et al. Partial trisomy 21 contributes to T-cell malignancies induced by JAK3-activating mutations in murine models. Blood Adv. 2018;2(13):1616-1627. doi:10.1182/bloodadvances.2018016089

84. Sharpless NE, Depinho RA. The mighty mouse: genetically engineered mouse models in cancer drug development. Nat Rev Drug Discov. 2006;5(9):741-754. doi:10.1038/nrd2110

85. Bastidas Torres AN, Cats D, Mei H, et al. Genomic analysis reveals recurrent deletion of JAK-STAT signaling inhibitors HNRNPK and SOCS1 in mycosis fungoides. Genes Chromosomes Cancer. 2018;57(12):653-664. doi:10.1002/gcc.22679

86. Basheer, F. and G. Vassiliou, Mouse Models of Myeloid Malignancies. Cold Spring Harb Perspect Med, 2021. 11(1)

87. Mouse Genome Sequencing Consortium, Waterston RH, Lindblad-Toh K, et al. Initial sequencing and comparative analysis of the mouse genome. Nature. 2002;420(6915):520-562. doi:10.1038/nature01262

88. Dummer R, Vermeer MH, Scarisbrick JJ, et al. Cutaneous T cell lymphoma. Nat Rev Dis Primers. 2021;7(1):61. Published 2021 Aug 26. doi:10.1038/s41572-021-00296-9

89. Hall B, Limaye A, Kulkarni AB. Overview: generation of gene knockout mice. Curr Protoc Cell Biol. 2009;Chapter 19:Unit-19.12.17. doi:10.1002/0471143030.cb1912s44

90. Aghajani K, Keerthivasan S, Yu Y, Gounari F. Generation of CD4CreER(T^2) transgenic mice to study development of peripheral CD4-T-cells. Genesis. 2012;50(12):908-913. doi:10.1002/dvg.22052

91. Casola S, Cattoretti G, Uyttersprot N, et al. Tracking germinal center B cells expressing germ-line immunoglobulin gamma1 transcripts by conditional gene targeting. Proc Natl Acad Sci U S A. 2006;103(19):7396-7401. doi:10.1073/pnas.0602353103

92. Fanok MH, Sun A, Fogli LK, et al. Role of Dysregulated Cytokine Signaling and Bacterial Triggers in the Pathogenesis of Cutaneous T-Cell Lymphoma. J Invest Dermatol. 2018;138(5):1116-1125. doi:10.1016/j.jid.2017.10.028

93. Harro CM, Perez-Sanz J, Costich TL, et al. Methyltransferase inhibitors restore SATB1 protective activity against cutaneous T cell lymphoma in mice. J Clin Invest. 2021;131(3):e135711. doi:10.1172/JCI135711

94. Viney JL. Transgenic and gene knockout mice in cancer research. Cancer Metastasis Rev. 1995;14(2):77-90. doi:10.1007/BF00665792

95. Anthony S, Schluns KS. Emerging roles for IL-15 in the activation and function of T-cells during immune stimulation. Research and Reports in Biology. 2015;6:25-37 doi:10.2147/RRB.S57685

96. Fehniger TA, Suzuki K, Ponnappan A, et al. Fatal leukemia in interleukin 15 transgenic mice follows early expansions in natural killer and memory phenotype CD8+ T cells. J Exp Med. 2001;193(2):219-231. doi:10.1084/jem.193.2.219

97. Mishra A, La Perle K, Kwiatkowski S, et al. Mechanism, Consequences, and Therapeutic Targeting of Abnormal IL15 Signaling in Cutaneous T-cell Lymphoma. Cancer Discov. 2016;6(9):986-1005. doi:10.1158/2159-8290.CD-15-1297

98. Sindaco P, Pandey H, Isabelle C, et al. The role of interleukin-15 in the development and treatment of hematological malignancies. Front Immunol. 2023;14:1141208. Published 2023 Apr 20. doi:10.3389/fimmu.2023.1141208

99. Kohnken R, McNeil B, Wen J, et al. Preclinical Targeting of MicroRNA-214 in Cutaneous T-Cell Lymphoma. J Invest Dermatol. 2019;139(9):1966-1974.e3. doi:10.1016/j.jid.2019.01.033

100. Kohnken R, Wen J, Mundy-Bosse B, et al. Diminished microRNA-29b level is associated with BRD4-mediated activation of oncogenes in cutaneous T-cell lymphoma. Blood. 2018;131(7):771-781. doi:10.1182/blood-2017-09-805663

2

In vivo modelling of Cutaneous T-cell lymphoma: The role of *SOCS1*

Yixin Luo[1], Maarten H. Vermeer[1], Frank R. de Gruijl[1], Willem H Zoutman[1], Marjolein Sluijter[2], Thorbald van Hall[2], Cornelis P Tensen[1]
1.Department of Dermatology, Leiden University Medical Center, Leiden, The Netherlands
2.Department of Medical Oncology, Oncode Institute, Leiden University Medical Center, Leiden, The Netherlands
Front Oncol. 2022 Nov; 12:1031052. doi: 10.3389/fonc.2022.1031052.

Abstract:

Mycosis fungoides (MF), the most common type of Cutaneous T cell Lymphoma (CTCL), is characterized by an inflamed skin intermixed with proliferating malignant mature skin-homing CD4+ T cells. Detailed genomic analyses of MF skin biopsies revealed several candidate genes possibly involved in genesis of these tumors and/or potential targets for therapy. These studies showed, in addition to common loss of cell cycle regulator *CDKN2A*, activation of several oncogenic pathways, most prominently and consistently involving JAK-STAT signaling. *SOCS1*, an endogenous inhibitor of the JAK-STAT signaling pathway, was identified as a recurrently deleted gene in MF, already occurring in the earliest stages of the disease. To explore the mechanisms of MF, we create *in vivo* mouse models of autochthonous CTCLs and these genetically engineered mouse models (GEMMS) can also serve as valid experimental models for targeted therapy.

We describe the impact of allelic deletion of *Socs1* in CD4+ T cells of the skin. To achieve this, we crossed inducible Cre-transgenic mice in the CD4 lineage with transgenic mice carrying floxed genes of *Socs1*. We first determined optimal conditions for *Socs1* ablation with limited effects on circulating CD4+ T-cells in blood. Next, we started time-course experiments mimicking sustained inflammation, typical in CTCL. FACS analysis of the blood was done every week. Skin biopsies were analyzed by immunocytochemical staining at the end of the experiment. We found that the *Socs1* knockout transgenic group had thicker epidermis of treated skin compared with the control group and had more CD3+ and CD4+ cells in the skin of the transgenic group compared to the control group. We also noted more activation of *Stat3* by staining for p-STAT3 in *Socs1* knockout compared to wt CD4+T cells in the skin. The results also indicated that single copy loss of *Socs1* in combination with sustained inflammation is insufficient to start a phenotype resembling early-stage mycosis fungoides within eight weeks in these mice.

In sum, we developed and optimized an autochthonous murine model permitting selective knockout of *Socs1* in skin infiltrating CD4+ T-cells. This paves the way for more elaborate experiments to gain insight in the oncogenesis of CTCL.

Key words: Cutaneous T cell lymphoma; *in vivo* modeling; Inflammation; Mycosis fungoides; Transgenic mouse.

1 Introduction

Mycosis fungoides (MF), the most common type of Cutaneous T cell Lymphoma (CTCL), is characterized by an inflamed skin intermixed with proliferating malignant mature skin-homing CD4+ T cells. (1-3) It presents in the early stage with cutaneous patches and/or plaques. The disease has a favorable prognosis in those early stages (IA-IB). However, approximately 25% of patients progress to the advanced stage, presented with cutaneous tumors or erythroderma or systemic involvement, and a dramatic reduction in five-year survival from approximately 80% to 25%.

The exact molecular mechanisms of MF pathology remained unclear despite some genomic and gene expression profile studies. Recent detailed genomic analyses (using next-generation sequencing) of MF skin biopsies revealed several candidate genes possibly involved in the genesis of these tumors and/or potential targets for therapy.(4) These studies showed, in addition to the common loss of cell cycle regulator *CDKN2A*, activation of several oncogenic pathways, most prominently and consistently involving JAK-STAT signaling. However, the precise genetic alterations driving these oncogenic pathways, the genetic drivers, remained unclear.

In mycosis fungoides, *SOCS1* (the suppressor of cytokine signaling 1) was identified as one of the highly recurrently deleted tumor suppressors and the gene rearrangements of *SOCS1* were already present in the earliest stages of MF.(5) *SOCS1* belongs to the suppressor of cytokine signaling (SOCS) family and is an endogenous inhibitor of the JAK-STAT signaling pathway, inhibiting JAK-STAT phosphorylation and activation via a negative feedback loop.(6) It plays critical roles in Th subset differentiation.(7) and the regulation of Tregs.(8) *SOCS1* is a unique tumor-suppressor gene that regulates inflammation-related tumorigenesis.(9)

In early disease stages, the skin lesions contain of a small population of malignant T cells immersed within a dense infiltrate of reactive immune cells. It is supposed that chronic inflammation precedes and gives rise to the malignant cell clone, which takes the upper hand as the tumor progresses. (10) It is now recognized that inflammation may not only combat the tumor but may promote its development. Immunologic processes, and in particular chronic inflammation, were added to Weinberg's and Hanahan's original hallmarks of cancer. (11)

To elaborate on the function of *SOCS1* and other identified genes in mycosis fungoides, in particular in the initiating events, we aim to use mouse models. The currently available mouse models (12) are nearly all based on cell lines and xenografts in immune

compromised mice and models that represent early stages of MF are lacking. Here we describe the development of a genetically engineered mouse model that aims to represent autochthonous CTCLs, permitting the necessary next steps in dissecting the precise role(s) of identified genes in the pathogenesis starting with *SOCS1*. We show that *Socs1* deletion in this *in vivo* model is limited to CD4+ T cells and chronic inflammation of the skin can be maintained and eventually used to promote and enhance the tumorigenic process. The irreplaceable merit of this autochthonous model is the possibility to study in detail the impact of the interaction between the imposed tumor cells transformation and an intact immune system. Finally, genetic mouse models might also serve as valid experimental models for targeted therapy.

2.Materials and Methods

2.1.Mice

Conditional *Socs1* knockout mice (13) (floxed *Socs1*) and tamoxifen-inducible *Cd4*-driven *CreER*^{T2}-knock-in mice (*Cd4CreER*^{T2}) (14) were crossed. The *Cd4*-driven *CreER*^{T2}-knock-in mice were purchased from Jackson's Laboratories (#:022356). Conditional *Socs1* knockout mice (with loxP sites on either side of exon 2 of the targeted *Socs1* gene; with inserted reporter human CD4) were kindly obtained from Professor Warren Alexander at Walter and Eliza Hall Institute. The first round of crossing yielded *Socs1 fl/wt Cd4CreER*^{T2}*+/-* and *Socs1 fl/wt Cd4CreER*^{T2}*-/-* mice. The resulting offspring will have exon2 of *Socs1* deleted in Cre-expressing CD4+ T cells up on administering tamoxifen.

Of note is the sub-Mendelian low yield of *Socs1 fl/fl Cd4CreER*^{T2} pups which hampered populating the experiments with an adequate number of these mice.

Genomic PCR was conducted to analyze the genotypes of mice using ear DNA and gene-specific primers for the *Socs1flox* transgene and *Cd4CreER*^{T2} construct.

All mice were housed in individually ventilated cages, maintained under specific pathogen-free conditions, and had access to food and water ad libitum.

All mouse experiments were supervised by the animal welfare committee (IvD) of the Leiden University Medical Center and approved by the national central committee of animal experiments (CCD) under the permit number AVD116002015271, in accordance with the Dutch Act on Animal Experimentation and EU Directive 2020/63/EU.

Mice entered the experiments at ages between 6 and 20 weeks. The mice were assigned to control or experimental groups based on genotype and were assigned randomly to

experimental treatments within each group.

2.2.Preparation and administration of Oxazolone and 4-hydroxy-Tamoxifen

Oxazolone (4-Ethoxymethylene-2-phenyl-2-oxazolin-5-one, Sigma-Aldrich, Netherlands) was dissolved in acetone. For every experiment performed, a freshly made solution was used. Mice were sensitized with 1.5% oxazolone (100 µL) on the shaved abdomen skin (2 cm x 2 cm) under anesthesia. After seven days, mice were challenged with 0.5% oxazolone (150 µL) on the shaved left flank skin (2 cm x 3 cm) and vehicle only (150 µL acetone) on the shaved right flank skin (2 cm x 3 cm). To maintain the skin inflammation, mice received 0.5% oxazolone (150 µL) on the shaved left flank skin (2 cm x 3 cm) and again vehicle only (150 µL acetone) on the shaved right flank skin (2 cm x 3 cm) three times a week.

4-hydroxy-Tamoxifen (4OH Tam Sigma-Aldrich, Netherlands) was dissolved in ethanol (20 mg/ml) and was sonicated for 2 minutes. Then it was stored at -20 °C for the experiments. For topical administration, 4OHT was reheated at 60 °C for 10 minutes and was administered 1mg per mouse topically on left shaved skin (2 cm x 3 cm).

2.3.Flow Cytometry

Blood (50l) was drawn from the tail veil every week. This was performed at least 24 hours after OXA application. Whole blood samples were processed using lysis buffer (from Hospital Pharmacy at LUMC) for 10 mins at 37 °C. Cells were incubated with monoclonal antibodies for 30 min on ice.

Fluorescence-labeled antibodies including anti-mouse CD3 (clone 145-2C11, BD, The Netherlands), anti-mouse CD19 (clone 1D3, Thermo Fisher Scientific, The Netherlands), anti-mosue CD4 (clone RM4-5, Thermo Fisher Scientific, The Netherlands), anti-mouse CD8 (clone 53-6.7, Biolegend, The Netherlands) and anti-ΔhCD4 (clone RPA-T4, eBioscience™, The Netherlands). Of note, the antibody for ΔhCD4 should be specifical clone that fits for the surrogated reporter in *Socs1flox* transgenic mouse. Samples were processed in a BD Fortessa flow cytometer and analyzed using the FlowJo software.

2.4.Histological and immunohistochemical analyses

Skin samples were fixed with 10% neutral buffered formalin, dehydrated with increasing grades of ethanol, cleared with xylene, and embedded in paraffin. Sections (4 µm-thick) were cut with a microtome (Leica 149MULTI0C1). Tissue sections were stained with hematoxylin and eosin to visualize general histological architecture.

For immunohistochemical analyses, paraffin-embedded skin sections were dewaxed with

xylene and rehydrated. After that, the sections were blocked for endogenous peroxidase using 0.3% hydrogen peroxide and nonspecific antibody binding using a blocking buffer (SuperBlock, Thermo Fisher Scientific, The Netherlands). Antigen retrieval was performed using citric acid (PH = 6.0) solution. The tissue sections were incubated with the following primary antibodies at 4°C overnight: anti-human CD4 (1:2000, EPR6855, Abcam, The Netherlands), anti-mouse CD3 (1:200, D7A6E, Cell Signaling Technology, The Netherlands), anti-mouse CD4 (1:100, D7D2Z, Cell Signaling Technology, The Netherlands), anti-mouse CD8 (1:1600, 4SM15, eBioscience™, The Netherlands), anti-phospho-STAT3 (1:150, D3A7, Cell Signaling Technology, The Netherlands).

Then sections were incubated with secondary antibody at room temperature for 60 min. Sections were visualized with Vectastain Elite Kit (Vector Labs, Netherlands) and diaminobenzidine (Dako Omnis, Agilent Dako, Netherlands). After counterstaining with hematoxylin, sections were mounted. The scanner (3DHISTECH, Pannoramic 250) was used for microscopic examination and image acquisition.

2.5.Immunohistochemical evaluation

The layers of the epidermis were counted within at least 5 high power fields (HPF) (20x magnification) of each slide, and the means were assessed for further statistical analysis.

The numbers of ΔhCD4+, CD3+, CD4+, CD8+ and phospho-STAT3 positive cells in the dermis were counted within 5 HPF (20x magnification) per case. The values were normalized to cells/mm^2, and the mean numbers were assessed for further statistical analysis. The evaluations were conducted by two independent individuals who were blinded to samples information.

2.6.Statistical Analysis

A paired *t*-test was used to compare treated skin and untreated skin from the same mouse group. Nonparametric test and an analysis of covariance were used to compare the skin between two different mouse groups.

All statistical analyses were performed using GraphPad Prism software version 8 (GraphPad). In all cases a *P*-value of 0.05 and below was considered significant (*), $P < 0.01$(**) and $P < 0.001$ (***) as highly significant.

3.Results

3.1.Generation of a specific conditional *Socs1* knockout mouse model

To knock out the *Socs1* gene in murine CD4+ (mCD4) T cells, we crossed conditional *Socs1* knockout mice (floxed *Socs1*) and tamoxifen-inducible *Cd4*-driven *CreER*^{T2}-knock-in mice (*Cd4CreER*^{T2}). The tamoxifen-inducible *Cd4*-driven *CreER*^{T2} transgenic mouse strain expresses a tamoxifen inducible Cre recombinase (*CreER*^{T2}) under the control of the *Cd4* gene promoter (**Figure 1A**). In the conditional *Socs1* knockout mouse, the endogenous *Socs1* gene was replaced with a modified *Socs1* gene flanked by LoxP sites. The modified *Socs1* gene harbors a 3' reporter, ΔhCD4, which comes under the control of the *Socs1* promoter. This reporter, ' Δ human CD4' contains an *F43I* mutation and intracellular truncation, which abrogates its function.

In *Socs1flox Cd4CreER*^{T2}*+/-* mice (*Socs1 fl/wt Cd4CreER*^{T2}*+/-* and *Socs1 fl/fl Cd4CreER*^{T2}*+/-*), *Cre* recombinase is activated selectively in CD4+ T cells upon tamoxifen and deletes the *Socs1* sequence between loxP sites. *Socs1* wild-type alleles, *Socs1* floxed alleles and *Cd4CreER*^{T2} transgene were determined by PCR using genomic DNA from ear clips. (**Figure 1B, & 1C**)

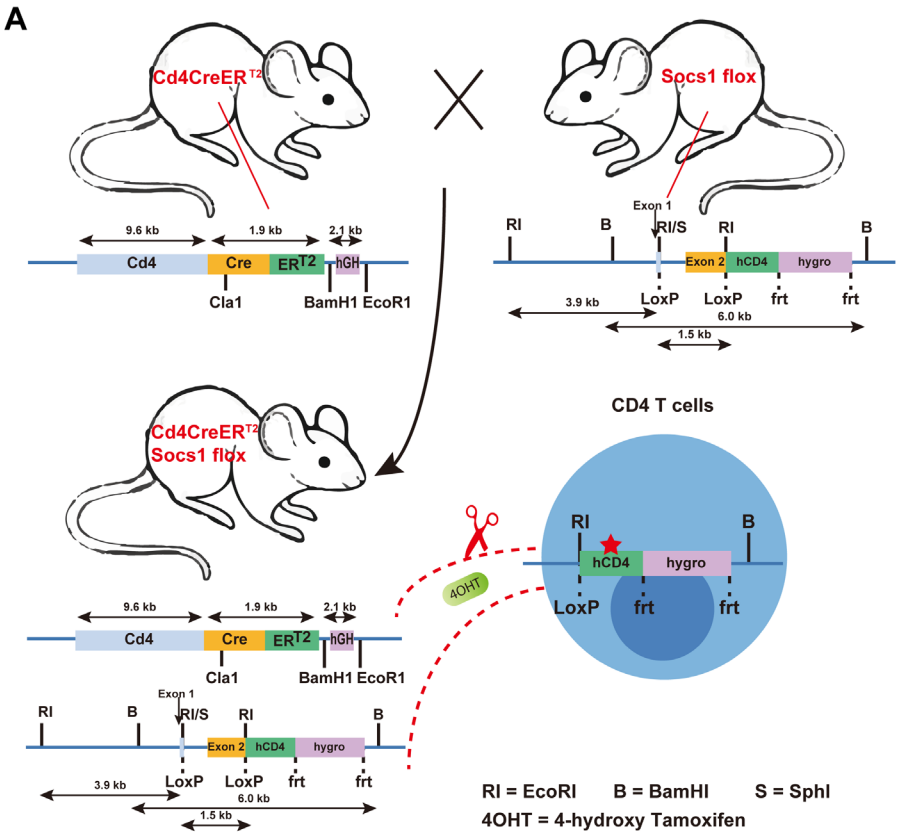
A
Cd4CreER T2
Socs1 flox
9.6 kb
1.9 kb
2.1 kb
Cd4
Cre
ER T2
hGH
Cla1
BamH1 EcoR1
Exon 1
RI
B
RI/S
Exon 2
hCD4
hygro
3.9 kb
LoxP
frt
6.0 kb
1.5 kb
CD4 T cells
4OHT
RI = EcoRI
B = BamHI
S = SphI
4OHT = 4-hydroxy Tamoxifen

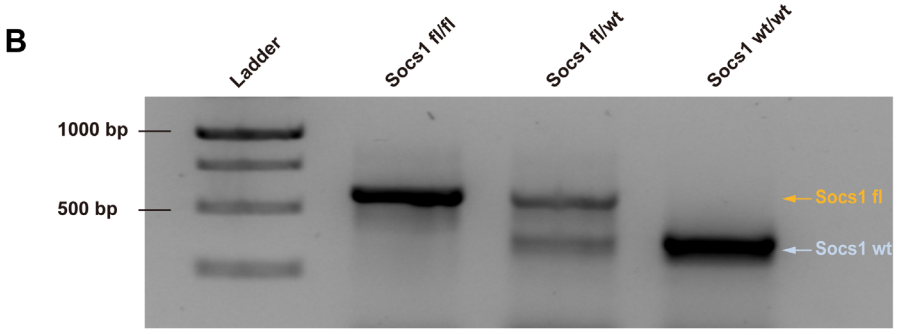
B
Ladder
Socs1 fl/fl
Socs1 fl/wt
Socs1 wt/wt
1000 bp
500 bp
Socs1 fl
Socs1 wt

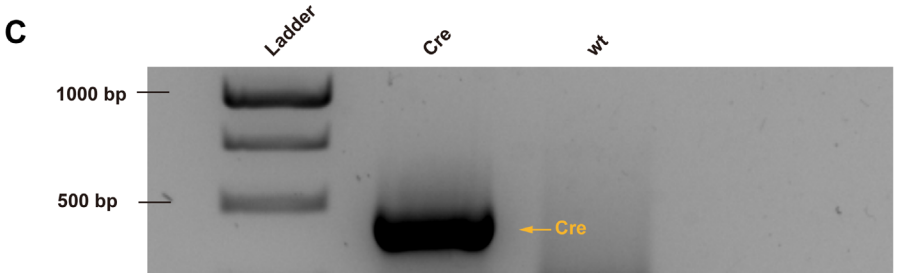
C
Ladder
Cre
wt
1000 bp
500 bp
Cre

Figure 1. Creation of conditional *Socs1* knockout mice permitting specific inactivation of the *Socs1* gene in CD4+ T cells. (A). Breeding scheme used to create on conditional knockout mice permitting specific deletion of functional *Socs1* in CD4+ T cells. The transgenic *Socs1flox Cd4CreER^{T2}+ (Socs1fl/wt Cd4CreER^{T2}+* and *Socs1fl/fl Cd4CreER^{T2}+*) mice were generated by crossing *Socs1flox* (in which the exon2 of *Socs1* is flanked by LoxP sites) with the inducible *Cd4CreER^{T2}* mice (in which *Cre* is under the control of *Cd4* promoter. Expression of the *Cre* recombinase gene is induced in CD4+ T cells by giving the mice the drug tamoxifen, (shown in the figure as 4OHT). Tamoxifen allows the Cre recombinase to enter the nucleus of CD4+ T cells and recombine the loxP sites. In the event that *Socs1fl* was deleted by *Cre*, the inserted reporter human CD4 (hCD4) will be under control of the endogenous *Socs1* promoter and expressed instead of *Socs1*. The human CD4 reporter contains a *F43I* mutation and intracellular truncation to abrogates its function. (B). Agarose gel electrophoresis image of the *Socs1* PCR product of *Socs1fl/fl, Socs1fl/wt* and *Socs1wt/wt* mice. Visible marker bands indicate fragment sizes of 1000, 750, 500 and 250 bps from top to bottom (lane 1). (C). Agarose gel electrophoresis image of the Cre PCR product of the *Cd4CreER^{T2}*+ and wildtype mice. Visible marker bands indicate fragment sizes of 1000, 750 and 500 bps from top to bottom (lane 1).

3.2.Three doses of 4OHT topical application have less systemic influence compared with five doses of 4OHT topical application

Two groups of *Socs1 fl/wt Cd4CreER^{T2}*+/- mice, with bilateral flank skin shaved, received topical 4OHT once daily on the left flank and acetone as a vehicle control once daily on the right flank for 5 and 3 consecutive days, respectively. Blood (50 µl) was taken from the tail vein before the 4OHT application and three days after the last 4OHT application. (**Figure 2A**)

The *Socs1* deletion, showed by the reporter gene ΔhCD4 on CD4+ T cells, was measured by flow cytometry in both groups. The results showed that *Socs1* was successfully deleted in circulating CD4+T cells after the 4OHT application in both groups of mice. Moreover, it confirmed that the activation of Cre-loxP system in our specific mouse model could be achieved by using five doses of 4OHT and three doses of 4OHT, which resulted in the deletion of *Socs1* in CD4+ T cells. (**Figure 2B**) After 4OHT, the S*ocs1 fl/wt Cd4CreER^{T2}+/-* mouse can be marked as the *Socs1-/wt Cd4CreER^{T2}+/-* (S+-C) mouse.

In quantifying the percentage of CD4+T cells with *Socs1* deletion in circulating CD4+T cells after 5 and 3 doses of 4OHT, we observed a clear dose effect: 3 doses resulted in statistically significantly less deletions than 5 doses. (**Figure 2C**)

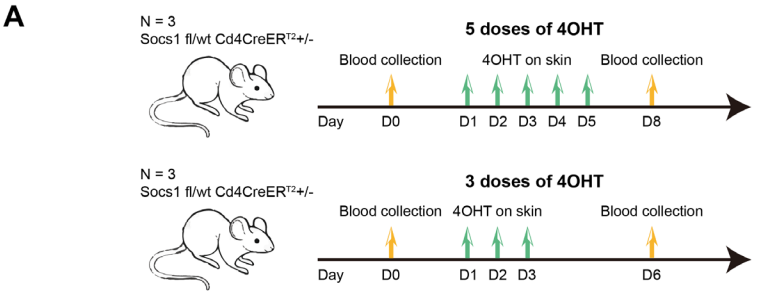
A
N = 3
Socs1 fl/wt Cd4CreER^{T2}+/-
5 doses of 4OHT
Blood collection
4OHT on skin
Blood collection
Day
D0
D1 D2 D3 D4 D5
D8
N = 3
Socs1 fl/wt Cd4CreER^{T2}+/-
3 doses of 4OHT
Blood collection
4OHT on skin
Blood collection
Day
D0
D1 D2 D3
D6

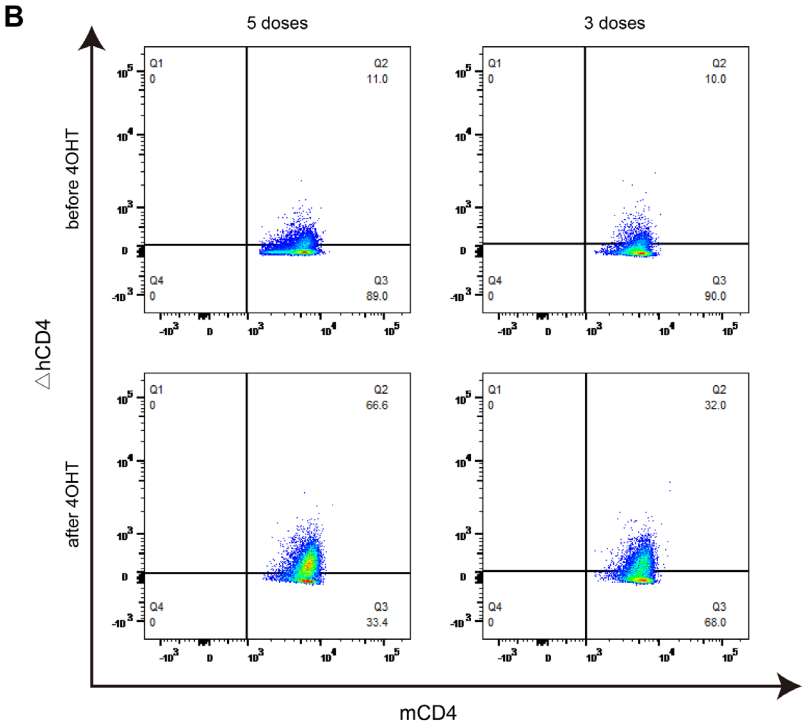
B
5 doses
3 doses
before 4OHT
after 4OHT
△hCD4
mCD4
Q1
Q2
Q3
Q4
11.0
89.0
10.0
90.0
66.6
33.4
32.0
68.0

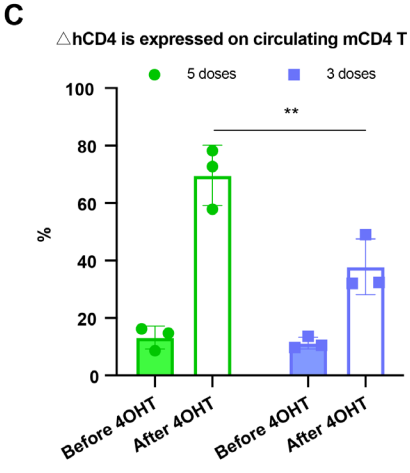
C
△hCD4 is expressed on circulating mCD4 T cells
5 doses
3 doses
**
%
100
80
60
40
20
0
Before 4OHT
After 4OHT
Before 4OHT
After 4OHT

Figure 2. Effect of five and three times 4OHT application on the skin. (A). Schematic representation of the experiment determining the effect of 5 and 3 doses of 4OHT. Blood (50 µL) was drawn from the tail veil before 4OHT application and 3 days after the last 4OHT application and subjected to FACS analysis. (B). Reporter ΔhCD4 expression in circulating murine CD4+T cells using FACS analysis. Representative flow plots of blood obtained before 5 doses of 4OHT, after 5 doses of 4OHT, before 3 doses of 4OHT, and after 3 doses of 4OHT. (C). Cells with *Socs1* deletion (resulting in ΔhCD4 expression) in percentage of total circulating murine CD4+ T cells in transgenic *Socs1fl/wt Cd4CreER^{T2}+/-* mice. Data are presented as mean ± SD. Symbols in bar graphs represent individual mouse. *P<0.05

3.3.Long-term low concentration OXA is suitable for inducing and maintaining an inflamed skin

In this experiment, we tried to avoid the damaging effect on murine skin of a high concentration of OXA thereby reducing mouse distress/scratching, and optimized the OXA dose to induce a sustainable skin inflammation in skin (no wounding from scratching). 1.5% OXA was used for sensitization on the shaved abdomen on day 1. 0.5% OXA was used for challenge on the shaved left flank seven days later. Then 4OHT on the shaved left flank was used for three consecutive days to knockout *Socs1*. After that, repeated dosing was performed on the shaved left flank until day 56, with each dose at least 48h apart. Skin samples were collected two weeks after the last dose. (**Figure 3**)

After 4OHT, *Socs1fl/fl Cd4CreER^{T2}+/-* mouse are abbreviated as S--C (*Socs1-/- Cd4CreER^{T2}+/-*) mouse, and the *Socs1wt/wt Cd4CreER^{T2}+/-* mouse as the C (control) mouse.

During the study, none of the mice showed open wounds or persistent severe pruritus on the skin. The treated skin had obvious inflammation symptoms like erythema, scaling, and skin roughness. The S--C group had the strongest skin inflammation among three groups. Meanwhile, the shaved right flank with vehicle had no inflammation phenotype in each group of mice. (**Supplementary Figure 1**) Flow cytometry data from weekly peripheral blood during the experiment also showed no significant abnormalities in the immune system of the mice.

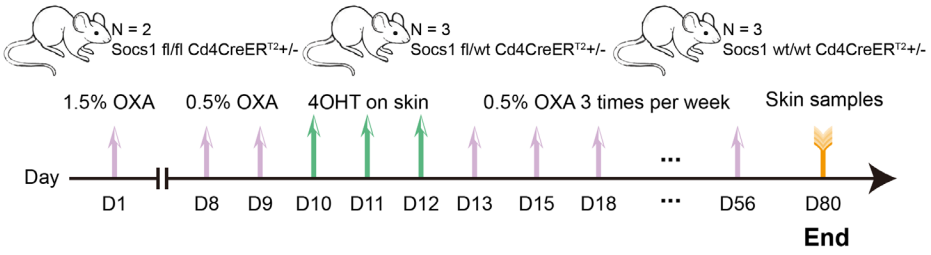

Figure 3. Scheme of the experiment performed using the conditional *Socs1* knockout mouse model. OXA also on the skin

3.4.*Socs1* was successfully deleted in circulating and skin-homing CD4+ T cells of the transgenic mouse.

To confirm the *Socs1* deletion in circulating CD4+ T cells, we measured the reporter ΔhCD4 in peripheral blood by flow cytometry. The results showed that *Socs1* was deleted in circulating CD4+ T cells in S--C and S+-C groups after the 4OHT application on the skin. In C group, no *Socs1* deletion was detected. (**Figure 4A**) The *Socs1* deletion level in circulating CD4+ T cells from S--C and S+-C groups was long-lasting during the experiment. (**Figure 4B**) It illustrates the stable knockout effect of our new transgenic mouse strain.

The *Socs1* deletion in skin resident CD4+ T cells, showed by reporter gene ΔhCD4, was confirmed by immunohistochemical staining. The results showed that there were ΔhCD4 positive cells in S--C and S+-C groups after the 4OHT application on the skin. The number of ΔhCD4 positive cells was most pronounced in the S--C group although this was not firmly quantifiable with only two mice in this genotype group (see M&M section). In the control group, no *Socs1* deletion was detected. (**Figure 4C**) Among transgenic mice (S- -C and S+-C), there is statistically significant more *Socs1* knockout in the dermis of the treated skin comparison with that of the untreated skin. **(Figure 4D)**

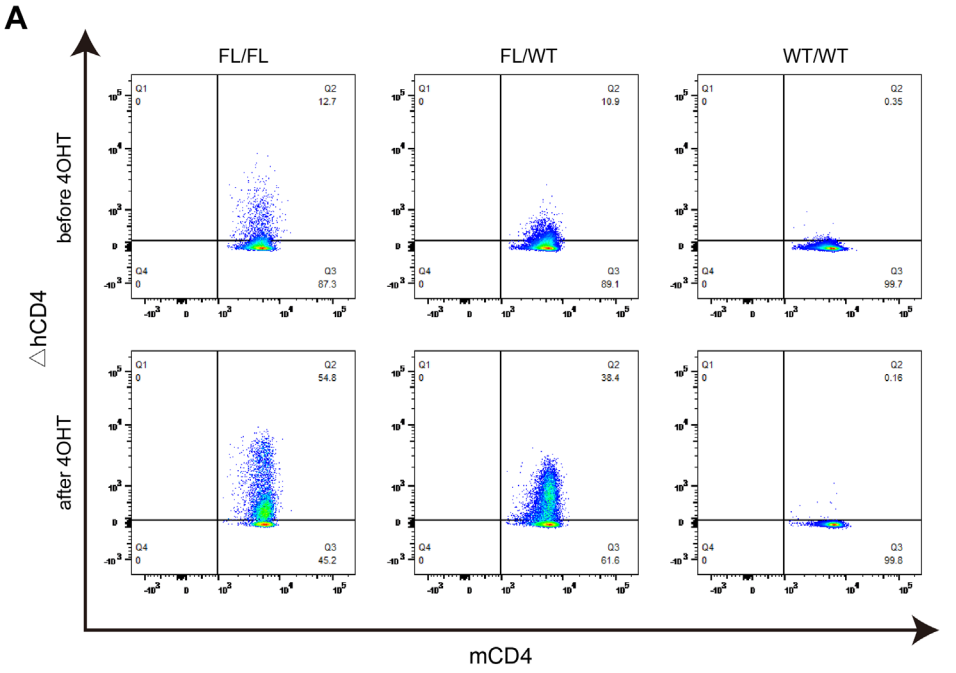
A
FL/FL
FL/WT
WT/WT
before 4OHT
after 4OHT
△hCD4
mCD4
Q1
Q2
Q3
Q4
12.7
87.3
10.9
89.1
0.35
99.7
54.8
45.2
38.4
61.6
0.16
99.8

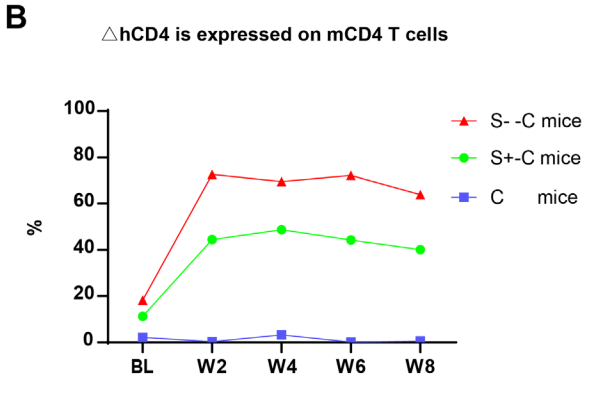
B
△hCD4 is expressed on mCD4 T cells
%
100
80
60
40
20
0
BL
W2
W4
W6
W8
S- -C mice
S+-C mice
C mice

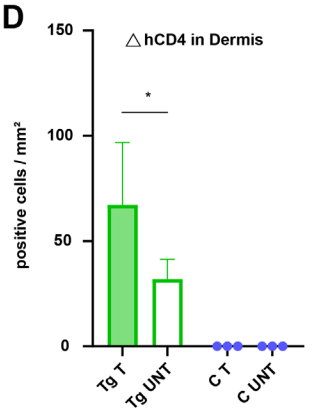
D
△hCD4 in Dermis
positive cells / mm²
150
100
50
0
*
Tg T
Tg UNT
C T
C UNT

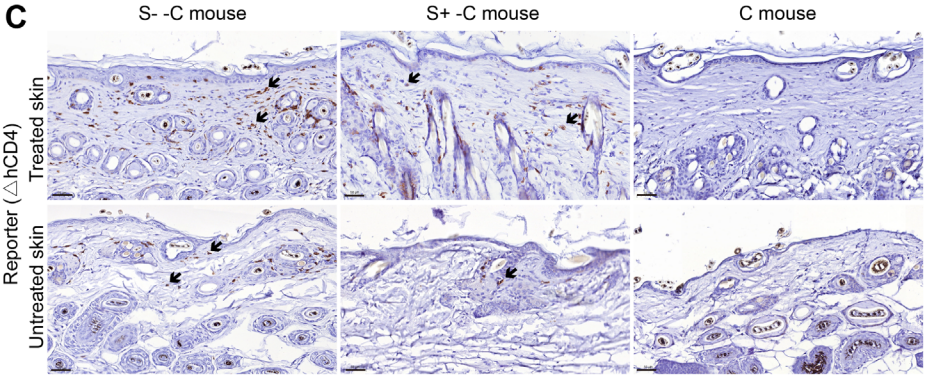
C
S- -C mouse
S+ -C mouse
C mouse
Reporter (△hCD4)
Treated skin
Untreated skin

Figure 4. *Socs1* can successfully be deleted in circulating and skin-homing CD4+ T cells of the transgenic mouse by 4OH Tamoxifen application. (A). Circulating murine CD4+ T cells were analyzed for ΔhCD4 expression by flow cytometry to show *Socs1* deletion. Representative flow cytometry plots for before and after 4OHT application in FL/FL (*Socs1fl/fl Cd4CreER^{T2}+/-*), FL/WT (*Socs1fl/wt Cd4CreER^{T2}+/-*) and WT/WT (*Socs1wt/wt Cd4CreER^{T2}+/-*) mice. (B). *Socs1* deletion (measured as ΔhCD4 expression) in cells as a percentage of total circulating murine CD4+ T cells in S--C mice, S+-C mice and C mice during the whole experiment. Each plot is the mean value of mice with the same genotype. BL is baseline. W is week. S--C is *Socs1 -/- Cd4CreER^{T2}+/-*; S+-C is *Socs1-/wt Cd4CreER^{T2}+/-*; C is control group. (C). Immunohistochemical staining of ΔhCD4+ To show Socs1 deletion in cells in the murine skin. Representative photomicrographs of ΔhCD4 expression in treated and untreated skin from S--C mice, S+-C mice and C mice respectively. Black arrows: ΔhCD4 positive cells. Scale bar: 50 μm. S--C is *Socs1 -/- Cd4CreER^{T2}+/-*; S+-C is *Socs1-/wt Cd4CreER^{T2}+/-*; C is control group. (D). Quantification of ΔhCD4 positive cells in dermis of transgenic group (S--C mice, S+-C mice) and C mice. Data are presented as mean ± SD (N= 5 in Tg and N=3 in C). * $P < 0.05$, ** $P < 0.01$, *** $P < 0.001$. Tg is transgenic group, C is control group. S--C is *Socs1 -/- Cd4CreER^{T2}+/-*; *S+-C is Socs1-/wt Cd4CreER^{T2}+/-*.

3.5.Augmented inflammation in *Socs1* knockout transgenic mouse

We performed immuno-histopathology on skin biopsies to characterize the effect of *Socs1* deletion in our transgenic mice with chronic skin inflammation. The H&E staining of the skin sections from the treated flanks of three group mice showed the thickness of the epidermis of treated skin was most pronounced in the S--C group although this could not be well evaluated statistically with only two mice. (**Figure 5A**) The epidermal layers were assessed and quantitated in the transgenic group (S- -C and S+-C) and the C groups. The transgenic group had thicker epidermis of treated skin compared with the control group. (**Figure 5B**)

The inflammatory response was confirmed by immunohistochemical staining of CD3+, CD4+and CD8+ of the skin sections of the mice. The numbers of inflammatory cells were most pronounced in the S--C group although this was again not well quantitated with only two mice in this genotype group. Quantifying positive staining cells showed a statistically significant increase in CD3+, CD4+ and CD8+ cells in the dermis of the treated skin of mice in the transgenic group (S- -C and S+-C) in comparison with the C group. In the untreated skin dermis, the numbers of CD3+ and CD4+ in the transgenic group (S- - C and S+-C) also showed a statistically significant increase comparison with the C group. The numbers of CD8+ in the untreated skin dermis of mice in the transgenic group (S- - C and S+-C) was not different from that in the untreated skin dermis of mice in the C group. (**Figure 5B**)

In the transgenic group (S- - C and S+-C), there was statistically significantly more CD3+

and CD4+ staining in the dermis of the treated flank than that of untreated skin. For CD8, the dermis of treated and untreated flank was not different. Moreover, there was no difference in inflammatory cells in the treated and non-treated skin of the control group. The CD3+ and CD4+ were more abundant in the skin of the transgenic group compared to the control group, suggesting that *Socs1* deletion can promote skin inflammation. **(Figure 5B)**

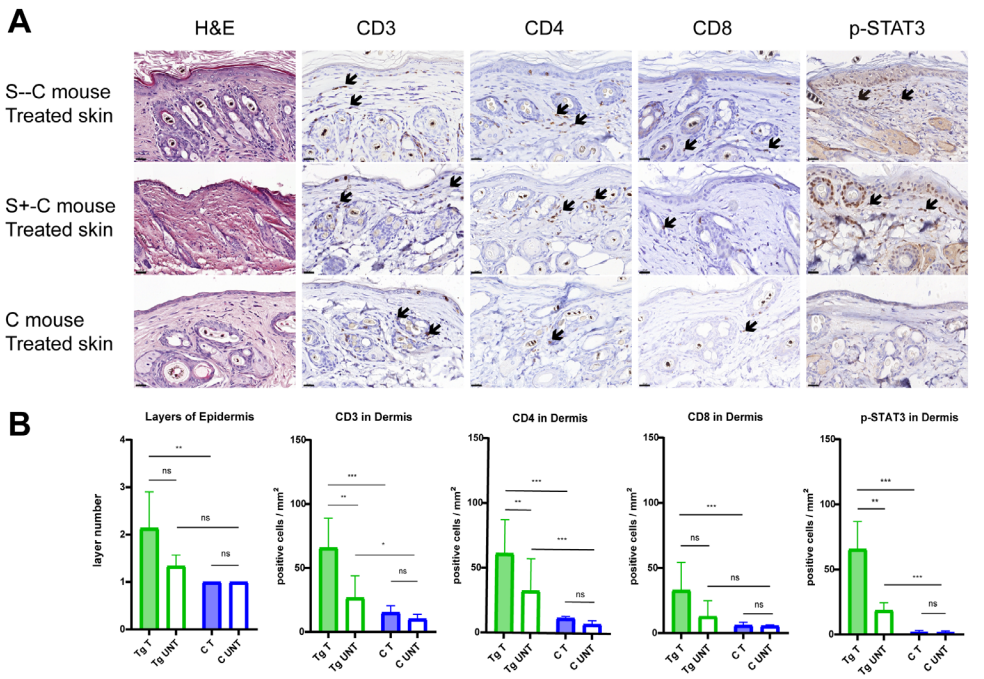

Figure 5. Detailed histological analyses using H&E and immunohistochemical staining of murine skin sections. (A). Representative photomicrographs of treated skin from S--C mice, S+-C mice and C mice respectively. Black arrows: positive cells. Scale bar: 50 µm. S--C is *Socs1 -/- Cd4CreER*^{T2}+/-; S+-C is *Socs1-/wt Cd4CreER*^{T2}+/-; C is control group. (B). Quantification of the layers of epidermis, inflammatory cells and p-STAT3 positive cells in the dermis from transgenic group (S--C mice, S+-C mice) and C mice. Data are presented as mean ± SD. (N=5 and 3 in each group). * $P < 0.05$, ** $P < 0.01$, *** $P < 0.001$. Tg is transgenic group, C is control group. S--C is *Socs1 -/- Cd4CreER*^{T2}+/-; S+-C is *Socs1-/wt Cd4CreER*^{T2}+/-.

3.6.phospho-STAT3 (p-STAT3) expression in CD4+ T cells of transgenic *Socs1* knockout mice

To further characterize the role of *SOCS1* in the JAK-STAT signaling pathway, we examined the p-STAT3 expression in skin biopsies by immunohistochemical staining. STAT3 activation

was confirmed by immunohistochemical staining of p-STAT3 of the skin sections of the three groups of mice. (**Figure 5A**) The number of p-STAT3 positive cells was most pronounced in S--C mice although, again, this could not be well statistically evaluated with only two mice in this genotype group. Quantifying positive staining cells showed a statistically significant increase in number of p-STAT3 cells in the dermis of treated skin of mice in the transgenic group (S--C and S+-C) compared to the treated skin in C group. The amount of p-STAT3 positive cells in the untreated skin dermis of mice in the transgenic group (S--C and S+-C) also showed a statistically significant increase comparison with the C group. (**Figure 5B**)

In the transgenic group (S--C and S+-C), there were statistically significantly more p-STAT3 positive cells in the dermis of the treated flank compared to untreated skin. In contrast, there was remarkably no difference in p-STAT3 positive cells in the treated and non-treated skin of the Control group. (**Figure 5B**)

4.Discussion

This study is, to our best knowledge, the first that specifically focused on the function of genes involved in mycosis fungoides by targeted deletion in skin homing T-cells in combination with chronic inflammation using GEMMs.

To overcome the prenatal lethality of *Socs1* deficiency during development (13, 15, 16) and frame the *Socs1* deletion in CD4+ T cells specifically, thus enabling studies on the contribution of *Socs1* in the pathogenesis of mycosis fungoides, we used cross breeding of two existing transgenic mouse strains (*Socs1flox* and *Cd4CreER*^{T2}). This resulted in the expected genotypes, however, a sub-Mendelian low yield of *Socs1 fl/fl Cd4CreER*^{T2} pups was observed probably due to leakage of *Cre*.

We first show that application of 4OH tamoxifen on the skin of these transgenes effectively targets local *Cd4-Cre* T-cells and that a decrease from five to three 4OHT applications statistically significantly reduces the systemic effect on circulating T cells. There are several ways to apply Tamoxifen to activate Cre-loxP systems depending on various research aims. (17, 18) A majority of studies use intraperitoneal injections as well as oral gavage to get the potent systemic effect and the commonly used dosing is usually on 5 consecutive days (Tamoxifen 1mg/per day/per mouse, 4OHT 1mg/per day/per mouse). (19, 20) Since our study's target tissue are immune cells in the skin, we reasoned that topical administration would be preferable. Five doses and three doses of 4OHT topical application have been applied in a few studies all targeting keratinocytes while studies that distinguish the systemic effect from topical application are not available. (21-23) This study shows that

Cre can be activated to knock out *Socs1* in skin resident T-cells in a way that minimized the systemic effect of 4OHT on other circulating immune cells animals.

Next, we determined optimal conditions for simulation of a chronic dermatosis without damaging skin integrity. Inflammation can exhibit tumor-promoting effects even at the early phases of neoplastic growth and is characteristic for early-stage mycosis fungoides. (11, 24) In addition, it can promote the progression of precancerous neoplasia into full-blown malignancies. (25-28) In our study we induced chronic skin inflammation using Oxazolone to add the possible tumor-promoting effects in the transgenic mouse, but also to attract T-cells to the skin before application of 4OHT to increase the probability to hit the target cells. In previous studies, mouse ears were mostly used as a model for OXA-induced long-term chronic skin inflammation. (29-32) Commonly used concentrations of oxazolone are 1.5% - 2% in the sensitization phase and 0.4-1% in the challenging phase. The maximum duration of repeated use of OXA for long-term chronic inflammation studies was 3 weeks. (29, 33) In our study, low concentrations of OXA were repeatedly applied 3 times per week on the flank of mice until 8 weeks (Day 56). The mice showed typical inflammatory reactions such as erythema, scaling, and skin roughness. However, open wounds, ulcers, and long-lasting, intense scratching were successfully avoided. It is important in this study not only to exclude a specific tumor promotion from severe skin trauma but also for the well-being of the experimental animals. (24)

Our immune-histochemical analyses additionally confirmed Socs1 was deleted successfully in CD4+ T cells in the skin of transgenic mice upon treatment with 4OHT. Expression of the ΔhCD4 reporter (surrogate marker for *Socs1* deletion) in CD4+ T cells was primarily observed in the left, treated flank of transgenic *Socs1 fl/wt Cd4CreER*^{T2}+/- mice.

The thickness of epidermis and the immune-histochemistry results of CD3+, CD4+ and CD8+ confirmed that *Socs1* deletion augment the skin inflammation in the dermis of *Socs1 flox Cd4CreER*^{T2} transgenic mouse specifically. Moreover, the numbers of CD3+ and CD4+ cells infiltration in the dermis of treated flanks are statistically higher than that of untreated flanks. We collected the skin samples two weeks after the last OXA administration to assess prolonged inflammation. The clinically observable skin inflammation in our mouse model was alleviated over this time interval but could still be observed. Histology results showed that the inflammatory response in the treated skin of *Socs1*-deleted mouse group was still obvious. *Socs1* deletion in CD4+ T cells increases prolonged skin inflammation. Consistent with our observation, previous research indicates *Socs1* loss relates to inflammation-associated tumor development. The germline loss-of-function mutations in the *SOCS1* gene were associated with early onset autoimmune manifestations in a whole exome/genome sequencing study. (34) *Socs1* deletion in murine dendritic cells from induce stronger

immune responses both *in vitro* and *in vivo*. (35) Finally, we determined whether JAK-STAT signaling was enhanced as a result of *Socs1* deletion by measuring p-STAT3. Our results indicated more activation of *STAT3* in *Socs1* knockout compared to wt CD4+T cells in the dermis.

These results are in line with the previous findings showing that the phosphorylation of STAT3 was elevated in splenic T cells of *Socs1*-deficient mice relative to those of wild-type mice. (36) Downregulation of *Socs1* in rat hepatocytes activates JAK2-STAT3 in an animal model of sepsis. (37) Aberrant activation of the JAK-STAT3 pathway due to down-regulation of *SOCS1* by miR-155 is observed in solid tumors, such as breast cancer and laryngeal carcinoma. (38, 39) In melanoma, melanoma cell-secreted exosomal miR-155 suppressed *SOCS1* expression in CAFs. Suppression of *SOCS1* in CAFs activated the JAK2-STAT3 signaling pathway. (40) In CTCL, especially in advanced stages, constitutive expression of STAT3 has been consistently observed. IL-21 leads to more specific activation of *STAT3* in Sézary Syndrome, which in turn directly upregulates IL-21 expression leading to an enhanced IL-21 autocrine signaling loop. (41) Constitutively active STAT3 can increase survival and resistance to apoptosis in malignant T cells by promoting bcl-2 expression. (42)

In contrast to tumors, reduced miR-155 expression, upregulated *SOCS1* expression, and significantly reduced STAT3 phosphorylation were found in CD4+ T cells in autoimmune SLE. IL21 expression was upregulated but induced STAT3 phosphorylation was inhibited. STAT3 phosphorylation was increased after miR-155 overexpression. (43) *SOCS1* is necessary for stability and suppressor functions of Treg cells: *SOCS1* protects Treg cells from harmful effects of inflammatory cytokines. STAT3 overactivation in *Socs1*-deficient Treg cells promotes the conversion of Treg cells to Th17-like cells. (8) Based on these and other data (4, 5), a model explaining the role of *SOCS1* in aberrant JAK-STAT signaling in MF was postulated.

We also observed keratinocytes with more activated STAT3 in the epidermis of *Socs1* knockout transgenic mice. STAT3 activation is associated with aberrant keratinocytes differentiation and hyperproliferation. (44) STAT3 plays a major role in epithelial carcinogenesis. This has been demonstrated in previous studies on wounds healing, UVB-induced skin carcinogenesis and keratinocytes-specific Stat3-deficient mice. (45, 46)

There are some limitations in this study. The first is that there is obvious inflammatory responses and STAT3 activation. However, this model has not yet shown significant skin tumors. The second one is the small size of samples. In the future, we will use the established model to conduct studies with larger sample sizes and longer-term experiments for carcinogenesis.

In sum, we developed and optimized an autochthonous murine model permitting selective knockout of *Socs1* in skin infiltrating CD4+ T-cells. Our results show that *Socs1* deletion specifically in CD4+ T cells can promote persisting inflammation in the skin of mice and activate STAT3. This paves the way for more elaborate experiments, e. g. extending the time of treatment, knockout of other genes to gain insight in the genesis of CTCL.

References

1. Willemze R, Jaffe ES, Burg G, Cerroni L, Berti E, Swerdlow SH, et al. WHO-EORTC classification for cutaneous lymphomas. Blood (2005) 105(10):3768-85. doi: 10.1182/blood-2004-09-3502
2. Willemze R, Cerroni L, Kempf W, Berti E, Facchetti F, Swerdlow SH, et al. The 2018 update of the WHO-EORTC classification for primary cutaneous lymphomas. Blood (2019) 33(16):1703-14. doi: 10.1182/blood-2018-11-881268
3. Kempf W, Mitteldorf C. Cutaneous T-cell lymphomas-An update 2021. Hematol Oncol (2021) Suppl 1:46-51. doi: 10.1002/hon.2850
4. Tensen CP, Quint KD, Vermeer MH. Genetic and epigenetic insights into cutaneous T-cell lymphoma. Blood (2022) 139(1):15-33. doi: 10.1182/blood.2019004256
5. Bastidas Torres AN, Cats D, Mei H, Szuhai K, Willemze R, Vermeer MH, et al. Genomic analysis reveals recurrent deletion of JAK-STAT signaling inhibitors HNRNPK and SOCS1 in mycosis fungoides. Genes Chromosomes Cancer (2018) 57(12):653-64. doi: 10.1002/gcc.22679
6. Tamiya T, Kashiwagi I, Takahashi R, Yasukawa H, Yoshimura A. Suppressors of cytokine signaling (SOCS) proteins and JAK/STAT pathways: regulation of T-cell inflammation by SOCS1 and SOCS3. Arterioscler Thromb Vasc Biol (2011) 31(5):980-5. doi: 10.1161/ATVBAHA.110.207464
7. Tanaka K, Ichiyama K, Hashimoto M, Yoshida H, Takimoto T, Takaesu G, et al. Loss of suppressor of cytokine signaling 1 in helper T cells leads to defective Th17 differentiation by enhancing antagonistic effects of IFN-gamma on STAT3 and Smads. J Immunol (2008) 180(6):3746-56. doi: 10.4049/jimmunol.180.6.3746
8. Takahashi R, Nishimoto S, Muto G, Sekiya T, Tamiya T, Kimura A, et al. SOCS1 is essential for regulatory T cell functions by preventing loss of Foxp3 expression as well as IFN-(34) and IL-17A production. J Exp Med (2011) 208(10):2055-67. doi: 10.1084/jem.20110428
9. Inagaki-Ohara K, Kondo T, Ito M, Yoshimura A. SOCS, inflammation, and cancer. JAKSTAT (2013) 2(3):e24053. doi: 10.4161/jkst.24053
10. Krejsgaard T, Lindahl LM, Mongan NP, Wasik MA, Litvinov IV, Iversen L, et al. Malignant inflammation in cutaneous T-cell lymphoma-a hostile takeover. Semin Immunopathol. (2017) 39(3):269-82. doi: 10.1007/s00281-016-0594-9
11. Hanahan D, Weinberg RA. Hallmarks of cancer: the next generation. Cell (2011) 144(5):646-74. doi: 10.1016/j.cell.2011.02.013
12. Gill RPK, Gantchev J, Martinez Villarreal A, Ramchatesingh B, Netchiporouk E, Akilov OE, et al. Understanding Cell Lines, Patient-Derived Xenograft and Genetically Engineered Mouse Models Used to Study Cutaneous T-Cell Lymphoma. Cells (2022) 11(4): 593 doi: 10.3390/cells11040593
13. Hanada T, Yoshida H, Kato S, Tanaka K, Masutani K, Tsukada J, et al. Suppressor of cytokine signaling 1 is essential for suppressing dendritic cell activation and systemic autoimmunity. Immunonity (2003) 19(3):437-50. doi: 10.1016/s1074-7613(03)00240-1
14. Aghajani K, Keerthivasan S, Yu Y, Gounari F. Generation of CD4CreER(T2) transgenic mice to study development of peripheral CD4-T-cells. Genesis (2012) 50(12):908-13. doi: 10.1002/dvg.22052
15. Marine JC, Topham DJ, McKay C, Wang D, Parganas E, Stravopodis D, et al. SOCS1 deficiency causes a lymphocyte-dependent perinatal lethality. cell (1999) 98(5):609-16. doi: 10.1016/s0092-

8674(00)80048-3
16. Feil S, Valtcheva N, Feil R. Inducible Cre mice. Methods Mol Biol (2009) 530:343-63. doi: 10.1007/978-1-59745-471-1_18
17. Gunschmann C, Chiticariu E, Garg B, Hiz MM, Mostmans Y, Wehner M, et al. Transgenic mouse technology in skin biology: inducible gene knockout in mice. J Invest Dermatol (2014) 134(7):1-4. doi: 10.1038/jid.2014.213
18. Faralli JA, Filla MS, Peters DM. Effect of alphavbeta3 Integrin Expression and Activity on Intraocular Pressure. Invest Ophthalmol Vis Sci (2019) 60(5):1776-88. doi: 10.1167/iovs.18-26038
19. Heger K, Seidler B, Vahl JC, Schwartz C, Kober M, Klein S, et al. CreER(T2) expression from within the c-Kit gene locus allows efficient inducible gene targeting in and ablation of mast cells. Eur J Immunol. (2014) 44(1):296-306. doi: 10.1002/eji.201343731
20. Chong MM, Cornish AL, Darwiche R, Stanley EG, Purton JF, Godfrey DI, et al. Suppressor of cytokine signaling-1 is a critical regulator of interleukin-7-dependent CD8+ T cell differentiation. 2003 (Immunity) 18(4):475-87. doi: 10.1016/s1074-7613(03)00078-5
21. Kataoka K, Kim DJ, Carbajal S, Clifford JL, DiGiovanni J. Stage-specific disruption of Stat3 demonstrates a direct requirement during both the initiation and promotion stages of mouse skin tumorigenesis. Carcinogenesis (2008) 29(6):1108-14. doi: 10.1093/carcin/bgn061
22. Stratis A, Pasparakis M, Markur D, Knaup R, Pofahl R, Metzger D, et al. Localized inflammatory skin disease following inducible ablation of I kappa B kinase 2 in murine epidermis. J Invest Dermatol (2006) 126(3):614-20. doi: 10.1038/sj.jid.5700092
23. Lopez-Rovira T, Silva-Vargas V, Watt FM. Different consequences of beta1 integrin deletion in neonatal and adult mouse epidermis reveal a context-dependent role of integrins in regulating proliferation, differentiation, and intercellular communication. J Invest Dermatol (2005) 125(6):1215-27. doi: 10.1111/j.0022-202X.2005. 23956.x
24. Schafer M, Werner S. Cancer as an overhealing wound: an old hypothesis revisited. Nat Rev Mol Cell Biol. (2008) 9(8):628-38. doi: 10.1038/nrm2455
25. DeNardo DG, Andreu P, Coussens LM. Interactions between lymphocytes and myeloid cells regulate pro-versus anti-tumor immunity. Cancer Metastasis Rev (2010) 29(2):309-16. doi: 10.1007/s10555-010-9223-6
26. Qian BZ, Pollard JW. Macrophage diversity enhances tumor progression and metastasis. Cell (2010) 141(1):39-51. doi: 10.1016/j.cell.2010.03.014
27. Grivennikov SI, Greten FR, Karin M. Immunity, inflammation, and cancer. Cell (2010) 140(6):883-99. doi: 10.1016/j.cell.2010.01.025
28. de Visser KE, Eichten A, Coussens LM. Paradoxical roles of the immune system during cancer development. Nat Rev Cancer (2006) 6(1):24-37. doi: 10.1038/nm.3394
29. Bertelsen T, Iversen L, Riis JL, Arthur JS, Bibby BM, Kragballe K, et al. The role of mitogen- and stress-activated protein kinase 1 and 2 in chronic skin inflammation in mice. Exp Dermatol (2011) 20(2):140-5. doi: 10.1111/j.1600-0625.2010.01153.x
30. Webb EF, Tzimas MN, Newsholme SJ, Griswold DE. Intralesional cytokines in chronic oxazolone-induced contact sensitivity suggest roles for tumor necrosis factor alpha and interleukin-4. J Invest Dermatol (1998) 111(1):86-92. doi: 10.1046/j.1523-1747.1998.00239.x.

31. Wang X, Fujita M, Prado R, Tousson A, Hsu HC, Schottelius A, et al. Visualizing CD4 T-cell migration into inflamed skin and its inhibition by CCR4/CCR10 blockades using in vivo imaging model. Br J Dermatol (2010) 162(3):487-96. doi: 10.1111/j.1365-2133.2009.09552.x

32. Liu B, Escalera J, Balakrishna S, Fan L, Caceres AI, Robinson E, et al. TRPA1 controls inflammation and pruritogen responses in allergic contact dermatitis. FASEB J (2013) 27(9):3549-63. doi: 10.1096/fj.13-229948

33. Ivetic Tkalcevic V, Cuzic S, Kramaric MD, Parnham MJ, Erakovic Haber V. Topical azithromycin and clarithromycin inhibit acute and chronic skin inflammation in sensitized mice, with apparent selectivity for Th2-mediated processes in delayed-type hypersensitivity. Inflammation (2012) 35(1):192-205. doi: 10.1007/s10753-011-9305-9

34. Hadjadj J, Castro CN, Tusseau M, Stolzenberg MC, Mazerolles F, Aladjidi N, et al. Early-onset autoimmunity associated with SOCS1 haploinsufficiency. Nat Commun (2020) 11(1):5341. doi: 10.1038/s41467-020-18925-4

35. Hanada T, Tanaka K, Matsumura Y, Yamauchi M, Nishinakamura H, Aburatani H, et al. Induction of hyper Th1 cell-type immune responses by dendritic cells lacking the suppressor of cytokine signaling-1 gene. J Immunol (2005) 174(7):4325-32. doi: 10.4049/jimmunol.174.7.4325

36. Guo H, Li R, Wang M, Hou Y, Liu S, Peng T, et al. Multiomics Analysis Identifies SOCS1 as Restraining T Cell Activation and Preventing Graft-Versus-Host Disease. Adv Sci (Weinh) (2022) e2200978. doi: 10.1002/advs.202200978

37. Yuan FH, Chen YL, Zhao Y, Liu ZM, Nan CC, Zheng BL, et al. MicroRNA-30a inhibits the liver cell proliferation and promotes cell apoptosis through the JAK/STAT signaling pathway by targeting SOCS-1 in rats with sepsis. J Cell Physiol (2019) 234(10):17839-53. doi: 10.1002/jcp.28410

38. Zhao XD, Zhang W, Liang HJ, Ji WY. Overexpression of miR -155 promotes proliferation and invasion of human laryngeal squamous cell carcinoma via targeting SOCS1 and STAT3. PLoS One (2013) 8(2):e56395. doi: 10.1371/journal.pone.0056395

39. Jiang S, Zhang HW, Lu MH, He XH, Li Y, Gu H, et al. MicroRNA-155 functions as an OncomiR in breast cancer by targeting the suppressor of cytokine signaling 1 gene. Cancer Res (2010) 70(8):3119-27. doi: 10.1158/0008-5472.CAN-09-4250

40. Zhou X, Yan T, Huang C, Xu Z, Wang L, Jiang E, et al. Melanoma cell-secreted exosomal miR-155-5p induce proangiogenic switch of cancer-associated fibroblasts via SOCS1/JAK2/STAT3 signaling pathway. J Exp Clin Cancer Res (2018) 37(1):242. doi: https://doi.org/10.1186/s13046-018-0911-3

41. van der Fits L, Out-Luiting JJ, van Leeuwen MA, Samsom JN, Willemze R, Tensen CP, et al. Autocrine IL-21 stimulation is involved in the maintenance of constitutive STAT3 activation in Sezary syndrome. J Invest Dermatol (2012) 132(2):440-7. doi: 10.1038/jid.2011.293

42. Nielsen M, Kaestel CG, Eriksen KW, Woetmann A, Stokkedal T, Kaltoft K, et al. Inhibition of constitutively activated Stat3 correlates with altered Bcl-2/Bax expression and induction of apoptosis in mycosis fungoides tumor cells. Leukemia (1999) 13(5):735-8. doi: 10.1038/sj.leu.2401415.

43. Rasmussen TK, Andersen T, Bak RO, Yiu G, Sorensen CM, Stengaard-Pedersen K, et al. Overexpression of microRNA-155 increases IL-21 mediated STAT3 signaling and IL-21 production in systemic lupus erythematosus. Arthritis Res Ther (2015) 17:154. doi: 10.1186/s13075-015-0660-z.

44. Sano S, Chan KS, Carbajal S, Clifford J, Peavey M, Kiguchi K, et al. Stat3 links activated keratinocytes and immunocytes required for development of psoriasis in a novel transgenic mouse

model. Nat Med(2005) 11(1):43-9. doi: 10.1038/nm1162.

45. Kim DJ, Angel JM, Sano S, DiGiovanni J. Constitutive activation and targeted disruption of signal transducer and activator of transcription 3 (Stat3) in mouse epidermis reveal its critical role in UVB-induced skin carcinogenesis. Oncogene (2009) 28(7):950-60. doi: 10.1038/onc.2008.453.

46. Kim DJ, Kataoka K, Rao D, Kiguchi K, Cotsarelis G, Digiovanni J. Targeted disruption of stat3 reveals a major role for follicular stem cells in skin tumor initiation. Cancer Res (2009) 69(19):7587-94. doi:10.1158/0008-5472.CAN-09-1180

Supplementary Information

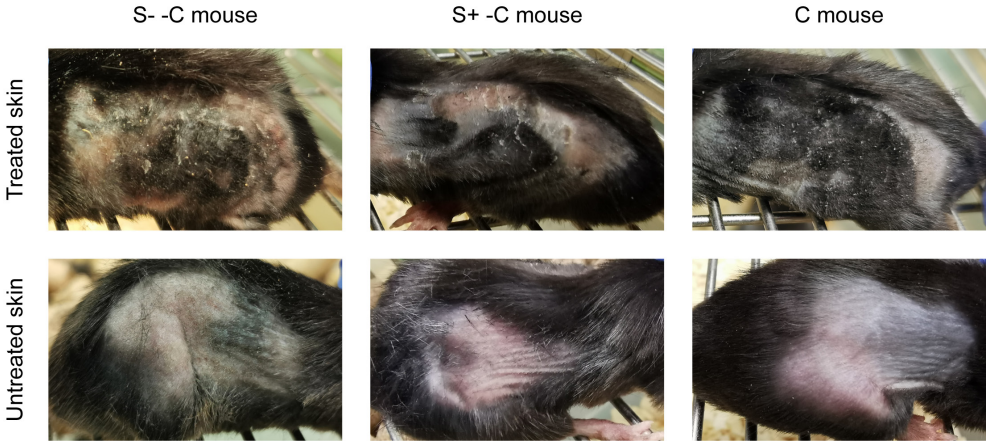

Supplementary Figure 1. Augmented skin inflammation induced by repeated low concentration oxazolone. Representative images of the shave treated skin and untreated skin of S--C mice, S+-C mice and C mice on day 35 during experiment. S--C is *Socs1 -/- Cd4CreER*^{T2}+/-; S+-C is *Socs1-/wt Cd4CreER*^{T2}+/-; C is *Socs1wt/wt Cd4CreER*^{T2}+/-.

3

Socs1-knockout in skin-resident CD4 T cells in a protracted contact-allergic reaction results in an autonomous skin inflammation with features of early-stage mycosis fungoides

Yixin Luo[1], Maarten H. Vermeer[1], Sanne de Haan[1], Priscilla Kinderman[3], Frank R. de Gruijl[1], Thorbald van Hall[2], and Cornelis P. Tensen[1]
1.Department of Dermatology, Leiden University Medical Center, Leiden, The Netherlands
2.Department of Medical Oncology, Oncode Institute, Leiden University Medical Center, Leiden, The Netherlands
3.Department of Gastroenterology and Hepatology, Leiden University Medical Center, Leiden, The Netherlands
Biochem Biophys Rep. 2023 Aug: 35:101535. doi: 10.1016/j.bbrep.2023.101535.

Abstract:

Recent detailed genomic analysis of mycosis fungoides (MF) identified suppressor of cytokine signaling 1 (*SOCS1*), an inhibitor of JAK-STAT signaling, as one of the frequently deleted tumor suppressors in MF, and one-copy deletion of *SOCS1* was confirmed in early-stage MF lesions. To better understand the functional role of *SOCS1* in the genesis of MF, we used a genetically engineered mouse model emulating heterozygous *SOCS1* loss in skin resident CD4+ T cells. In these mice an experimentally induced contact-allergic reaction was maintained for 20 weeks. Ten weeks after discontinuing contact-allergic challenges, only the skin with locally one-copy deletion of *Socs1* in CD4+ T cells still showed high numbers of CD3+/CD4+ *Socs1* k.o. cells in the dermis ($p < 0.0001$) with prevalent STAT3 activation ($p < 0.001$). And in one out of 9 mice, this had progressed to far more dramatic increases, including the thickened epidermis, and with an explosive growth of *Socs1* k.o. T cells in circulation; indicative of a cutaneous lymphoma. Hence, we show that *Socs1* mono-allelic loss in CD4+ T cells locally in a protractedly inflamed skin results in an autonomous skin inflammation with features of early-stage MF.

Key words: CD4+ T cells; Inflammation; Mycosis fungoides; *Socs1*; Transgenic mouse.

1 Introduction

Mycosis fungoides (MF) is characterized by the proliferation of malignant mature skin resident CD4+ T cells (1-3). Early-stage MF often presents with limited skin lesions such as red, scaly patches or plaques and with the features of a substantial infiltration of reactive immune cells and a small group of malignant T cells (4). In advanced stage, more infiltrated plaques, generalized erythroderma or tumors can develop with extracutaneous involvement (blood, lymph nodes, and other visceral organs) (2, 3, 4). The pathogenesis of MF remains elusive. Genetic investigation of advanced MF indicates involvement of the NF-kB, TCR, and JAK-STAT pathways (5, 6). *SOCS1* is a member of the suppressor of cytokine signaling (SOCS) family and inhibits immune-associated inflammatory responses mediated by the JAK-STAT pathway and controls cancer-related inflammation (7, 8). Recent research of our group has identified *SOCS1* as one of the frequently deleted tumor suppressors in MF and deletions have been detected in early-stage of MF (9).

Genetically engineered mouse models (GEMMs) have been established as versatile tools to study the function of tumor suppressors and oncogenes, facilitated by the development of advanced genetic techniques. In contrast to models inoculated with patient-derived cancer cells (xenografts), GEMMs grow de novo tumors in an immune-competent natural microenvironment as an experimentally accessible model of the pathogenesis (10, 11). Thus, GEMMs can be used for the validation of candidate oncogenes, evaluation of treatment and dissection of the role of the tumor microenvironment. In mycosis fungoides, most *in vivo* models are xenografts and a pathogenic model of early-stage MF is lacking (12,13). Early-stage MF skin lesions are densely infiltrated with reactive immune cells and a small group of malignant T cells. A crucial step in the progression of MF from an early, indolent stage to an advanced illness is the change in the inflammatory environment associated with the tumor (4, 14). We created and improved an autochthonous mouse model that allows selective *Socs1* deletion in skin-infiltrating CD4+ T cells (15), based on the observation that *Socs1* is one of the most prevalent genetic changes in MF. The mouse model has the CRE-loxP conditional knockout system controlled by the CD4 promoter. The deletion of *Socs1* in CD4+ T cells can be controlled in time and location by using 4-hydroxy-tamoxifen (4OHT) to activate CRE (15).

This study is a follow-up and extension of our previous small exploratory study (15), to firm up the causal role of a *SOCS1* allelic loss in the development of MF. Here, we used larger group sizes (8-9) to strengthen statistics and extended the duration of the experiment to establish more firmly what happens in the long run. A 20-week regimen of contact allergic challenges was followed by an extended 10-week observational period to study the course of skin inflammation long after discontinuing of contact allergic challenges. This 30-

week experiment would also provide more time for the anticipated tumor development. Moreover, we diminished the initial systemic effects of 4-repeated hydroxy-tamoxifen applications by reducing it to just one application, which was proven to be adequate.

As chronic skin inflammation is suspected to precede MF, our experiment was targeted to answer one main question: what is the impact of allelic loss of *Socs1* in a protracted skin inflammation – is it sufficient to lead up to MF? Therefore, the main experimental comparison focuses on comparing a protractedly inflamed skin with a mono-allelic loss of *Socs1* in CD4+ T cells to one without this allelic loss. Thus, we clearly demonstrate that mice with one-copy deletion of *Socs1* in skin resident CD4+ T cells in protractedly inflamed skin lead up to an autonomous inflammation and the features of early-stage mycosis fungoides.

2.Materials and Methods

2.1.Mouse models

Socs1 fl/wt Cd4CreER^{T2}+/- and *Socs1 fl/wt Cd4CreER*^{T2} -/- were generated as presented in our previous study (15). However, compared with the previous study, this experiment lasted more than 20 weeks longer, used a larger number of mice, and had less systemic effects by only using a single dose of 4OHT.

All mice were housed in individually ventilated cages, maintained under specific pathogen-free conditions, and had access to food and water ad libitum.

All mouse experiments were supervised by the animal welfare committee (IvD) of the Leiden University Medical Center and approved by the national central committee of animal experiments (CCD) under the permit number AVD116002015271, in accordance with the Dutch Act on Animal Experimentation and EU Directive 2020/63/EU.

2.2.Flow cytometry

Blood (50 µL) was collected weekly 24 hours after OXA application. Whole blood samples were processed using lysis buffer (from Hospital Pharmacy at LUMC) for 10 mins at 37℃ . Cells were incubated with monoclonal antibodies for 30 min on ice.

Fluorescence-labeled antibodies including anti-mouse CD3 (clone 145-2C11, BD, The Netherlands), anti-mouse CD19 (clone 1D3, Thermo Fisher Scientific, The Netherlands), anti-mouse CD4 (clone RM4-5, Thermo Fisher Scientific, The Netherlands), anti-mouse CD8 (clone 53-6.7, Biolegend, The Netherlands) and anti-ΔhCD4 (clone RPA-T4, eBioscience™, The Netherlands). Of note, the antibody for ΔhCD4 should be specific for this fragment of

human-CD4 as a reporter in the Socs1flox transgenic mouse. Samples were processed in a BD Fortessa flow cytometer and analyzed using the FlowJo software.

2.3.Histological and immunohistochemical analysis

All staining experiments were done on 4-µm-thick sections from formalin-fixed paraffin-embedded skin. Tissue sections were stained with hematoxylin and eosin to visualize general histological architecture. We used anti-human CD4 (1:2000, EPR6855, Abcam, The Netherlands), anti-mouse CD3 (1:200, D7A6E, Cell Signaling Technology, The Netherlands), anti-mouse CD4 (1:100, D7D2Z, Cell Signaling Technology, The Netherlands), anti-mouse CD8 (1:1600, 4SM15, eBioscience™, The Netherlands), anti-phospho-STAT3 (1:150, D3A7, Cell Signaling Technology, The Netherlands). The scanner (3DHISTECH, Panoramic 250) was used for microscopic examination and image acquisition.

2.4.Immunohistochemical evaluation

The layers of the epidermis were counted within at least 5 high power fields (HPF) (20x magnification) of each slide, and the means were assessed for further statistical analysis.

The numbers of ΔhCD4+, CD3+, CD4+, CD8+ and phospho-STAT3 positive cells in the dermis were counted within at least 5 HPF (20x magnification) per case. The values were normalized to cells/mm^2, and the mean numbers were assessed for further statistical analysis. The evaluations were conducted by two independent individuals who were blinded to samples information.

2.5.Statistical Analysis

A paired t-test was used to compare treated skin and untreated skin from the same mouse group. An analysis of covariance was used to compare the epidermis layers, CD3+, CD4+ and p-STAT3 positive cells in the treated skin between two different mouse groups. A nonparametric test was used to compare the number of CD8+ in the treated skin between two different mouse groups.

All statistical analyses were performed using GraphPad Prism software version 8 (GraphPad). In all cases a *P*-value of 0.05 and below was considered significant (*), $P < 0.01$(**), $P < 0.001$ (***) and $P < 0.0001$ as highly significant.

3.Results

3.1.Experimental design

We used three groups of transgenic mce with the both genders (the gender was not significant in the study) and with the age from 7 to 9 weeks: a. an experimental group (n = 9, 4 females, 5 males) with a floxed *Socs1* gene deleted through tamoxifen-activated Cre under the control of a *Cd4* promoter (*Socs1fl/wt Cd4CreER*^{T2}+/- mice, abbreviated as S+-C), b. a control group with *Socs1wt/wt Cd4CreER*^{T2}+/- mice (n=8, 5 females, 3 males, abbreviated as C), and c. a blank group with *Socs1fl/wt Cd4CreER*^{T2}+/- mice (n=9, 2 females, 7 males) not receiving any experimental intervention. **(Figure 1)**

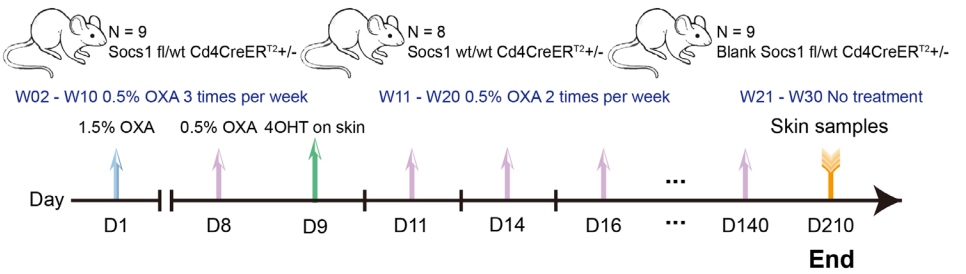

Figure 1. Experimental scheme employing the Socs conditional knockout mouse model. OXA: oxazolone. 4OHT: 4-hydroxy-tamoxifen. D: day. W: week. OXA application on the skin: 3 times per week from W02 to W10; 2 times per week from W11 to W20. Blank (Untreated) *Socs1 fl/wt Cd4CreER*^{T2}+/- is without experimental intervention during the whole experiment. Blood (50 µL) was collected weekly and was performed after 24 hours after OXA application. Skin samples were collected at the end of the experiment.

Chronic skin inflammation was induced by maintaining a contact allergic reaction to oxazolone, as described previously (15). To knock out *Socs1*, a single dose of 4OHT (20mg/ml in ethanol, 1mg 4OHT per mouse) was used on the shaved left flank after inducing a first contact allergic skin reaction to oxazolone, OXA (sensitizing with 1.5% concentration in acetone on the shaved abdomen and evoking with 0.5% in acetone). (**Figure 1**) After that, repeated dosing of OXA (0.5% concentration) was applied on the shaved left flank three times a week from week 2 to week 10 and twice a week from week 11 to week 20, with each dose at least 48h apart. (**Figure 1**) The shaved right flank was only treated with a vehicle. Skin samples were collected on day 210. (**Figure 1**) The shaved left flank was marked as treated skin and right flank as untreated skin.

The mice in the blank group did not show any phenotypical deviations, and no abnormalities were seen in FACS or IHC. The data are available but not presented in the figures.

3.2.Single dose topical application of 4OHT is sufficient to delete *Socs1* in CD4+ T cells

We used a single application of 4OHT on the skin to delete *Socs1* by activating the CRE-loxP system. We detected the expression of truncated human CD4, (ΔhCD4), on cells in the blood and the skin as a reporter only expressed upon deletion of the floxed fragment in the *Socs1* gene (15-17).

A single dose of 4OHT applied topically to the skin of S+-C mice resulted in significantly increased ΔhCD4+ CD4+ T cells over baseline in circulation, signifying induced *Socs* loss in these cells, as detected by flow cytometry. (**Figure 2A & 2B**) No *Socs1* knockout (ΔhCD4+) was observed in the control group. (**Figure 2A**) This single application importantly reduced the number of *Socs1* ko cells in circulation in comparison to our previous exploratory experiment (lower systemic effect).

The flow cytometry results showed one mouse from the experimental group, mouse S+-C8, with a strongly growing percentage of *Socs1* knockout cells among the circulating CD4+ T cells starting from week 16. Compared to S+-C8, other mice in this group had a stable, enhanced percentage of *Socs1* knockout cells in the circulating CD4+ T cell. **(Figure 2C)**

Immunohistochemical staining showed a persistent presence of *Socs1* knocked out in skin resident CD4+ T cells on day 210 in the treated flanks of S+-C mice, as flagged by ΔhCD4 expression. There were no ΔhCD4+ cells in the control group mice (**Figure 2D**) In the experimental group, the S+-C8 mouse was an outlier. (**Figure 2E**) In the dermis of S+-C mice, the quantification of ΔhCD4+ cells revealed that the treated flank harbored statistically significantly more cells with *Socs1* knockout cells than the untreated flank. There was no *Socs1* knockout detected in the control group. **(Figure 2F)**

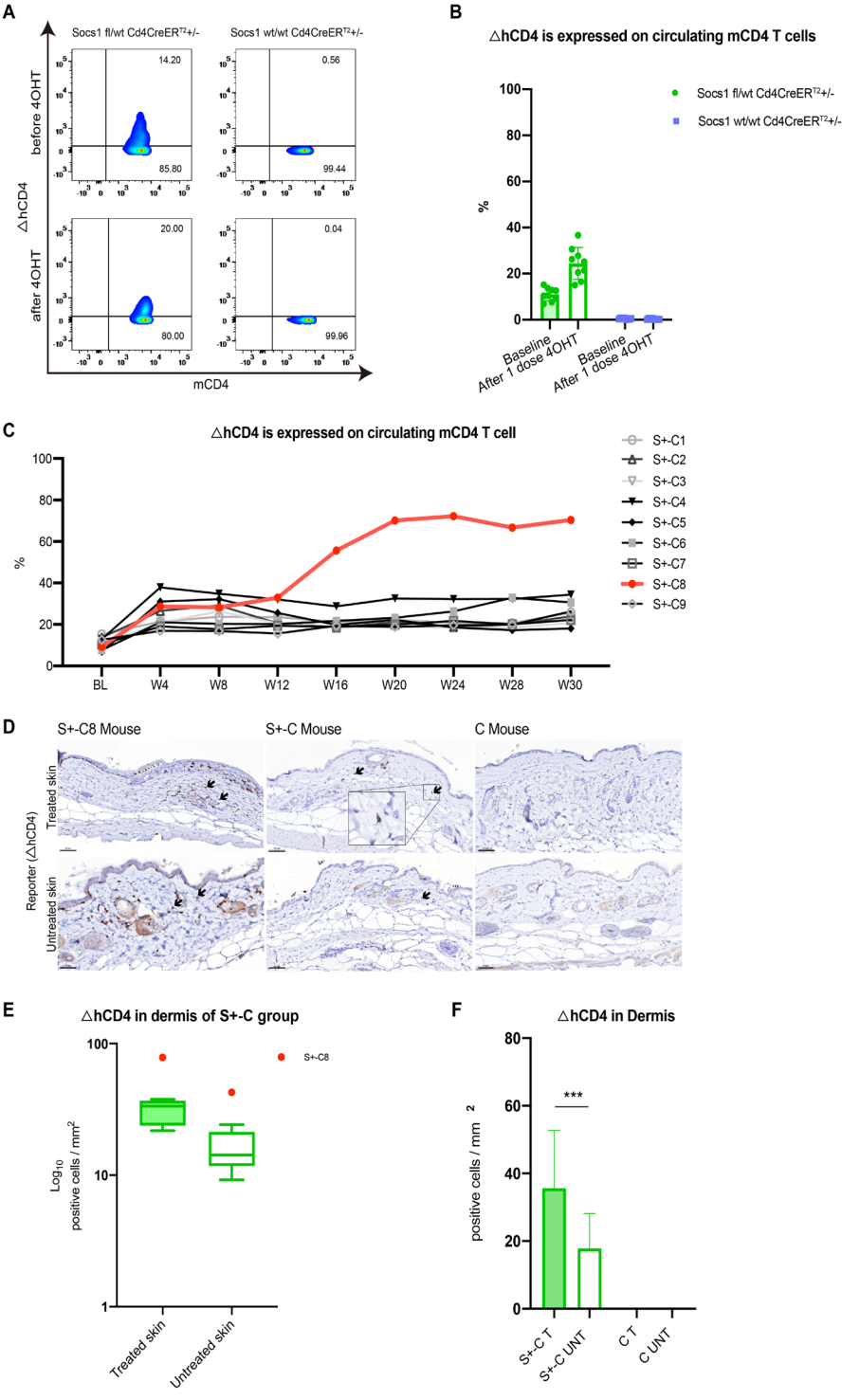
A
Socs1 fl/wt Cd4CreER^{T2}+/-
Socs1 wt/wt Cd4CreER^{T2}+/-
before 4OHT
after 4OHT
△hCD4
14.20
85.80
0.56
99.44
20.00
80.00
0.04
99.96
mCD4
B
△hCD4 is expressed on circulating mCD4 T cells
Socs1 fl/wt Cd4CreER^{T2}+/-
Socs1 wt/wt Cd4CreER^{T2}+/-
%
Baseline
After 1 dose 4OHT
Baseline
After 1 dose 4OHT
C
△hCD4 is expressed on circulating mCD4 T cell
%
S+-C1
S+-C2
S+-C3
S+-C4
S+-C5
S+-C6
S+-C7
S+-C8
S+-C9
BL
W4
W8
W12
W16
W20
W24
W28
W30
D
S+-C8 Mouse
S+-C Mouse
C Mouse
Treated skin
Untreated skin
Reporter (△hCD4)
E
△hCD4 in dermis of S+-C group
S+-C8
Log$_{10}$ positive cells / mm^2
Treated skin
Untreated skin
F
△hCD4 in Dermis
***
positive cells / mm^2
S+-C T
S+-C UNT
C T
C UNT

Figure 2. Single dose application of 4OHT knocked out Socs1 in circulating and skin-homing CD4+ T cells in *Socs1 fl/wt Cd4CreER*^{T2} +/- mouse. (A). The flow cytometry results of periphery blood before and after a single dose application of 4OHT on the skin. The loss of *Socs1* (measured as ΔhCD4 expression) in murine CD4+ T cells was analyzed. (B). The percentage of cells with loss of Socs1 (measured as ΔhCD4 expression) in total circulating murine CD4+ T cells in *Socs1 fl/wt Cd4CreER*^{T2} +/- group and *Socs1 wt/wt Cd4CreER*^{T2} +/- group before and after single dose application of 4OHT on the skin. Symbols in bar graphs represent individual mice. Data are presented as mean ± SD. ***P < 0.001. (C). The overview of the percentage of cells with loss of Socs1 deletion (measured as ΔhCD4 expression) in total circulating murine CD4+ T cells in *Socs1 fl/wt Cd4CreER*^{T2} +/- group during the whole experiment. Lines represent individual mice. BL is baseline. W is week. S+-C is Socs1 fl/wt Cd4CreER^{T2} +/-. (D). Immunohistochemical staining results of ΔhCD4 (to demonstrate Socs1 knockout) in the dermis from S+-C mouse and C mouse. S+-C is *Socs1 fl/wt Cd4CreER*^{T2} +/-. C is *Socs1 wt/wt Cd4CreER*^{T2} +/-. Scale bar: 50 μm. Black arrows: positive cells. (E). Box and Whisker plots representing the quantification of ΔhCD4-positive cells in the dermis of the S+-C group. S+-C is *Socs1 fl/wt Cd4CreER*^{T2} +/-. The box in each plot spans the interquartile range of the data, with the median indicated by a horizontal line within the box. The whiskers extend to the minimum and maximum values within 1.5 times the IQR from the first and third quartiles, respectively. Outlier S+-C8 beyond this range is displayed as an individual data point. (F). Quantifying dermal ΔhCD4-positive cells in S+-C and C mice. S+-C is *Socs1 fl/wt Cd4CreER*^{T2} +/-. C is *Socs1 wt/wt Cd4CreER*^{T2} +/-. T is 4OHT and OXA treated skin; UNT is untreated skin. S+-C8 was excluded as an outliner. Data are presented as mean ± SD. ***P < 0.001.

3.3.Persistent skin inflammation with mono-allelic *Socs1* loss in CD4+ T cells

The immunohistopathology of skin samples from different groups of mice showed a clear effect of *Socs1* knockout in CD4+ T cells in chronic skin inflammation. We excluded S+-C8 as an outlier when we compared the S+-C group with the C group to avoid excessive skewing by this outlier.

The HE staining and counting of the epidermal layers demonstrated that the treated skin was thicker than the untreated skin in both the S+-C and C groups. **(Figure 3A & 3B**) There was no difference between the epidermal layers of the S+-C and C groups' treated skin. **(Figure 3B)**

The immunohistochemical staining of T cells showed an augmented inflammation in the skin of the S+-C group (**Figure 3A**). Quantifying the staining of cells showed that in the S+-C group, the treated skin had a statistically significant increased number of CD3+, CD4+, and CD8+ cells in comparison with the untreated skin. (**Figure 3B**) In the C group, the treated skin also had a statistically significantly increased number of CD3+ and CD4+

cells compared to the untreated skin. (**Figure 3B**) An elevated skin inflammatory response by Socs1 deletion was demonstrated by the statistically more CD3+ and CD4+ cells in the treated dermis through the S+-C group compared to the C group. **(Figure 3B)**

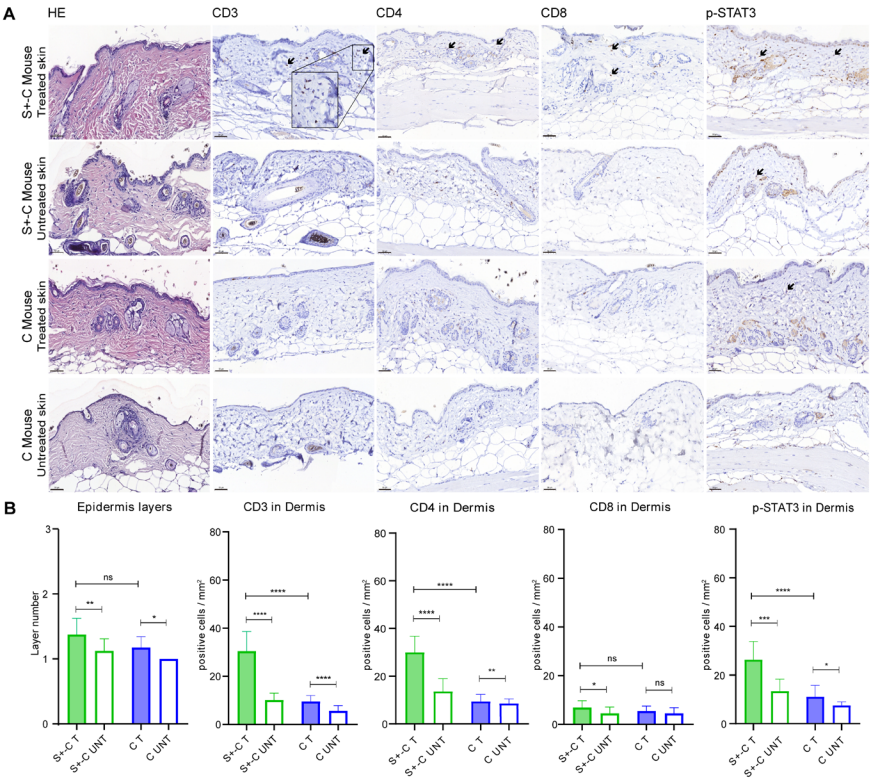

Figure 3. The histological and immunohistochemical results of the skin samples in different groups. (A). The HE and immunohistochemical staining for CD3, CD4, CD8, and p-STAT3 on the skin of S+-C and C group. S+-C is *Socs1 fl/wt Cd4CreER*^{T2} +/-. C is control group. S+-C8 was excluded. Scale bar: 50 µm. Black arrows: positive cells. (B). Quantifying the epidermal layers, dermal inflammatory cells (CD3+, CD4+, and CD8+), and p-STAT3 positive cells in S+-C group and C group. S+-C is *Socs1 fl/wt Cd4CreER*^{T2} +/-. S+-C8 was excluded as an outlier. C is control group. T is 4OHT and OXA treated skin; UNT is untreated skin. Data are presented as mean ± SD. **P* < 0.05, ***P* < 0.01, ****P* < 0.001, *****P* < 0.0001 and ns is not significant.

3.4.More STAT3 activation in skin resident T cells after the loss of one-copy *Socs1* in CD4+ T cells

We used immunohistochemistry to quantify the expression of p-STAT3 (activated STAT3) in the skin to determine how the absence of *Socs1* in CD4+ T cells affected the JAK-STAT

signaling pathway in mice. (**Figure 3A**) Quantification of these results showed that the treated skin in both the S+-C and C groups had statistically more p-STAT3 positive cells in the dermis when compared to the corresponding untreated skin (**Figure 3B**). In comparing these two groups, there was, however, a clear increase in p-STAT3 positive cells that is statistically significant in the dermis of treated skin in the S+-C group (**Figure 3B**) Hence, Socs1 knockout in cutaneous CD4+ T cells appears to boost STAT3 activation.

3.5.Pathological expansion of lymphocytes in circulation and in the skin

After 16 weeks in the experiment, one mouse, S+-C8, among the S+-C mice appeared to show explosive growth of ΔhCD4 expressing circulating CD4+ T cells, which prompted further analyses. The ratio between circulating CD3+ to CD19+ in S+-C8 decreased slightly from week 20 but increased more obviously from week 24 compared to the other mice in the same group (**Supplementary Figure 1**). The ratio between circulating CD4+ to CD8+ decreased more obviously from week 20 compared to the other mice in the same group (**Supplementary Figure 2**), indicating that there was ultimately a dominating expansion of circulating CD8+ cells in this mouse. Importantly, we only observed mild patches on the treated flank of this mouse. (**Supplementary Figure 3**) There were no severe clinical skin manifestations like open wounds and ulcers. (**Supplementary Figure 3**)

We also performed immunohistochemical staining and analysis of skin samples from S+-C8 (Figure 4). CD3+, CD4+, and CD8+ cells infiltrating the epidermis and dermis were observed. (**Figure 4**) The infiltrate predominantly consisted of CD3+ and CD4+ cells. (**Figure 4**) The numbers of epidermal layers, inflammatory cells (CD3+, CD4+, and CD8+), and cells with p-STAT3 expression in the dermis of this mouse were all higher than in the remainder of the S+-C group. (**Figure 4**) These data demonstrated that this mouse developed a pathological expansion of immune cells in the system and skin after the Socs1 knockout in skin-resident CD4+ T cells.

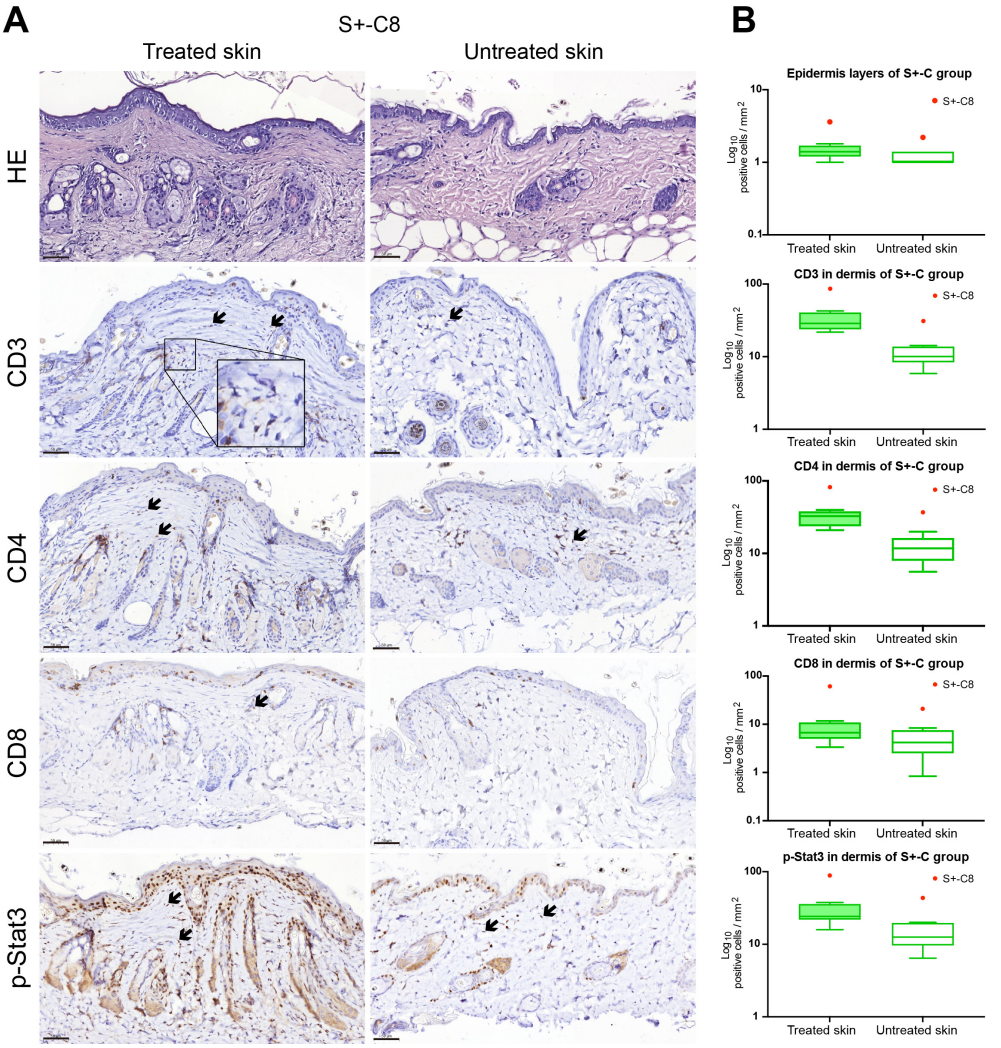

Figure 4. The histological and immunohistochemical results of the skins samples of S+-C8 mouse. (A). The HE and immunohistochemical staining for CD3, CD4, CD8, and p-STAT3 on the treated and untreated skin of S+-C8 mouse. S+-C is *Socs1 fl/wt Cd4CreER*^{T2} +/-. Black arrows: positive cells. Scale bar: 50 µm. (B). Box and Whisker plots representing the epidermal layers, dermal inflammatory cells (CD3+, CD4+, and CD8+), and p-STAT3 positive cells in treated and untreated skin of S+-C group. S+-C is *Socs1 fl/wt Cd4CreER*^{T2} +/-. The box in each plot spans the interquartile range (IQR) of the data, with the median indicated by a horizontal line within the box. The whiskers extend to the minimum and maximum values within 1.5 times the IQR from the first and third quartiles, respectively. Outlier S+-C8 beyond this range is displayed as an individual data point.

4.Discussion

In MF, one-copy deletion of *SOCS1* was detected in early-stage lesions and *SOCS1* was found to be a tumor suppressor frequently deleted in MF (9). Considering the grave effects caused by *SOCS1* absence (18) and more particularly one-copy deletion of *SOCS1* in CD4+ T cells in MF, the present long-term *in vivo* experiments focused on the impact of conditional Socs1 knockout in CD4+ T cells to mimic early-stage mycosis fungoides.

A single dose of 4OHT topical application was confirmed to be sufficient to knock out *Socs1* in our transgenic mice. The *Socs1* knockout level was stable during the whole experiment in the S+-C group (excluding S+-C8). The statistical differences between the number of inflammatory cells and STAT3 activation in treated skin of S+-C (excluding S+-C8) and treated skin of the C group show that knockout of *Socs1* in skin resident CD4 T cells activate STAT3 and maintains and promotes the inflammatory response. The infiltration of lymphocytes occurred mainly in the dermis. This is consistent with the results of the previous study (15). The JAK-STAT signaling pathway is inhibited by members of the SOCS family. *SOCS1* stands out as one of the most effective family members and its role is to interfere with JAK1 or JAK3, effectively reducing immune-associated inflammatory responses mediated by the JAK-STAT system. When *SOCS1* is silenced, the JAK-STAT signaling pathway becomes dysregulated (8). In lymphomas, there is evidence of DNA hypermethylation affecting the *SOCS1* gene, which in turn can promote cell proliferation by enhancing JAK2 activity (19). Studies have also reported the loss of *SOCS1* in early-stage mycosis fungoides patients (9). In 18% of MF cases, the *SOCS1* promoter is inactivated due to DNA methylation (20). Additionally, miR155, a microRNA targeting SOCS1 mRNA, has been found to be upregulated in MF cases (21). The exacerbated inflammatory response in the skin also aligns with the fact that patients may experience more severe inflammatory lesions as mycosis fungoides disease progresses.

In the S+-C group (without S+-C8), there was a statistical difference between the number of T cells (CD3+, CD4+) and STAT3 activation in oxazolone treated versus untreated skin. Furthermore, the *Socs1* knockout transgenic mice did not show other systemic abnormalities. This suggests that this mouse model produces a dense infiltrate of reactive immune cells and malignant T cells, which fits the features of early-stage mycosis fungoides (4). This *in vivo* modelling preserves the microenvironment after *Socs1* knockout in CD4+ T cells and the interaction between the oncogenic pathway and the immune system (5, 12). In the C group, the treated skin had a statistically significantly thicker epidermis, more inflammatory cells (CD3+ and CD4+), and STAT3 activation of T cells in the dermis than the untreated skin. It was evidently due to the long-term induction of chronic inflammation in the treated skin (22, 23). However, only with a loss of one-copy *Socs1* in skin-resident CD4+

cells, in S+-C mice, the inflammatory response persisted and became more pronounced.

The most interesting observation is that under these conditions, one mouse in the experimental S+-C group showed a growing dominance of loss of *Socs1* among circulating CD4+ T cells after week 16. The circulating CD8+ cells in this mouse appeared to expand strongly after week 20, perhaps in a reactive response to the prior expansion of CD4+ cells with Socs1 knockout. The skin samples showed a thicker epidermis with lymphocyte infiltration. The epidermis of treated and untreated skin from this mouse was thicker than other S+-C mice. The numbers of inflammatory cells CD3+, CD4+, and CD8+ in the dermis were also higher than in other S+-C mice. The number of CD4+ cells in the skin of this mouse was much higher than that of CD8+ cells, but in circulation, the latter ultimately dominated. The immune response toward the malignant cells, similar to the early inflammation in MF, includes a cell-mediated anti-tumor response that actively suppresses the malignant cell's expansion (24-26). It also agrees with earlier findings that OXA-induced inflammation contains both CD4+ and CD8+ cells (23, 27). All the data showed a strong pathological expansion of immune cells in the skin and blood in this one mouse. Moreover, the STAT3 activation of T cells in the dermis of this mouse was also much more increased than in other S+-C mice according to the quantification of IHC staining. The constitutive STAT3 activation of T cells in the dermis and the STAT3 activation of keratinocytes in the epidermis (10 weeks after the last challenge with OXA) is also evidence of early stages of carcinogenesis and malignant progression *in vivo* (28-31).

There are some limitations to the present study. The first is that only one mouse developed noticeable signs of tumorigenesis, also reflected in circulating lymphocytes. The skin showed a noticeably thicker epidermis, massive inflammatory cell infiltration and increased STAT3 activation. But the persisting skin infiltration of CD4+ T cells in all skin samples within the mono-allelic *Socs1* in CD4+ T cells can be considered as a potential skin condition from which MF may develop. The observation from the one outliner mouse merely as an initial indication, suggests the need for further investigation. To establish more robust findings, it is crucial to conduct a more extensive and prolonged experiment that includes a larger sample size. Another limitation is that we were unable to include S*ocs1 fl/fl Cd4CreER*^{T2} +/- mice because of a none Mendelian extremely low yield of this genotype from our breeding colony. In further research, we will perform again longer-term experiments with more mice to increase the number of mice with the features of lymphoma development.

In summary, this long-term experiment confirmed that *Socs1*-knockout in skin-resident CD4+ T cells in a protracted contact-allergic reaction results in an autonomous skin inflammation with features of early-stage mycosis fungoides.

References

1. Willemze R, Jaffe ES, Burg G, Cerroni L, Berti E, Swerdlow SH, et al. WHO-EORTC classification for cutaneous lymphomas. Blood. (2005) 105: 3768-85. doi:10.1182/blood-2004-09-3502
2. Willemze R, Cerroni L, Kempf W, Berti E, Facchetti F, Swerdlow SH, et al. The 2018 update of the WHO-EORTC classification for primary cutaneous lymphomas. Blood. (2019) 133: 1703-14. doi:10.1182/blood-2018-11-881268
3. Dummer R, Vermeer MH, Scarisbrick JJ, Kim YH, Stonesifer C, Tensen CP, et al. Cutaneous T cell lymphoma. Nat Rev Dis Primers. (2021) 7: 61. doi: 10.1038/s41572-021-00296-9
4. Krejsgaard T, Lindahl LM, Mongan NP, Wasik MA, Litvinov IV, Iversen L, et al. Malignant inflammation in cutaneous T-cell lymphoma-a hostile takeover. Semin Immunopathol. (2017) 39: 269-82. doi: 10.1007/s00281-016-0594-9
5. Tensen CP, Quint KD, Vermeer MH. Genetic and epigenetic insights into cutaneous T-cell lymphoma. Blood (2022) 139: 15-33. doi: 10.1182/blood.2019004256
6. Patil K, Kuttikrishnan S, Khan AQ, Ahmad F, Alam M, Buddenkotte J, et al. Molecular pathogenesis of Cutaneous T cell Lymphoma: Role of chemokines, cytokines, and dysregulated signaling pathways. Semin Cancer Biol. (2022) 86: 382-99. doi: 10.1016/j.semcancer.2021.12.003
7. Tamiya T, Kashiwagi I, Takahashi R, Yasukawa H, Yoshimura A. Suppressors of cytokine signaling (SOCS) proteins and JAK/STAT pathways: regulation of T-cell inflammation by SOCS1 and SOCS3. Arterioscler Thromb Vasc Biol. (2011) 31: 980-5. doi:10.1161/ATVBAHA.110.207464
8. Inagaki-Ohara K, Kondo T, Ito M, Yoshimura A. SOCS, inflammation, and cancer. JAKSTAT. (2013) 2: e24053. doi: 10.4161/jkst.24053
9. Bastidas Torres AN, Cats D, Mei H, Szuhai K, Willemze R, Vermeer MH, et al. Genomic analysis reveals recurrent deletion of JAK-STAT signaling inhibitors HNRNPK and SOCS1 in mycosis fungoides. Genes Chromosomes Cancer. (2018) 57: 653-64. doi: 10.1002/gcc.22679
10. Hill W, Caswell DR, Swanton C. Capturing cancer evolution using genetically engineered mouse models (GEMMs). Trends Cell Biol. (2021) 31: 1007-18. doi: 10.1016/j.tcb.2021.07.003.
11. Kersten K, de Visser KE, van Miltenburg MH, Jonkers J. Genetically engineered mouse models in oncology research and cancer medicine. EMBO Mol Med. (2017) 9: 137-53. doi: 10.15252/emmm.201606857
12. Gill RPK, Gantchev J, Martinez Villarreal A, Ramchatesingh B, Netchiporouk E, Akilov OE, et al. Understanding Cell Lines, Patient-Derived Xenograft and Genetically Engineered Mouse Models Used to Study Cutaneous T-Cell Lymphoma. Cells. (2022) 11: 539. doi: 10.3390/cells11040593
13. Bresin A, Caprini E, Russo G, Narducci MG. Challenging Cutaneous T-Cell Lymphoma: What Animal Models Tell us So Far. J Invest Dermatol. (2022) 142: 1533-40. doi: 10.1016/j.jid.2021.12.007
14. Hanahan D, Weinberg RA. Hallmarks of cancer: the next generation. Cell. (2011) 144: 646-74. doi: 10.1016/j.cell.2011.02.013
15. Luo Y, Vermeer MH, de Gruijl FR, Zoutman WH, Sluijter M, van Hall T, et al. In vivo modelling of cutaneous T-cell lymphoma: The role of SOCS1. Front Oncol. (2022) 12: 1031052. doi: 10.3389/fonc.2022.1031052

16. Chong MM, Cornish AL, Darwiche R, Stanley EG, Purton JF, Godfrey DI, et al. Suppressor of cytokine signaling-1 is a critical regulator of interleukin-7-dependent CD8+ T cell differentiation. Immunity. (2003) 18: 475–87. doi: 10.1016/s1074-7613(03)00078-5

17. Aghajani K, Keerthivasan S, Yu Y, Gounari F. Generation of CD4CreER(T^2) transgenic mice to study development of peripheral CD4-T-cells. Genesis. (2000) 50: 908–13. doi: 10.1002/dvg.22052

18. Marine JC, Topham DJ, McKay C, Wang D, Parganas E, Stravopodis D, et al. SOCS1 Deficiency Causes a Lymphocyte-Dependent Perinatal Lethality. Cell. (1999) 98: 609–16. doi: 10.1016/s0092-8674(00)80048-3

19. Melzner I, Bucur A, Brüderlein S, Dorsch K, Hasel C, Barth TFE, et al. Biallelic mutation of SOCS-1 impairs JAK2 degradation and sustains phospho-JAK2 action in the MedB-1 mediastinal lymphoma line. Blood. (2005) 105: 2535-42. doi: 10.1182/blood-2004-09-3701

20. Ferrara G, Pancione M, Votino C, et al. A specific DNA methylation pro le correlates with a high risk of disease progression in stage I classical (Alibert-Bazin type) mycosis fungoides. Br J Dermatol.(2014) 170:1266–75.doi: 10.1111/bjd.12717

21. Tensen CP, Vermeer MH. MicroRNA-155 potentiates tumour development in mycosis fungoides. Br J Dermatol. (2017) 177:618–20.doi: 10.1111/bjd.15785

22. Fyhrquist N, Wolff H, Lauerma A, Alenius H. CD8+ T cell migration to the skin requires CD4+ help in a murine model of contact hypersensitivity. PLoS One. (2012) 7: e41038. doi: 10.1371/journal.pone.0041038

23. Lehtimaki S, Tillander S, Puustinen A, Matikainen S, Nyman T, Fyhrquist N, et al. Absence of CCR4 exacerbates skin inflammation in an oxazolone-induced contact hypersensitivity model. J Invest Dermatol (2010) 130: 2743-51. doi: 10.1038/jid.2010.208

24. Echchakir H, Bagot M, Dorothée G, Dorothée G, Martinvalet D, Le Gouvello S, et al. Cutaneous T cell lymphoma reactive CD4+ cytotoxic T lymphocyte clones display a Th1 cytokine profile and use a fas-independent pathway for specific tumor cell lysis. J Invest Dermatol. (2000) 115: 74-80. doi: 10.1046/j.1523-1747.2000.00995.x

25. Vermeer MH, van Doorn R, Dukers D, Bekkenk MW, Meijer CJ, Willemze R. CD8+ T cells in cutaneous T-cell lymphoma: expression of cytotoxic proteins, Fas Ligand, and killing inhibitory receptors and their relationship with clinical behavior. J Clin Oncol. (2001) 19: 4322-9. doi: 10.1200/JCO.2001.19.23.4322

26. Hsi AC, Lee SJ, Rosman IS, Carson KR, Kelley A, Viele V, et al. Expression of helper T cell master regulators in inflammatory dermatoses and primary cutaneous T-cell lymphomas: diagnostic implications. J Am Acad Dermatol. (2015) 72: 159-67. doi: 10.1016/j.jaad.2014.09.022

27. Zhang L, Tinkle SS. Chemical activation of innate and specific immunity in contact dermatitis. J Invest Dermatol. (2000) 115: 168-76. doi: 10.1046/j.1523-1747.2000.00999.X

28. Zhang L, Kuca K, You L, Zhao Y, Musilek K, Nepovimova E, et al. Signal transducer and activator of transcription 3 signaling in tumor immune evasion. Pharmacol Ther. (2022) 230: 107969. doi: 10.1016/j.pharmthera.2021.107969

29. Gluud M, Pallesen EMH, Buus TB, Gjerdrum LMR, Lindahl LM, Kamstrup MR, et al. Malignant T cells induce skin barrier defects through cytokine-mediated JAK/STAT signaling in cutaneous T-cell lymphoma. Blood. (2023) 141: 180-93. doi: 10.1182/blood.2022016690

30. Zhu F, Wang KB, Rui L. STAT3 Activation and Oncogenesis in Lymphoma. Cancers (Basel). (2019) 12:19. doi: 10.3390/cancers12010019

31. Nielsen M, Kaestel CG, Eriksen KW, Woetmann A, Stokkedal T, Kaltoft K, et al. Inhibition of constitutively activated Stat3 correlates with altered Bcl-2/Bax expression and induction of apoptosis in mycosis fungoides tumor cells. Leukemia. (1999) 13: 735-8. doi: 10.1038/sj.leu.2401415

Supplementary Information

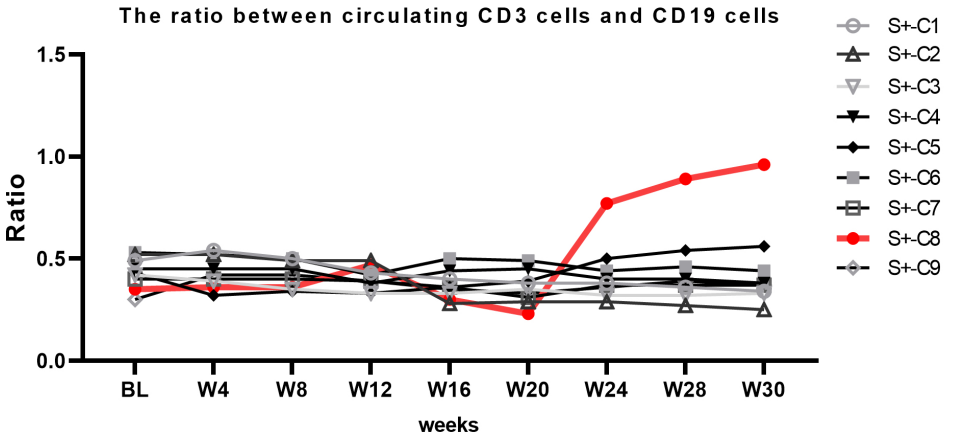

Supplementary Figure 1. The overview of the ratio between circulating CD3 and CD19 in *Socs1 fl/wt Cd4CreER^{T2}* +/- group during the whole experiment. Lines represent individual mice. BL is baseline. W is week. S+-C is *Socs1 fl/wt Cd4CreER^{T2}* +/-.

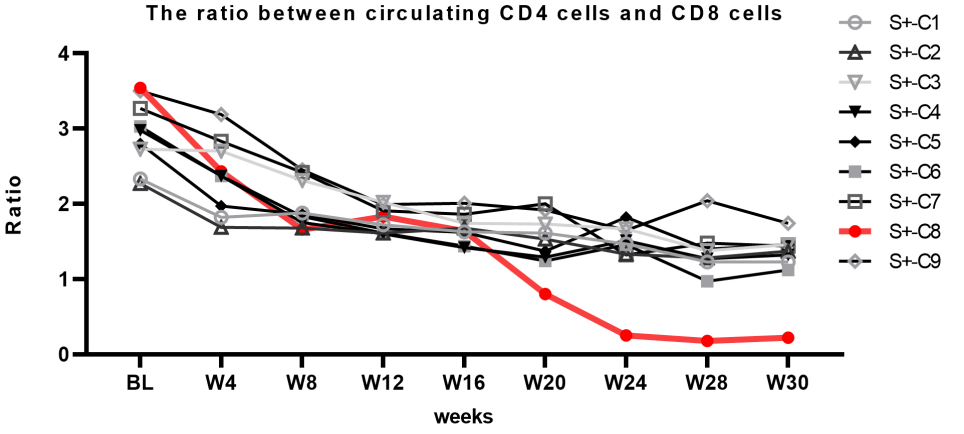

Supplementary Figure 2. The overview of the ratio between circulating CD4 and CD8 in *Socs1 fl/wt Cd4CreER^{T2}* +/- group during the whole experiment. Lines represent individual mice. BL is baseline. W is week. *S+-C is Socs1 fl/wt Cd4CreER^{T2}* +/-.

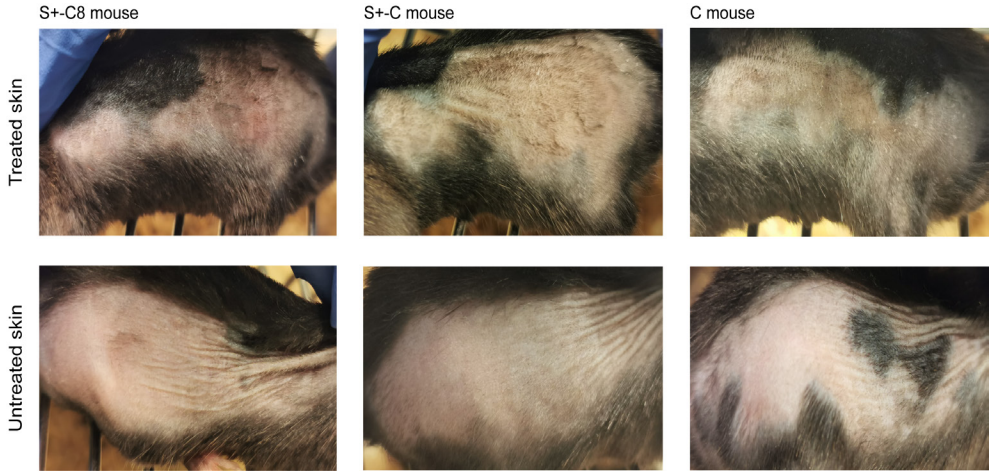

Supplementary Figure 3. Augmented skin inflammation induced by repeated low concentration oxazolone. Representative images of the shave treated skin and untreated skin of S+-C mice and C mice on day 168 (W24) during the experiment. *S+-C is Socs1 fl/wt Cd4CreER^{T2} +/-*, C is control group.

4

A novel knockout mouse model to assess the impact of one-copy loss of *Hnrnpk* in CD4+ T cells in chronically inflamed skin as a prelude to CTCL

Yixin Luo[1], Maarten H. Vermeer[1], Margot M. Linssen[2], Conny Brouwers[2], Jill Claassens[2], Frank R. de Gruijl [1], Peter Hohenstein 2, Cornelis P. Tensen [1]
1.Department of Dermatology, Leiden University Medical Center, Leiden, The Netherlands
2.Transgenic Facility Leiden, Central Animal Facility, Leiden University Medical Center, The Netherlands

The manuscript is currently under review by Scientific Reports

Abstract:

Cutaneous T-cell lymphomas (CTCLs), particularly Mycosis fungoides (MF), frequently exhibit deletions and reduced expression of *HNRNPK* in CD4+ T cells. To enable *in vivo* studies, we developed a conditional *Hnrnpk* knockout mouse that thrives, facilitating the investigation of *HNRNPK*'s role in CTCL onset. We generated mice with a floxed *Hnrnpk* allele, then crossbred them with *Cd4CreER*^{T2} mice to generate *Hnrnpk* flox *Cd4CreER*^{T2} mice, all in BL6 background. PCR confirmed the targeted the deletion of *Hnrnpk* in CD4+ T cells after tamoxifen i.p. injection. Skin allergic reactions were induced with oxazolone, and *Cre* was activated in skin-infiltrating CD4+ T cells using tamoxifen topically after the first allergic skin reaction. The mice exhibited no immediately obvious phenotype. Flow cytometry and histopathological analysis were conducted on blood and skin samples collected throughout the experiment. Following 20 weeks of sustained allergic reactions, inflammation persisted over 20 weeks after challenges ceased, demonstrating early CTCL characteristics such as chronic skin inflammation, CD3+ CD4+ T cell infiltration, and stable peripheral blood parameters. This mouse model provides experimental access to the complex microenvironment and immune responses involved in early inflammatory stages, providing opportunities for further research into the role of *HNRNPK* in CTCL and the development of effective therapeutic interventions for this challenging malignancy

Key words: Cutaneous T-cell lymphomas; Mycosis fungoides; CD4+ T cells; *HNRNPK*; Transgenic mouse

1 Introduction

Cutaneous T-cell lymphomas (CTCL) are a diverse group of non-Hodgkin's lymphomas (NHL) characterized by the localization of neoplastic T lymphocytes to the skin. (1, 2) Recent advancements have significantly contributed to our understanding of the molecular mechanisms underlying CTCL, revealing the involvement of genes such as heterogenous nuclear ribonucleoprotein K (*HNRNPK*) and Suppressor of cytokine signaling 1(*SOCS1*). (3-5) However, a comprehensive understanding of CTCL requires the development of appropriate model systems that can capture the complex nature of the disease and facilitate the identification of effective therapeutic strategies. (6)

The role of the tumor microenvironment within the lesions in the development, progression and treatment resistance of CTCL has become an important area of research due to its complicated pathogenesis. (7) *In vitro* models, although valuable, have limitations in simulating essential factors such as the tumor microenvironment and intact immune system, emphasizing the need for *in vivo* models. (8-10) Therefore, more sophisticated tools, such as genetically engineered mouse models, are indispensable for comprehensively exploring T-cell malignancies.

HNRNPK, a DNA and RNA-binding protein, regulates numerous cellular processes through transcriptional, posttranscriptional, and translational mechanisms. (11,12) Notably, its oncogenic and tumor-suppressive functions are context-dependent. Both overexpression and abnormally low expression of *HNRNPK* can be pathogenic, likely due to the dysregulation of multiple cellular oncogenes or tumor suppressor genes. (13) In the context of hematological malignancies, it has been observed that a 9q21.32 deletion encompassing the *HNRNPK* gene occurs in acute myeloid leukemia patients, resulting in the loss of one copy of *HNRNPK*. (14,15) Interestingly, the recurrent deletion of *HNRNPK* has been reported in mycosis fungoides (MF) and other CTCL subtypes. (16,17) Therefore, there is a compelling need to establish a CD4+ T-cell-specific murine model of *Hnrnpk* that accurately represents the intact immune system and tumor microenvironment. Such a model would be pivotal in elucidating the intricate and multifaceted role of *HNRNPK* in CTCL, ultimately leading to a better understanding of the disease and developing more effective therapeutic interventions.

This work describes a novel *Hnrnpk* mouse model designed based on the CTCL gene sequencing results. Here, we primarily wanted to examine the basic impact of *Hnrnpk*-ko limited to CD4+ T cells in an inflamed skin site on subsequent chronic (allergic) inflammation at this site as suspected prelude to CTCL. In this mouse model, the immune homeostasis in peripheral blood remains relatively undisturbed under chronic antigen

exposure, while T-cell infiltration is confined to the skin. The skin lesions predominantly exhibit lymphocytic infiltration characterized by CD3+ CD4+ cells, and the infiltration persists without regression, aligning with early-stage CTCL characteristics.

2.Result

2.1.Generation of *Hnrnpk flox* and *Hnrnpk flox Cd4CreER^{T2}* mice

To generate conditional knockout *Hnrnpk* mice, we employed CRISPR/Cas9 RNPs and 200 bp single-stranded oligodeoxynucleotides (ssODN) to sequentially target intron 2 and in the resulting mouse intron 6 of the *Hnrnpk* gene, in murine oocytes on C57BL/J background We designed the 5' ssODN (for intron 2) with a LoxP site, and introduced it into oocytes along with the CRISPR/Cas9 RNP complex.(**Figure 1A**) Additionally, we designed the 3' ssODN (for intron 6) with a LoxP site, , and 3' HA, and introduced it into the resulting mouse line to target the LoxP site in intron 6. (**Figure 1B**) (gRNA, ssODN listed in **Supplementary Table 1**)

We screened the offspring for the correct insertion of the LoxP sites on genomic DNA from ear-clip biopsies by PCR and Sanger Sequencing (primers listed in **Supplementary Table 2**). (**Figure 1 C, 1D, & 1E**). To confirm correct integration loxP site in intron 6, TOPO-TA PCR product subcloning was performed. As shown in **Figure 1F**, the *Hnrnpk flox* mice were inserted with two loxP sites flanked exon 3 to 5. We bred these conditional mice to homozygosity and the offsprings are healthy.

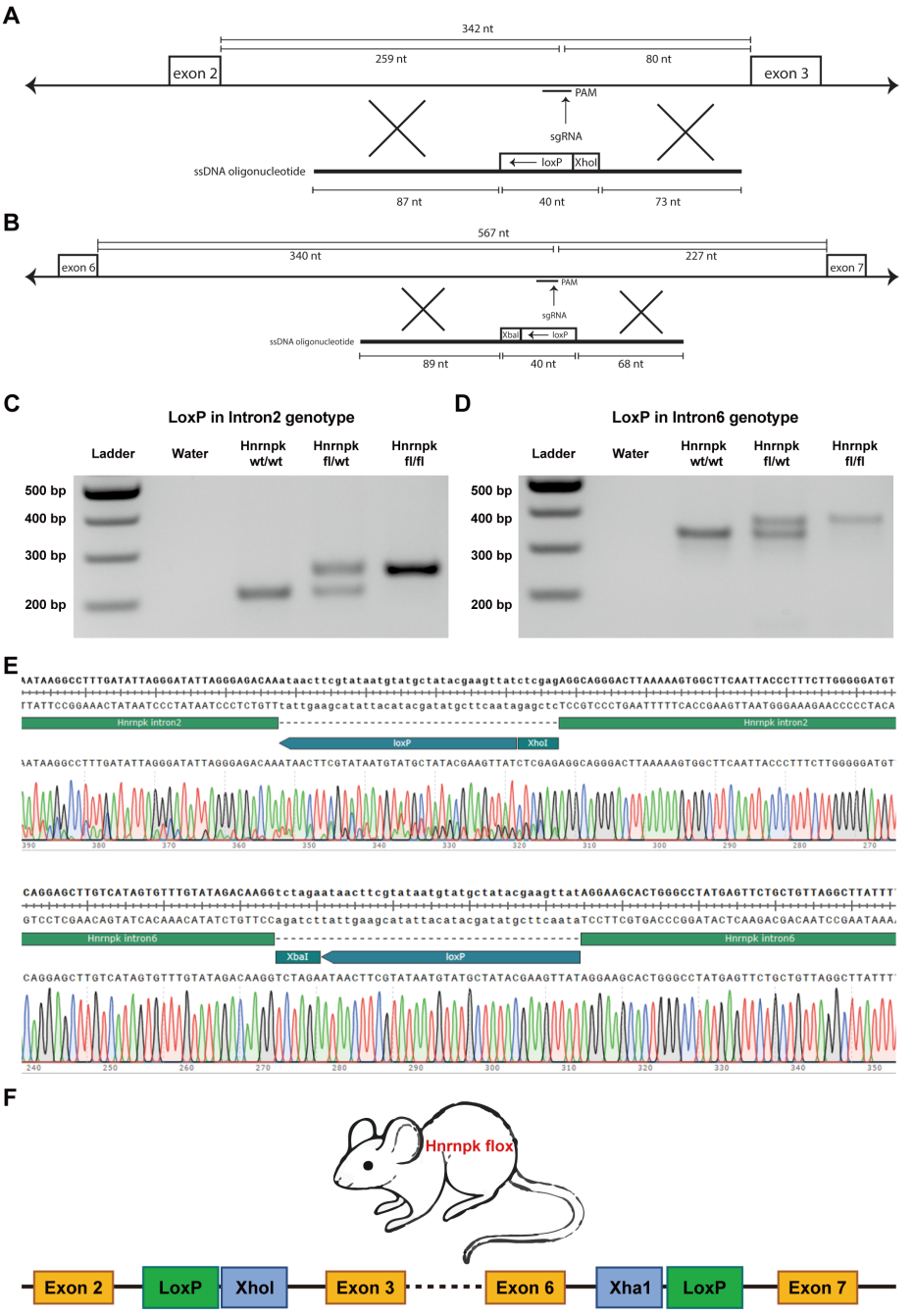

Figure 1. (A, B) The structure of designed single-stranded oligodeoxynucleotides (ssODN) for intron 2 and intron 6 of *Hnrnpk*. (C, D) Agarose gel electrophoresis image showing the PCR product of LoxP inserted in intron 2 and intron 6 of *Hnrnpk*. (E) Sanger sequencing chromatogram of both

modifications. (F). The structure of the *Hnrnpk* flox modified gene with two LoxP sites in *Hnrnpk* flox mouse.

2.2.*Hnrnpk* Knockout in CD4+ T cells confirmation

To induce *Hnrnpk* knockout in CD4+ T cells, we crossed *Cd4CreER*^{T2} mice with *Hnrnpk* flox mice. Details of the cross-breeding scheme can be found in **Figure 2A**. *In Cd4CreER*^{T2} mice, *Cre* recombinase is controlled by the *Cd4* gene promoter and can be induced by tamoxifen. Homozygous *Hnrnpk* flox (*Hnrnpk fl/fl*) mice were crossed with the transgenic mice expressing *Cre* recombinase under the control of the CD4 promoter (*Cd4CreER*^{T2} mice) to yield heterozygous littermates with the *Cd4CreER*^{T2} transgene. Offspring inherited both the targeted *Hnrnpk fl/wt* allele and the *Cd4CreER*^{T2} transgene.

In *Hnrnpk flox Cd4CreER*^{T2} mice, tamoxifen can selectively knock out *Hnrnpk* in CD4+ T cells. After five consecutive days of intraperitoneal tamoxifen injections in *Hnrnpk fl/wt Cd4CreER*^{T2}+ mice, splenocytes were collected and CD4+ T cells were enriched. (**Figure 2B**) Flow cytometry analysis showed that CD4+ T cells accounted for approximately 94.1% after enrichment. (**Figure 2C**). DNA was extracted from the enriched CD4+ T cells. Successful *Hnrnpk* deletion in CD4+ T cells of *Hnrnpk flox Cd4CreER*^{T2} mice treated with tamoxifen was confirmed through PCR analysis (primers listed in **Supplementary Table 3**) showing the recombinant *Hnrnpk* (*Hnrnpk* KO). In contrast, the spleen CD4+ T cells enriched from mice not receiving tamoxifen injections showed no recombinant gene fragments following *Hnrnpk* deletion (*Hnrnpk* WT). (**Figure 2D**).

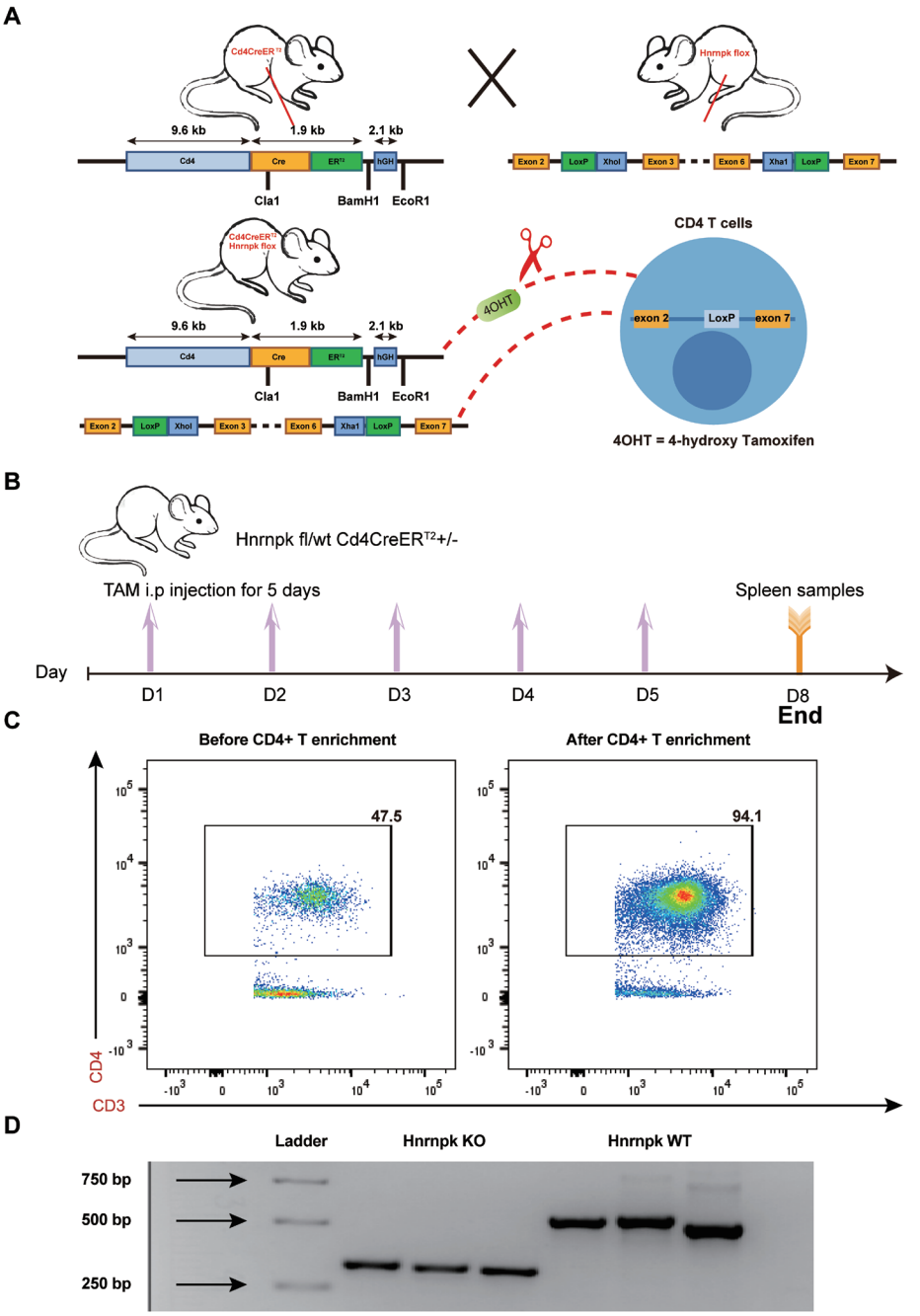

Figure 2. (A) Breeding scheme used to create *Hnrnpk flox/wt Cd4CreER*^{T2} mouse. (B) Schematic diagram illustrating the *Hnrnpk* knockout using Tamoxifen in *Hnrnpk flox/wt Cd4CreER*^{T2} mouse.

Tamoxifen was administered to mice for 5 continuous days via intraperitoneal injection (i.p.). On day 8, the spleen was collected, and CD4+ T cells were enriched. TAM: tamoxifen, i.p: intraperitoneal. (C) Representative flow cytometry plots showing CD3+ CD4+ T cells in splenocytes before and after CD4+ T cell enrichment. (D) Agarose gel electrophoresis image displaying the PCR product of recombinant *Hnrnpk* following *Hnrnpk* deletion (*Hnrnpk* KO) using three different sets of primers, and unrecombined *Hnrnpk* (*Hnrnpk* WT) also using three different sets of primers.

2.3.T-cell infiltration limited to cutaneous region and undisturbed immune homeostasis in peripheral blood in the conditional knockout mice with single-copy *Hnrnpk* deficiency in skin-resident CD4+ T cells

In this experiment, *Hnrnpk fl/wt Cd4CreER*^{T2} mice were used to induce sustained chronic inflammation in the skin using OXA and topically applied tamoxifen to knock out *Hnrnpk* in CD4+ T cells within the skin. (**Figure 3A**) One flank was treated and the collateral flank was left untreated as matched internal control. The specific application of reagents was implemented as previously described. (18,19) From these earlier experiments we know that without tamoxifen (no recombination at floxed sites) the chronic inflammation faded after discontinuation of the allergic challenges very much to a level observed in untreated flanks in the test animals.

Flow cytometry analysis of peripheral blood during the 40-week experiment showed that repeated topical application of low-concentration OXA did not result in significant abnormalities in immune cell populations. The ratio of CD3+ cells to CD19+ cells in peripheral blood of all mice did not exhibit noticeable fluctuations (**Figure 3B**). Similarly, the ratio of CD4+ cells to CD8+ cells in peripheral blood of all mice also did not show significant fluctuations. (**Figure 3C**). The ratios of immune cell subpopulations remained relatively stable throughout the experiment.

Flow cytometry analysis showed successful cell extraction from mouse skin, and the proportion of CD4+ and Cd8+ cells among CD3+ cells was determined. In the cells extracted from the skin, the percentage of CD4+ cells among CD3+ cells in the left flank (treated flank) was significantly higher compared to the percentage of CD4+ cells among CD3+ cells in the right flank (untreated flank) to a statistically significant level. (**Figure 3D, & 3E**). Similarly, the percentage of CD8+ cells among CD3+ cells in the left flank was significantly higher than that of CD8+ cells among CD3+ cells in the right flank. (**Figure 3F, & 3G**)

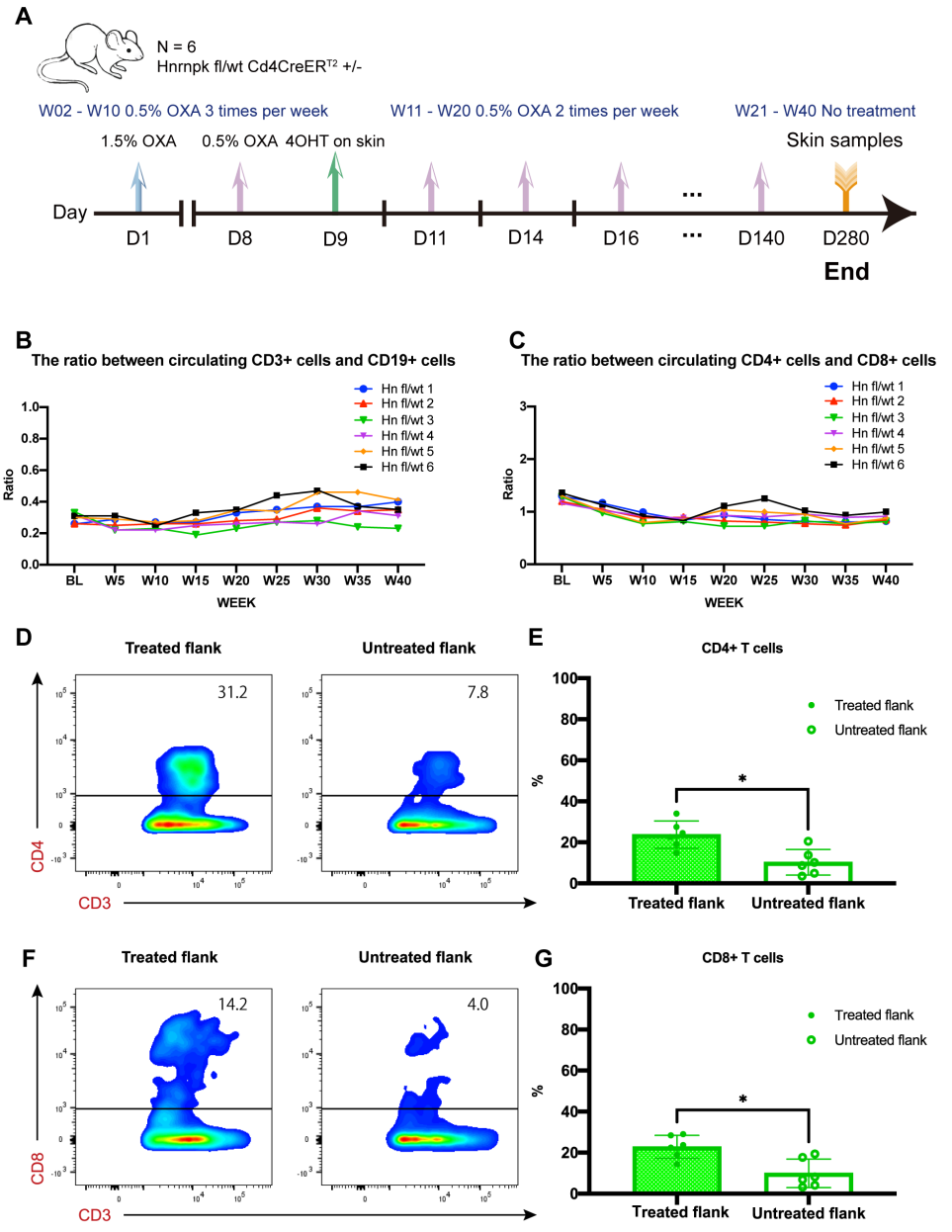

Figure 3. (A) Schematic diagram illustrating the experiment in *Hnrnpk flox CD4CreER*^{T2} transgenic mice. D: day, W: week, OXA: oxazolone, 4OHT: 4-hydroxy-tamoxifen. Blood collection was performed 24 hours after OXA application. Skin samples were collected at the end of the experiment. (B, C) Overview of the ratio between CD3+ cells and CD19+ cells, and between CD4+ cells and CD8+ cells in peripheral blood throughout the experiment. (D, E) Representative flow cytometry plots

and quantitative analysis of CD3+ CD4+ T cells in treated and untreated flanks. P = 0.0159. (F, G) Representative flow cytometry plots and quantitative analysis of CD3+ CD8+ T cells in treated and untreated flanks. P= 0.0111. The data were presented as means ± SDs. Statistical analysis was performed using a pair t-test. Differences were considered statistically significant when $P < 0.05$ (*$p <$ 0.05).

2.4.Increased skin inflammation with dermal infiltrating lymphocytes, primarily characterized by CD3+ CD4+ cells in transgenic mice with single-copy *Hnrnpk* deficiency in skin-resident CD4+ cells

In addition to isolation of intact cells from mouse skin, we made sections of paraffin embedded formalin fixed biopsies of mouse skin and performed histopathological analysis using haematoxylin and eosin (H&E) staining and immunohistochemistry (IHC). The H&E staining revealed a minor amount of epidermal cell swelling and lymphocyte infiltration in the dermis of the treated flanks. (**Figure 4A**) No significant abnormalities were observed in the epidermis and dermis of the untreated flanks. Quantitative statistical analysis of the epidermal layers showed that the treated flanks exhibited thicker epidermis than the untreated flanks. (**Figure 4A**)

Furthermore, we conducted immunohistochemical staining on the mouse skin samples using T-cell (inflammation) markers CD3, CD4, and CD8. The staining results revealed scattered or focal distribution of CD3+ and CD4+ cells in the dermis of the treated flanks, and the presence of CD8+ cells, although with a scattered distribution. In contrast, the untreated flanks showed fewer CD3+, CD4+, and CD8+ lymphocyte infiltrations. (**Figure 4B**) Quantitative analysis of CD3+, CD4+, and CD8+ infiltration in the dermis demonstrated a significant increase in the number of CD3+, CD4+, and CD8+ cells in the treated flanks compared to the untreated flanks. (**Figure 4B**)

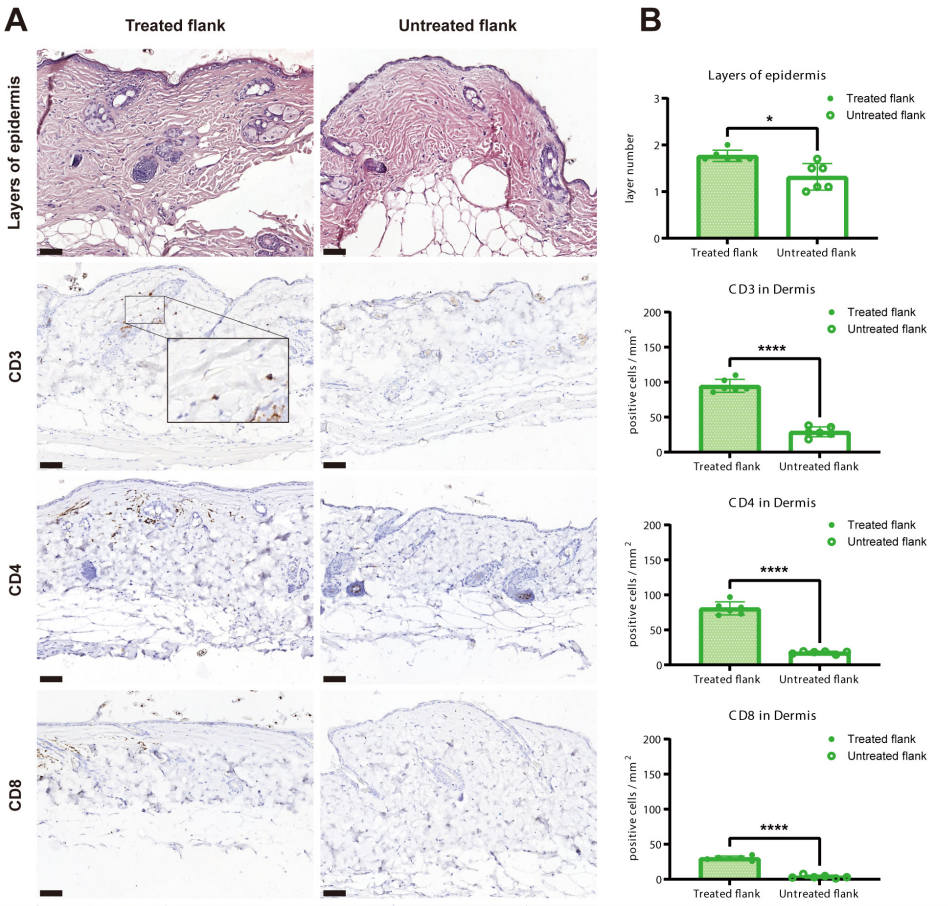

Figure 4. (A) Representative HE staining images and immunohistochemistry staining image of CD3, CD4 and CD8. in treated flanks and untreated flanks. (B) Quantitative analysis of the layer numbers of epidermis (P = 0.0312) and the quantitative analysis of CD3 (P = 0.000052), CD4 (P = 0.000019) and CD8 (P = 0.000002). The results were obtained by counting within five high-power fields (HPFs) at 20x magnification for each slide, with the mean values displayed in the figure. Scale bar = 50 µm. The data were presented as means ± SDs. A paired t-test or non-parametric test was used. A p-value of 0.05 or below was considered significant (*) and $p < 0.0001$ (****) was considered highly significant.

3.Discussion

We established a novel controlled knockout transgenic mouse model to study the function of one-copy loss of *Hnrnpk* in CD4+ T cells. *HNRNPK* has a dual role in tumor suppression and tumor promotion, and its expression may be upregulated or downregulated in different types of tumors. (13, 20, 21) Previous RNA sequencing studies have shown downregulation of *HNRNPK* expression in CD4+ T cells from patient skin lesions of MF, the

most common type of CTCL. (5, 22) This abnormality may lead to *HNRNPK* dysfunction, affecting RNA processing and gene expression regulation. (23) Deletions in *HNRNPK* have also been identified in malignant cells from patients with Sézary syndrome and skin tumor samples from patients with MF. (17)

In further validating our *Hnrnpk flox Cd4CreER^{T2}* model, we conducted a comparison with the established *Socs1 flox Cd4CreER^{T2}* transgenic mouse model. (19) The *Socs1 flox Cd4CreER^{T2}* mice serve as targeting skin GEMMs (Genetically Engineered Mouse Models) in CTCL research. Specifically, the inflammatory responses observed following the deletion of *Socs1* in CD4+ T cells suggest that *Socs1* deletion may act as a potential initiator for CTCL. (18) This is similar to our approach in the *Hnrnpk flox Cd4CreER^{T2}* model, where the *Socs1 flox Cd4CreER^{T2}* mice employ a targeted gene knockout strategy. This method has effectively simulated the very early characteristics of CTCL, underscoring the relevance and applicability of our technique in studying CTCL pathogenesis. The precision in gene manipulation and the resulting phenotypic manifestations observed in the *Socs1 flox Cd4CreER^{T2}* model lend credibility to the skin painting method and gene knockout technique used in our study.

Thanks to the reporter gene, deletion of the *Socs1* gene in the CD4+ T cells of these hybrid mice can be detected via flow cytometry. (24) In the *Hnrnpk flox Cd4CreER^{T2}* mice, the knockout of Hnrnpk, which lacks a reporter gene, is verified by extracting DNA from enriched CD4+ T cells and employing PCR technology. These procedures have effectively confirmed the efficacy of the *Cd4CreER^{T2}* knockout tool.

In the *Socs1 flox Cd4CreER^{T2}* model, deletion of the Socs1 gene, combined with topical sensitizing stimuli, leads to autonomous skin inflammation exhibiting early MF characteristics. This closely mirrors the conditions observed in early-stage human CTCL. (25) Similarly, in our *Hnrnpk flox Cd4CreER^{T2}* mice, the targeted gene knockout resulted in a phenotype that accurately reflects early CTCL characteristics, particularly in early-stage MF. This similarity not only validates our methodological approach but also significantly enhances the potential of our model in revealing new insights into the molecular basis of CTCL. The ability to precisely knockout genes of interest, as demonstrated in both the *Socs1 flox Cd4CreER^{T2}* and our *Hnrnpk flox Cd4CreER^{T2}* models, is crucial for dissecting the complex interplay of genetic factors in the pathogenesis and progression of CTCL.

Our novel mouse model shows no significant disturbances in the immune cell population in peripheral blood, aligning with the localized nature of MF in CTCL and the challenge of distinguishing benign and malignant T cells in early-stage MF skin lesions. (4,8) In our new mouse model, skin inflammation persists even after the stimulus is removed,

indicating a sustained chronic inflammatory response locally. However, there were no significant disturbances observed in the immune cell population in the peripheral blood. This pattern aligns with the early manifestations MF in CTCL, characterized by long-lasting and persistent inflammation limited to the skin. (2,26) Most MF patients also suffer from localized skin diseases, and distinguishing between benign and malignant T cells in early-stage MF lesions is challenging due to their shared T-cell characteristics and overlapping phenotypes. (27)

CTCL involves the coexistence of malignant CD4+ T cells, secreting cytokines, and normal tissue-resident memory T cells (TRM cells) that also contribute to the complex microenvironment through cytokine secretion.(28) CTCL cells, and CD4+ TRM cells, share a common tissue differentiation program likely influenced by the skin microenvironment. (29) In our mouse model, dermal infiltrating lymphocytes in *Hnrnpk* knockout mice primarily consisted of CD3+ CD4+ cells, mirroring the lymphocyte profile seen in human CTCL skin lesions. The increase in CD8+ T cells was less pronounced, suggesting an expansion of cytotoxic CD8+ T cells followed by gradual depletion.

Next to introducing the new mutant mouse model in this study, several limitations need to be addressed. The first limitation is the sample size of mice in long-term experiments. Additionally, further investigations are needed to validate the findings from sequencing studies in CTCL patients and explore the role of *HNRNPK* deletion in CTCL development and progression.

In conclusion, we established a novel genetically modified mouse model with conditional *Hnrnpk* knockout specifically in CD4+ T cells to investigate its role in CTCL pathogenesis. This model exhibits features consistent with CTCL, such as chronic skin inflammation, lymphocytic infiltration predominantly composed of CD3+ CD4+ cells. Our work provides insights into the mechanisms underlying CTCL progression and validates findings from sequencing studies in CTCL patients. Future mice studies with larger sample sizes and longer follow-up are necessary to further enhance our understanding of *HNRNPK* involvement in CTCL.

4.Materials and Methods

4.1.Animals

All mouse experiments were supervised by the animal welfare committee (IvD) of the Leiden University Medical Center and approved by the national central committee of animal experiments (CCD) under the permit number AVD116002015271, in accordance with the Dutch Act on Animal Experimentation and EU Directive 2020/63/EU.

Hnrnpk flox (*Hnrnpk*em1Lumc; MGI:99894) mice where loxP sites were introduced in *Hnrnpk* intron 2 and intron 6 were generated at LUMC. *Hnrnpk* flox mice using CrisprCas9 RNP and 200 bp single-stranded oligodeoxynucleotides (ssODN). (all from IDT) *Cd4CreER*^{T2} mice (Tg(*Cd4-cre/ER*^{T2})11Gnri/J; MGI:5493114; JAX:022356) expressing *CreER*^{T2} recombinase under the control of the *Cd4* promoter were purchased from The Jackson Laboratory (JAX). *Hnrnpk* flox mice were mated with *Cd4CreER*^{T2} mice to generate *Hnrnpk flox Cd4CreER*^{T2} mice. The offspring inherited both the targeted *Hnrnpk flox* allele and the *Cd4CreER*^{T2} transgenes.

Male *Hnrnpk flox/wt Cd4CreER*^{T2}+ mice, 12-15 weeks old, were housed in a temperature-controlled room with a 12-hour light-dark cycle. Throughout the experiment, food and tap water were available ad libitum.

4.2.Tamoxifen and oxazolone application

Tamoxifen (TAM, Sigma-Aldrich, Netherlands) was dissolved in peanut oil at a concentration of 10 mg/ml, and 4-hydroxy-Tamoxifen (4OHT, Sigma-Aldrich, Netherlands) was dissolved in ethanol (20 mg/ml) and sonicated for 2 minutes. Tamoxifen was administered at a dose of 1 mg per mouse per day by intraperitoneal injection for 5 consecutive days. 4OHT was topically administered at a dose of 1mg per mouse on the left shaved skin (2 cm × 3 cm). Oxazolone (4-Ethoxymethylene-2-phenyl-2-oxazolin-5-one, Sigma-Aldrich, Netherlands) was dissolved in acetone. A freshly made solution of oxazolone was used for each experiment. The application schedule was as follows: On the first day, 1.5% OXA was applied to the abdomen for induction. On the eighth day, 0.5% OXA was applied to the left flank. On the ninth day, the CRE-Lox system was activated with 4OHT to knock out *HNRNPK* in CD4+ T cells. From week 2 to week 10, 0.5% OXA was applied three times per week to the left flank. From week 11 to week 20, 0.5% OXA was applied twice per week to the left flank. From week 21 to week 40, the mice were monitored for their overall condition, particularly their skin condition. The corresponding right flank was used as the control using the vehicle only.

Peripheral blood samples were collected from mice via the tail vein weekly or biweekly, and flow cytometry was performed to analyze the immune cell populations in the peripheral blood. At the end of week 40, skin specimens were collected from both the left and right flanks of the mice for cell extraction and preparation of paraffin-embedded sections.

4.3.Cell isolation and DNA isolation

Intact skin cells were isolated by taking a 4 mm^2 skin biopsy, which was then digested

using the whole skin dissociation Kit (Miltenyi Biotec, NL) following the manufacturer's instructions. CD4+ T splenocytes were isolated and enriched by processing the spleen using lysis buffer (from Hospital Pharmacy at LUMC) to obtain splenocytes. CD4+ T cells were enriched from the splenocyte suspension using The BD IMag™ Mouse CD4+ T Lymphocyte Enrichment Set (BD Biosciences, NL). DNA was isolated from ear-clips and the CD4+ T cells from splenocytes using DNeasy Blood & Tissue Kits (Qiagen, NL).

Genomic PCR was conducted to analyze the genotypes of mice using ear DNA and gene-specific primers (**Supplementary Table 1**) for the *Hnrnpk* flox transgene and *Hnrnpk* wildtype gene. Genomic PCR was conducted on the DNA from enriched CD4+ splenoctyes to detect the recombinant *Hnrnpk* transgene and unrecombined *Hnrnpk* wildtype gene using the three different sets of gene-specific primers respectively (**Supplementary Table 2**).

4.4.Flow cytometry

Samples from isolated skin cells, splenocytes before and after CD4+ T cell enrichment, and blood were used for flow cytometry. Blood samples were handled and stained as described previously. (18) Fluorescence-labeled antibodies, including Live/Dead marker (clone Zombie, BD, Netherlands), anti-mouse CD3 (clone 145-2C11, BD, Netherlands), anti-mouse CD19 (clone 1D3, Thermo Fisher Scientific, Netherlands), anti-mouse CD4 (clone RM4-5, Thermo Fisher Scientific, Netherlands), and anti-mouse CD8 (clone 53-6.7, Biolegend, Netherlands), were used. Samples were processed in a BD Fortessa flow cytometer, and the data were analyzed using FlowJo software.

4.5.Histological and immunohistochemical analyses

Skin samples were fixed with 4% paraformaldehyde, dehydrated, and paraffin-embedded. Sections (4 μm-thick) were cut with a microtome (Leica 149MULTI0C1). Tissue sections were stained with hematoxylin and eosin. For immunohistochemistry analyses, tissue sections were deparaffinized, rehydrated, and blocked for endogenous peroxidase using 0.3% hydrogen peroxide and nonspecific antibody binding using a blocking buffer (SuperBlock, Thermo Fisher Scientific, The Netherlands). Antigen retrieval was performed using citric acid (pH 6.0) solution. The tissue sections were incubated with the following primary antibodies at 4°C overnight: anti-mouse CD3 (1:200, D7A6E, Cell Signaling Technology, Netherlands), anti-mouse CD4 (1:100, D7D2Z, Cell Signaling Technology, Netherlands), anti-mouse CD8 (1:1600, 4SM15, eBioscience™, Netherlands). Then, sections were incubated with secondary antibodies at room temperature for 60 minutes. Sections were visualized with the Vectastain Elite Kit (Vector Labs, Netherlands) and

diaminobenzidine (Dako Omnis, Agilent Dako, Netherlands). After counterstaining with hematoxylin, sections were mounted. The scanner (3DHISTECH, Pannoramic 250) was used for microscopic examination and image acquisition.

The layers of the epidermis were counted within 5 high-power fields (HPF) (20x magnification) of each slide, and the mean values were calculated for subsequent statistical analysis. The numbers of CD3+, CD4+, and CD8+ lymphocytes in the dermis were counted within 5 HPF (20x magnification) per case. The values were normalized to cells/ mm^2, and the mean numbers were assessed for further statistical analysis. The evaluations were conducted by two independent individuals who were blinded to sample information.

4.6.Statistical analysis

Statistical analysis was performed using GraphPad Prism software (version 8.0.1). A paired *t*-test was used to compare the treated flank and untreated flank in mice. A *p*-value of 0.05 or below was considered significant (*), $p < 0.01$ (**), $p < 0.001$ (***) and $P < 0.0001$ (****) was considered highly significant.

References

1 Willemze, R. Primary cutaneous lymphoma: the 2018 update of the WHO-EORTC classification. Presse Med 51, 104126, doi:10.1016/j.lpm.2022.104126 (2022).

2 Rein Willemze, L. C., Werner Kempf, Emilio Berti,Fabio Facchetti,5 Steven H. Swerdlow,and Elaine S. Jaffe. The 2018 update of the WHO-EORTC classification for primary cutaneous lymphomas. Blood (2018).

3 Tensen, C. P., Quint, K. D. & Vermeer, M. H. Genetic and epigenetic insights into cutaneous T-cell lymphoma. Blood 139, 15-33, doi:10.1182/blood.2019004256 (2022).

4 Ren, J. et al. Integrated transcriptome and trajectory analysis of cutaneous T-cell lymphoma identifies putative precancer populations. Blood Adv 7, 445-457, doi:10.1182/bloodadvances.2022008168 (2023).

5 Bastidas Torres, A. N. et al. Genomic analysis reveals recurrent deletion of JAK-STAT signaling inhibitors HNRNPK and SOCS1 in mycosis fungoides. Genes Chromosomes Cancer 57, 653-664, doi:10.1002/gcc.22679 (2018).

6 Gill, R. P. K. et al. Understanding Cell Lines, Patient-Derived Xenograft and Genetically Engineered Mouse Models Used to Study Cutaneous T-Cell Lymphoma. Cells 11, doi:10.3390/cells11040593 (2022).

7 Kalliara, E., Belfrage, E., Gullberg, U., Drott, K. & Ek, S. Spatially Guided and Single Cell Tools to Map the Microenvironment in Cutaneous T-Cell Lymphoma. Cancers (Basel) 15, doi:10.3390/cancers15082362 (2023).

8 Han, Z. et al. MicroRNA Regulation of T-Cell Exhaustion in Cutaneous T Cell Lymphoma. J Invest Dermatol 142, 603-612 e607, doi:10.1016/j.jid.2021.08.447 (2022).

9 Trochopoulos, A. G. X. et al. Micellar Curcumin Substantially Increases the Antineoplastic Activity of the Alkylphosphocholine Erufosine against TWIST1 Positive Cutaneous T Cell Lymphoma Cell Lines. Pharmaceutics 14, doi:10.3390/pharmaceutics14122688 (2022).

10 Patil, K. et al. Molecular pathogenesis of Cutaneous T cell Lymphoma: Role of chemokines, cytokines, and dysregulated signaling pathways. Semin Cancer Biol 86, 382-399, doi:10.1016/j.semcancer.2021.12.003 (2022).

11 Barboro, P., Ferrari, N. & Balbi, C. Emerging roles of heterogeneous nuclear ribonucleoprotein K (hnRNP K) in cancer progression. Cancer Lett 352, 152-159, doi:10.1016/j.canlet.2014.06.019 (2014).

12 Mucha, B. et al. Tumor suppressor mediated ubiquitylation of hnRNPK is a barrier to oncogenic translation. Nat Commun 13, 6614, doi:10.1038/s41467-022-34402-6 (2022).

13 Gallardo, M. et al. Aberrant hnRNP K expression: All roads lead to cancer. Cell Cycle 15, 1552-1557, doi:10.1080/15384101.2016.1164372 (2016).

14 Naarmann-de Vries, I. S. et al. Characterization of acute myeloid leukemia with del(9q) - Impact of the genes in the minimally deleted region. Leuk Res 76, 15-23, doi:10.1016/j.leukres.2018.11.007 (2019).

15 Dayyani, F. et al. Loss of TLE1 and TLE4 from the del(9q) commonly deleted region in AML cooperates with AML1-ETO to affect myeloid cell proliferation and survival. Blood 111, 4338-4347, doi:10.1182/blood-2007-07-103291 (2008).

16 Gallardo, M. et al. hnRNP K Is a Haploinsufficient Tumor Suppressor that Regulates Proliferation and Differentiation Programs in Hematologic Malignancies. Cancer Cell 28, 486-499, doi:10.1016/j.ccell.2015.09.001 (2015).

17 Park, J., Daniels, J., Wartewig, T., Ringbloom, K. G., Martinez-Escala, M. E., Choi, S., Thomas, J. J., Doukas, P. G., Yang, J., Snowden, C., Law, C., Lee, Y., Lee, K., Zhang, Y., Conran, C., Tegtmeyer, K., Mo, S. H., Pease, D. R., Jothishankar, B., Kwok, P. Y., … Choi, J. Integrated genomic analyses of cutaneous T-cell lymphomas reveal the molecular bases for disease heterogeneity. Blood, doi:10.1182/blood.2020009655 (2021).

18 Luo Y, V. M., de Haan S, Kinderman P, de Gruijl FR, van Hall T, et al. . Socs1-knockout in skin-resident CD4(+) T cells in a protracted contact-allergic reaction results in an autonomous skin inflammation with features of early-stage mycosis fungoides. Biochem Biophys Rep 35, 101535, doi:10.1016/j.bbrep.2023.101535 (2023).

19 Luo, Y. et al. In vivo modelling of cutaneous T-cell lymphoma: The role of SOCS1. Front Oncol 12, 1031052, doi:10.3389/fonc.2022.1031052 (2022).

20 Wang Z, Q. H., He J, Liu L, Xue W, Fox A, et al. The emerging roles of hnRNPK. J Cell Physiol 235, 1995-2008, doi:10.1002/jcp.29186 (2020).

21 Chen Y, Z. Y., Xiao Z, Chen S, Li Y, Zou J, et al. Role of heterogeneous nuclear ribonucleoprotein K in tumor development. J Cell Biochem 120, 14296-14305, doi:10.1002/jcb.28867 (2019).

22 Fan, X. et al. Cytoplasmic hnRNPK interacts with GSK3beta and is essential for the osteoclast differentiation. Sci Rep 5, 17732, doi:10.1038/srep17732 (2015).

23 Xu, Y. et al. New Insights into the Interplay between Non-Coding RNAs and RNA-Binding Protein HnRNPK in Regulating Cellular Functions. Cells 8, doi:10.3390/cells8010062 (2019).

24 Aghajani, K., Keerthivasan, S., Yu, Y. & Gounari, F. Generation of CD4CreER(T2) transgenic mice to study development of peripheral CD4-T-cells. Genesis 50, 908-913, doi:10.1002/dvg.22052 (2012).

25 Krejsgaard, T. et al. Malignant inflammation in cutaneous T-cell lymphoma-a hostile takeover. Semin Immunopathol 39, 269-282, doi:10.1007/s00281-016-0594-9 (2017).

26 Vieyra-Garcia, P. et al. Benign T cells drive clinical skin inflammation in cutaneous T cell lymphoma. JCI Insight 4, doi:10.1172/jci.insight.124233 (2019).

27 Roediger, B. & Schlapbach, C. T cells in the skin: Lymphoma and inflammatory skin disease. J Allergy Clin Immunol 149, 1172-1184, doi:10.1016/j.jaci.2022.02.015 (2022).

28 Stolearenco, V. et al. Cellular Interactions and Inflammation in the Pathogenesis of Cutaneous T-Cell Lymphoma. Front Cell Dev Biol 8, 851, doi:10.3389/fcell.2020.00851 (2020).

29 Bertschi, N. L., Bazzini, C. & Schlapbach, C. The Concept of Pathogenic TH2 Cells: Collegium Internationale Allergologicum Update 2021. Int Arch Allergy Immunol 182, 365-380, doi:10.1159/000515144 (2021).

Supplementary Information

Supplementary Table 1. Sequence information

	Sequence	
5'Loxp ssODN		
	GCAGTACAGTTTTTCCAACCAACATTTTAA TCCTTTGAAATACTTATTAAAATAAGGCCTT TGATATTAGGGATATTAGGGAGACAAataac ttcgtataatgtatgctatacgaagttatctcgagAGG CAGGGACTTAAAAAGTGGCTTCAATTACC CTTTCTTGGGGGATGTTTCTAATTGAAAAT TTAAACTTTAA	Homology arms in uppercase; loxP+ restrictionsite in lowercase
5'sgRNA intron 2	AGGGATATTAGGGAGACAA	
3'Loxp ssODN		
	GGAAGTTTATTTATAGTTCAGTTCCAGGTT ACTTCCATCTTAGGCAGTTGCAGCTACAG GAGCTTGTCATAGTGTTTGTATAGACAAGG tctagaataacttcgtataatgtatgctatacgaagtta tAGGAAGCACTGGGCCTATGAGTTCTGCT GTTAGGCTTATTTTCTTTATTAACATTAAGA GTCTAATCA	Homology arms in uppercase; loxP+ restrictionsite in lowercase
3'sgRNA intron 6	TAGTGTTTGTATAGACAAGG	

Supplementary Table 2. Primer information

Primer	Sequence
Hn_int2_Fw	TTCTTGCACAGGTTAAAAAGCA
Hn_int2loxP_Fw	TCGAGAGGCAGGGACTTAAA
Hn_ex3_Rev	CCATATCTTCTGCAGGGCGT
Hn_int6_Fw	AGGCTGGCCATTCCTAGAGT
Hn_int6loxP_Fw	TAGGCAGTTGCAGCTACAGG
Hn_ex7_Rev	ACAGCATCAGATTCGAGCGG
Hn_KO_Fw	AGTAACCTTTTCTTGCACAGGT
Hn_KO_Rev	CGTGATCAGGCTATTGTCGC

Supplementary Table 3. Primer information

Primer	Sequence
hnRNPK_KO_F1	AGTAACCTTTTCTTGCACAGGT
hnRNPK_KO_R1	CGTGATCAGGCTATTGTCGC
hnRNPK_KO_F2	CCTTTTCTTGCACAGGTTAAAAAGC
hnRNPK_KO_R2	CAGGCTATTGTCGCATATATTGGT
hnRNPK_KO_F3	AGCAGTACAGTTTTTCCAACCA

hnRNPK_KO_R3	AGTGTCTAGCGTGATCAGGC
hnRNPK_WT_F1	TTCCCCAACACCGAAACCAA
hnRNPK_WT_R1	CAGTAGAGTGAGGGCAGCAC
hnRNPK_WT_F2	TCAGAGTCTGGCAGGAGGAA
hnRNPK_WT_R2	CCATGCCATCATAGCGGTCT
hnRNPK_WT_F3	GTGCTGCCCTCACTCTACTG
hnRNPK_WT_R3	GGGCTCCATGTGTCAATTGC

Supplementary Figure 1. Representative images of the shave treated flank and untreated flank on D19(week 3) and D67 (week 67) during experiment.

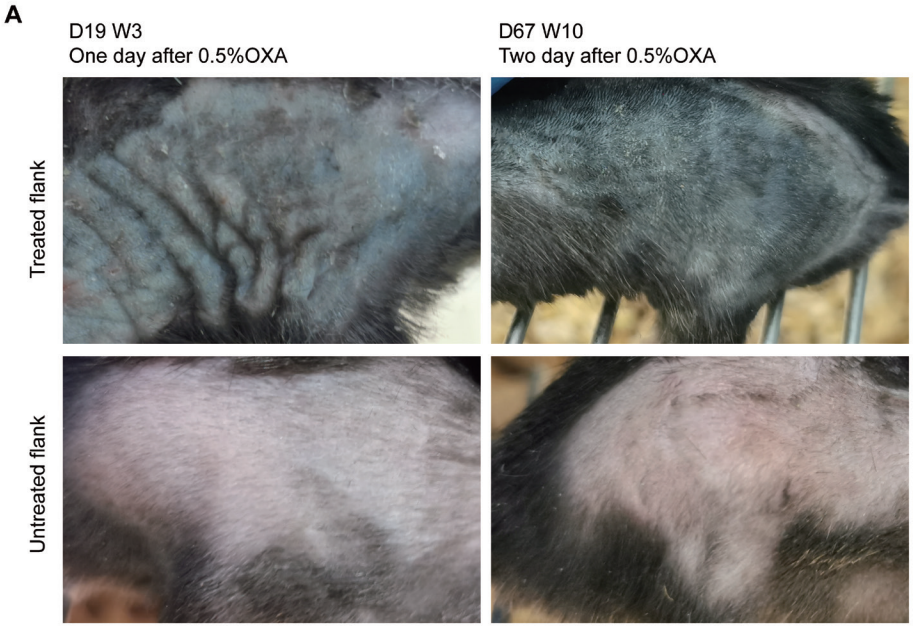

5

Role of *HNRNPK* Deletion in Initiating Cutaneous T-Cell Lymphoma Pathogenesis: An Inducible Knockout Mouse Model

Yixin Luo[1], Maarten H. Vermeer[1], Julia Van de Bie[1], Sanne de Haan[1], Peter Hohenstein[2], Frank R. de Gruijl[1], Cornelis P. Tensen[1]
1.Department of Dermatology, Leiden University Medical Center, Leiden, The Netherlands
2.Transgenic Facility Leiden, Central Animal Facility, Leiden University Medical Center, The Netherlands

The manuscript has been prepared and is ready for submission

Abstract:

Background: Recent genomic analysis has unveiled recurrent heterogeneous nuclear ribonucleoprotein K (*HNRNPK*) gene deletions in cutaneous T-cell lymphoma (CTCL). *HNRNPK* acts as a tumor suppressor by inhibiting the JAK-STAT pathway. **Objective**: This study investigates the pivotal role of *Hnrnpk* deletion in initiating CTCL pathogenesis using a transgenic mouse model. **Methods and Results**: *Hnrnpk* was knocked out in skin-infiltrating CD4+ T cells in transgenic mice (oxazolone, OXA, contact allergic reaction followed by topical tamoxifen to activate k.o.) which were then subjected to repeated applications of OXA (3-2/wk for 20 wks). After discontinuing OXA, autonomous inflammation persisted. Remarkably, *Hnrnpk* haploinsufficiency alone was sufficient to elicit these phenotypic changes. Comprehensive flow cytometry analyses of blood samples in the course of the experiment showed no evident effect but post mortem analyses of skin samples corroborated and characterized the persistent inflammation. Histological examinations revealed increased epidermal thickness and inflammatory cell infiltration, particularly CD3+ CD4+ T-cells, in *Hnrnpk* knockout mice exposed to long-term OXA treatment. Immunohistochemistry demonstrated heightened cell proliferation (Ki-67 expression) and augmented JAK-STAT signaling (p-STAT3) in these mice – all reminiscent of early CTCL. **Conclusion**: Our results underscore the significance of *Hnrnpk* deletion in CD4+ T-cells leading to autonomous skin inflammation, emulating early stages of CTCL, thereby confirming *HNRNPK*'s tumor-suppressive role. This *in vivo* model gives experimental access to the intricate processes involving *HNRNPK* in T-cell modulation, affecting epidermal homeostasis, and in CTCL pathogenesis, opening new avenues for potential therapeutic interventions.

Key words: Cutaneous T-cell lymphomas; JAK-STAT Pathway; CD4+ T cells; *HNRNPK*; Transgenic mouse

1 Introduction

Recent genomic analysis of cutaneous T-cell lymphoma (CTCL) has revealed recurrent deletion of the heterogeneous nuclear ribonucleoprotein K (*HNRNPK*) gene in two of the most common subtypes of CTCL, mycosis fungoides (MF) and Sézary syndrome (SS). (1-3) *HNRNPK* is a tumor suppressor gene that inhibits the JAK-STAT signaling pathway, and its deletion can lead to dysfunction of *HNRNPK*, which affects RNA processing and gene expression regulation. (4-6)

The potential impact of haploinsufficiency in this tumor suppressor gene is one of the notable characteristics of *HNRNPK*. *HNRNPK* haploinsufficiency resulted in reduced survival, increased tumor formation, genomic instability, and the development of transplantable hematopoietic neoplasms with myeloproliferation. (7) Haploinsufficiency of tumor suppressor genes (TSGs) can contribute to tumor development and progression by reducing levels of proteins, accelerating tumor development, promoting cancer progression, and collaborating with other haploinsufficient TSGs. (8-10)

The deletion of *HNRNPK* and other tumor suppressor genes (such as *SOCS1*, *STK11*, and *CDKN2A/B*) involved in commonly deregulated pathways in MF has been identified through next-generation sequencing (NGS) analysis. (1) A new mouse model with conditional *HNRNPK* knockout has been successfully established, which solves the lethality issue of direct *HNRNPK* knockout and confirms that this new mouse strain maintains relatively undisturbed immune homeostasis in the peripheral blood under chronic antigen exposure.

This study utilized a novel strain of homozygous and heterozygous mice to elucidate the role of *Hnrnpk* as an initiating factor when deleted in skin-homing CD4+ T cells, combined with repeated exposure to OXA simulation skin inflammation. Even after discontinuing 20 weeks of OXA applications, lymphocytic infiltration persisted, resulting in an authonomous inflammation with increased cell proliferation and sustained JAK-STAT pathway activation; features consistent with precursor stages of CTCL. A comparison between *Hnrnpk* double-copy deletion and *Hnrnpk* single-copy deletion mice revealed that the loss of a single allele of the *Hnrnpk* gene was already sufficient to cause this phenotypical change.

In sum, we investigated the role of *Hnrnpk* deletion as an initiating factor in the pathogenesis of CTCL in skin-homing CD4+ T cells, confirming the tumor-suppressive function of *Hnrnpk* and the impact of haploinsufficiency.

2.Result

2.1.Contact-allergic reaction in inducible *Hnrnpk* knock-out mice from long-term and

short-term oxazolone treatment groups

To determine the effect of oxazolone (OXA) treatment in inducing and maintaining inflamed skin in inducible *Hnrnpk* knock-out mice, a 1.5% concentration of OXA was administered topically on the shaved abdominal skin to sensitize *Hnrnpk fl/fl Cd4CreER^{T2}*+/- (FL/FL), *Hnrnpk fl/wt Cd4CreER^{T2}*+/- (FL/WT), and *Hnrnpk wt/wt Cd4CreER^{T2}*+/- (WT/WT) mice. Subsequently, a 0.5% concentration of OXA was applied 3 times a week (initially, and then twice after 10 weeks) on the shaved left flank from week 2 to week 20 (**Figure 1A**). This regimen established the experimental group as the long-term OXA group. An additional group of mice was included as a control group for the initial short-term OXA exposure. This group did not receive any application of 0.5% OXA on their skin from week 2 to week 20, as depicted in **Figure 1B.**

In both experimental groups, none of the mice displayed any signs of wounding from scratching in response to a possible pruritus (**Supplementary Figures 1 and 2**). Visible signs of inflammation, such as redness, flaking, and a rough texture, were observed on the treated flanks of all mice one day after the first application of 0.5% OXA on the skin. In contrast, the untreated skins of all mice in both long-term and short-term OXA treatment groups did not show any indication of inflammation.

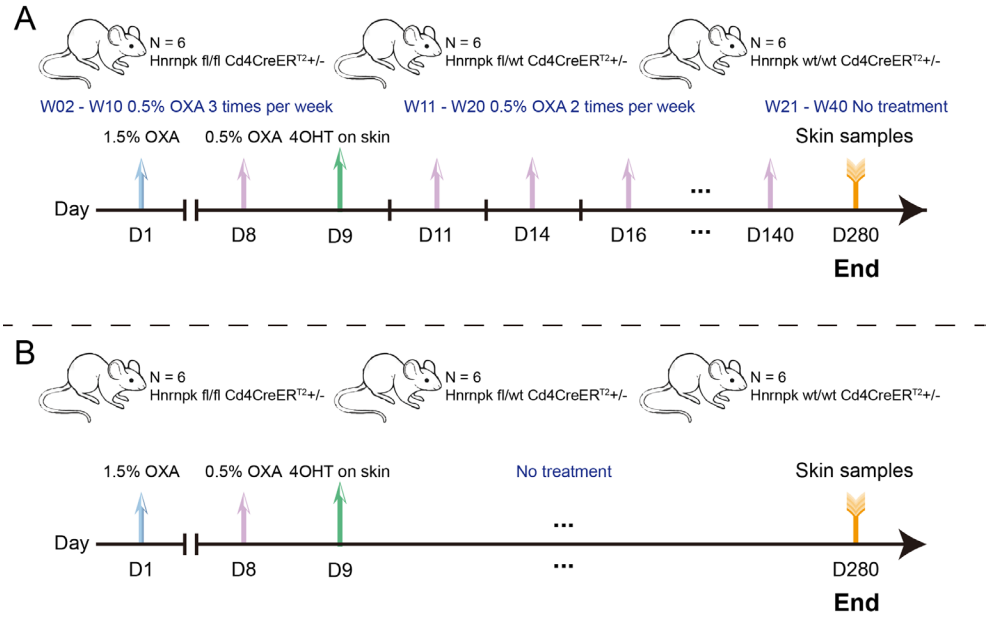

Figure 1. Schematic time-course representation of the experimental groups and different treatment

periods with oxazolone. (A). Long-term treatment period: the left flanks of *Hnrnpk fl/fl Cd4CreER^{T2}*+/-, *Hnrnpk fl/wt Cd4CreER^{T2}*+/- and *Hnrnpk wt/wt Cd4CreER^{T2}*+/- mice were treated with OXA 3 times per week from week 2 to 10 and 2 times per week from week 11 to 20. From week 21 to 40, no OXA was administrated on the skin of the mice. B) Short-term treatment period: *Hnrnpk fl/fl Cd4CreER^{T2}*+/-, *Hnrnpk fl/wt Cd4CreER^{T2}*+/- and *Hnrnpk wt/wt Cd4CreER^{T2}*+/- mice without OXA treatment from week 2 to 40. In both treatment groups the mice were treated on day 1 and 8 with OXA and 4OHT was applied on day 9. Mice were sacrificed on day 280. n is 6 per genotype. Abbreviations: D is day, W is week, OXA is oxazolone, 4OHT is 4-hydroxy-tamoxifen. Blood collection was performed 24 hours after OXA application. Skin samples were collected at the end of the experiment.

2.2.Long-term oxazolone application caused local skin inflammation rather than systemic effect

Flow cytometry analysis showed successful cell extraction post mortem from mouse skin, and the proportion of CD4+ and CD8+ cells among CD3+ cells was determined. (**Figure 2A**) The long-term OXA group exhibited a statistically significant increase in the proportion of CD4+ cells among CD3+ cells in the treated flanks of *Hnrnpk* knockout mice (FL/FL and FL/WT), as compared to the treated flanks of WT/WT mice. No statistically significant disparity is observed in the proportion of CD4+ cells among CD3+ cells in the treated flanks when comparing FL/FL and FL/WT conditions. (**Figure 2B**) In addition, there was a notable rise in the proportion of CD4+ cells to CD3+ cells in the treated flanks of *Hnrnpk* knockout mice (FL/FL and FL/WT) compared to the untreated flanks. Similar results were seen for the fraction of CD8+ cells among CD3+ cells. (**Figure 2C**) In the short-term OXA treatment group, no statistically significant differences were observed between the treated and untreated flanks when comparing across all groups.

Flow cytometry analysis was performed on the peripheral blood samples collected weekly from the mice in both experimental groups. The ratio of circulating CD3+ and CD19+ cells and CD4+ and CD8+ cells was measured to assess the overall status of the mice's immune system. In both the long-term and short-term groups, the peripheral blood of all mice did not show any disturbance in the ratio of CD3+ cells to CD19+ cells. (**Figure 2D**) Likewise, the proportion of CD4+ cells to CD8+ cells in the peripheral blood of all mice exhibited no noticeable variations. (**Figure 2E**) Throughout the investigation, the sub-population ratios of immune cells remained relatively stable.

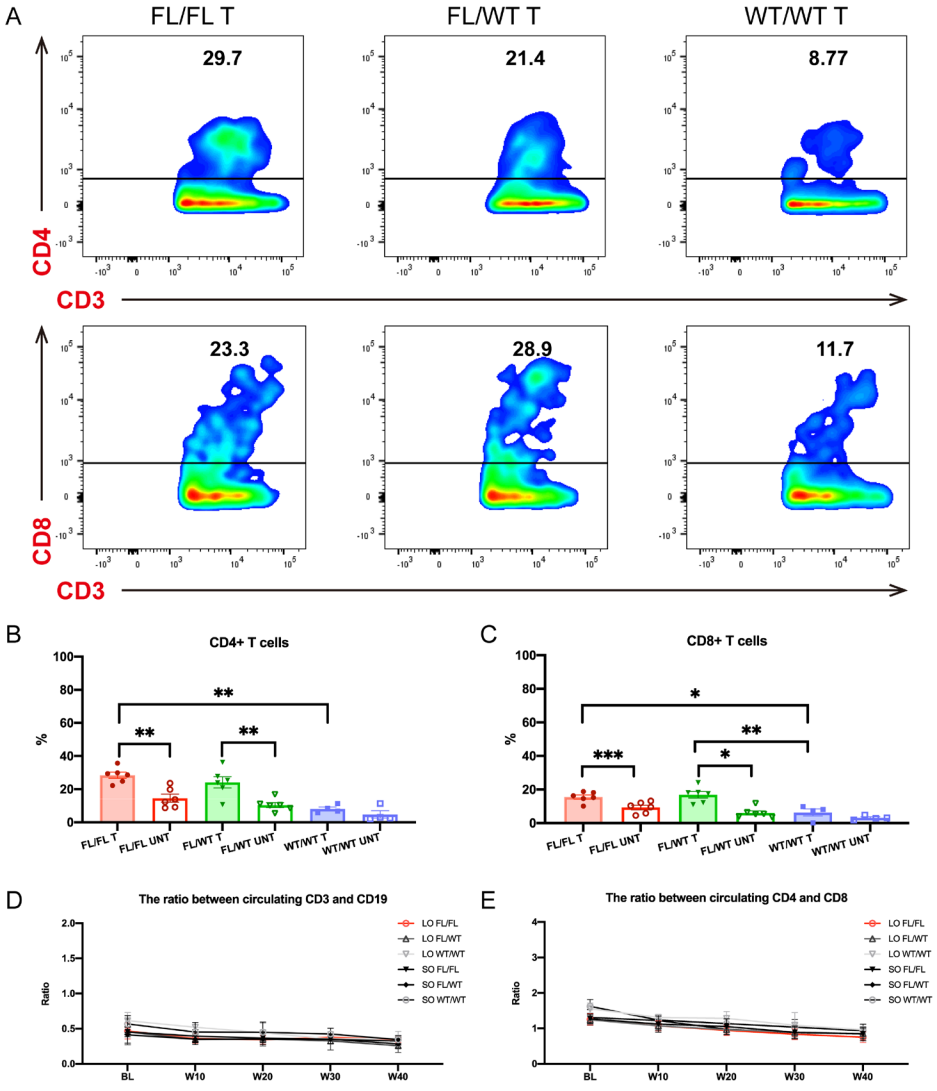

Figure 2. Flow cytometry analysis of skin and peripheral blood of *Hnrnpk fl/fl Cd4CreER*^{T2}+/-, *Hnrnpk fl/wt Cd4CreER*^{T2}+/- and *Hnrnpk wt/wt Cd4CreER*^{T2}+/- mice from the long-term and short-term OXA treatment groups showed T cells infiltration in skin and no systemic inflammation. (A). Representative flow cytometry plots and quantitative analysis of CD3+ CD4+ T cells and CD3+ CD8+ T cells in treated flanks of mice from the long-term group. (B) The quantitative analysis of CD3+ CD4+ T cells in the flanks of mice from long-term group. (C) The quantitative analysis of CD3+ CD8+ T cells in the flanks of mice from long-term group. (D) The ratio of CD3 to CD19 cells isolated from peripheral blood of mice in both long-term and short-term groups. (E) The ratio of CD4 to CD8 cells isolated from peripheral blood of mice in both long-term and short-term groups. Abbreviations: FL/FL is *Hnrnpk*

fl/fl Cd4CreER^{T2}+/-. FL/WT is *Hnrnpk fl/wt Cd4CreER*^{T2}+/-. WT/WT is *Hnrnpk wt/wt Cd4CreER*^{T2}+/-. T is treated flank. UNT is untreated flank. 'LO' is the long-term OXA treatment group, and 'SO' is the short-term OXA treatment group.

2.3.*Hnrnpk* deletion with long-term oxazolone treatment caused autonomous skin inflammation

HE staining was conducted on skin samples to assess and quantify the number of epidermal layers in the long-term and short-term treatment groups (**Figure 3, & Supplementary Figure 3**). In the long-term OXA group, the number of epidermal layers in treated flanks from FL/FL and FL/WT mice were significantly greater than those in untreated sides (**Figures 3A, & 3B**). There were no significant differences between genotypes. In the short-term treatment group, there were no statistically significant differences in the number of epidermal layers between the FL/FL and FL/WT mice and the WT/WT mice and the treated and untreated flanks from the same genotype. This showed that *Hnrnpk* deletion, in combination with long-term OXA treatment, caused a significant inflammatory response.

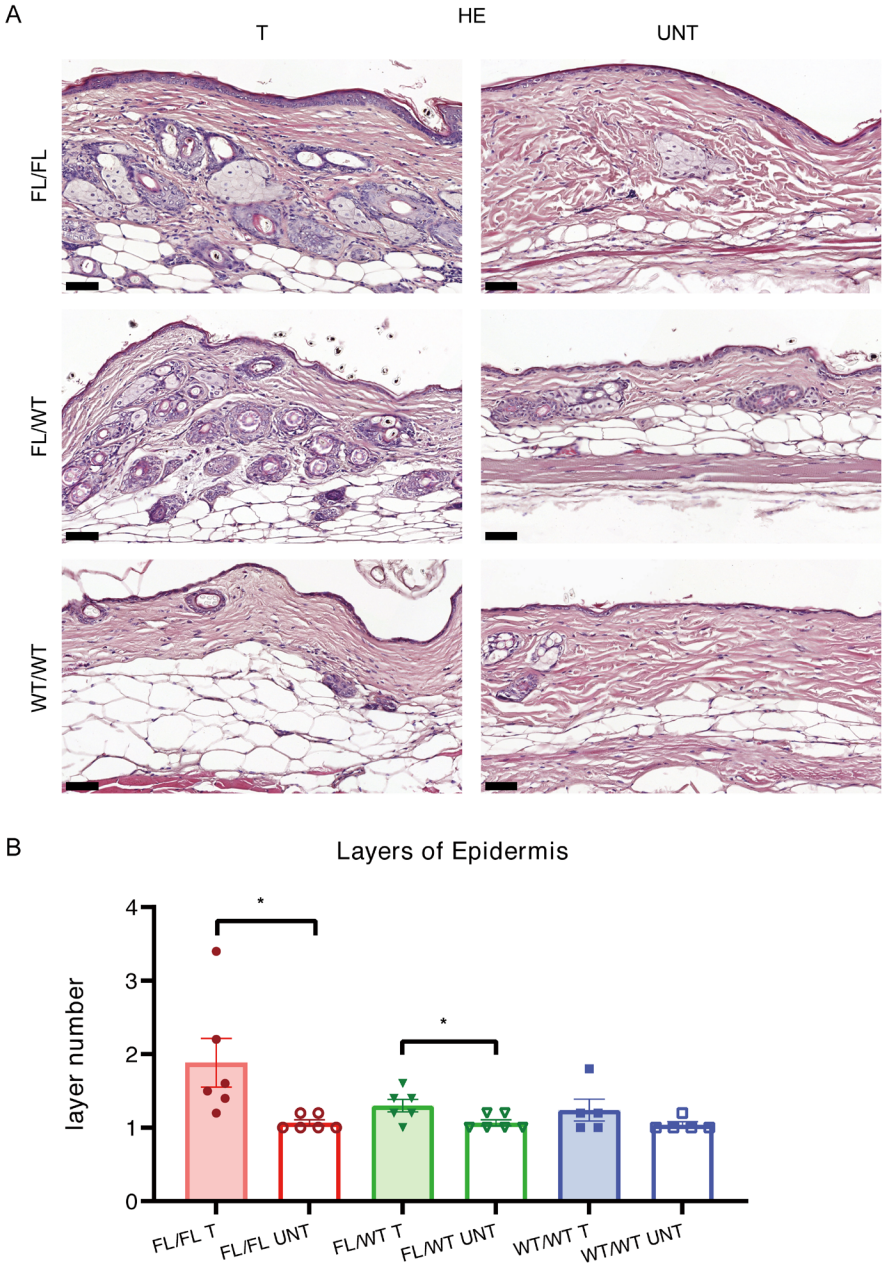

Figure 3. Histological examination of skin sections from the long-term treatment group indicated an increased number of epidermal layers in the treated flanks of *Hnrnpk fl/fl Cd4CreER*^{T2}+/- and *Hnrnpk fl/wt Cd4CreER*^{T2}+/- mice. (A). HE stained sections from treated and untreated flanks of mice in the long-term treatment group. Magnification is 20x and scale bar is 50 µm. (B) Quantification of the

number of epidermal layers of treated and untreated skin of the mice from long-term treatment group. Paired t-test and two-way ANOVA with a Tukey's post hoc test were used for statistical analysis. Error bars represent SEM and * indicates a significant difference (*$P < 0.05$). n is 5 or 6 per genotype. Abbreviations: FL/FL is *Hnrnpk fl/fl Cd4CreER^{T2}*+/-. FL/WT is *Hnrnpk fl/wt Cd4CreER^{T2}*+/-. WT/WT is *Hnrnpk wt/wt Cd4CreER^{T2}*+/-. T is treated flank. UNT is untreated flank.

2.4.*Hnrnpk* deletion increased the number of lymphocytes and caused autonomous skin inflammation

To evaluate the inflammatory response in the skin of transgenic mice, IHC staining was conducted to quantify the amount of CD3+, CD4+, and CD8+ T-cells in the dermis of the long-term and short-term OXA groups (**Figure 4; Supplemental Figures 4, 5 & 6**). The number of CD3+ and CD4+ positive stained cells in the treated flanks of transgenic mice (FL/FL and FL/WT) was considerably and statistically significantly higher in the long-term OXA group compared to the treated flanks of WT/WT mice (**Figure 4A, 4B, & 4C**). Moreover, the number of CD3+ and CD4+ cells in the dermis of the treated flanks of FL/FL and FL/WT mice was statistically significantly higher than in the untreated flanks (**Figures 4A, 4B, & 4C; Supplemental Figure 5**). Similar observations were made for CD8+ positive stained cells (**Figures 4A, & 4D; Supplemental Figure 5**). However, no significant change was seen between the treated flank sections of FL/FL mice and FL/WT mice. CD3+, CD4+, and CD8+ T-cells in the long-term OXA group showed in clusters. The short-term OXA group had no significant increases in inflammatory cells within or between groups. (**Supplementary Figures 4, & 6**). In untreated flanks, these findings showed that CD3+, CD4+, and CD8+ T-cells were more abundant in the treated skin sections of the transgenic mice in the long-term OXA group, particularly in the FL/FL and FL/WT mice when compared to the WT/WT mice, clearly showing that *Hnrnpk* loss along with long-term OXA treatment increased the skin inflammatory response.

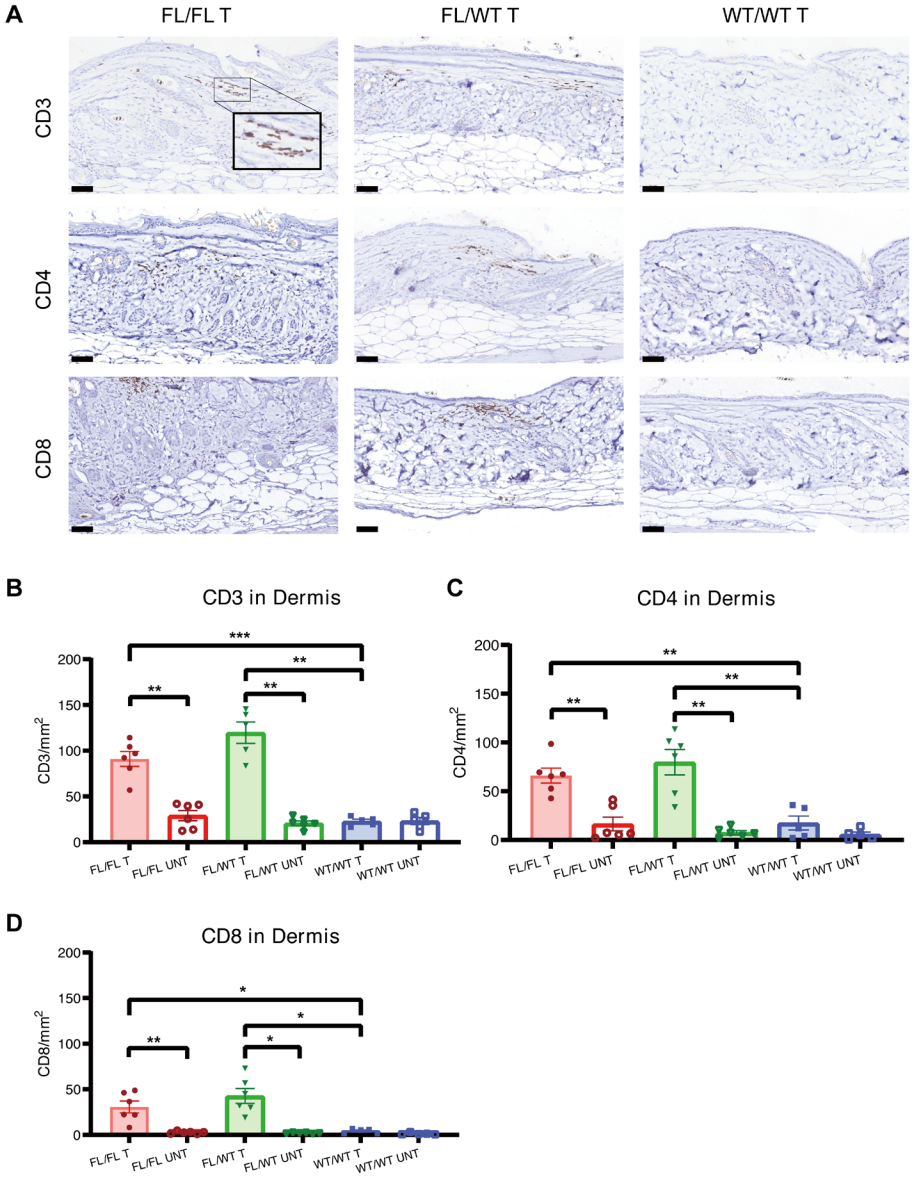

Figure 4. Histological analysis of treated skins from *Hnrnpk fl/fl Cd4CreER*^{T2}+/-, *Hnrnpk fl/wt Cd4CreER*^{T2}+/- and *Hnrnpk wt/wt Cd4CreER*^{T2}+/- mice of the long-term treatment group revealed increased number of CD3+, CD4+ and CD8+ cells in dermis. (A). Skin sections from the treated flanks of mice in the long-term treatment group, stained with markers for CD3, CD4, and CD8. Magnification is 20x and scale bar is 50 µm. (B, C, D) Quantification of the positive stained CD3+ (B), CD4+ (C) and CD8+ (D) cells in the dermis of treated (T) and untreated (UNT) flanks of the mice in

long-term treatment group. Paired *t*-test and two-way ANOVA with a Tukey's post hoc test were used for statistical analysis. Error bars represent SEM and * indicates a significant difference (*$P < 0.05$, **$P < 0.01$, ***$P < 0.001$, ****$P < 0.0001$). n is 5 or 6 per genotype. Abbreviations: FL/FL is *Hnrnpk fl/fl Cd4CreER^{T2}+/-*. FL/WT is *Hnrnpk fl/wt Cd4CreER^{T2}+/-*. WT/WT is *Hnrnpk wt/wt Cd4CreER^{T2}+/-*. T is treated flank. UNT is untreated flank.

2.5.Loss *Hnrnpk* in autonomous skin inflammation affected cell proliferation index

To investigate the impact of *Hnrnpk* deletion in CD4+ T-cells Ki-67 immunohistochemical staining was conducted on dermal samples of both the long-term and short-term treatment groups. The results of this analysis are presented in **Figure 5** and Supplementary **Figure 7**. The long-term treatment group exhibited a notable increase in Ki-67 positive cells in the flanks of FL/FL and FL/WT mice compared to WT/WT mice (**Figure 5A, & 5B**). Furthermore, a notable increase in Ki-67 activation was observed in both the dermis of the treated compared to those untreated flanks in FL/FL and FL/WT groups (**Figure 5A, & 5B**). No significant changes were found within and between the genotypes in the short-term therapy group (**Supplemental Figure 7**). The results of this study indicated that the levels of Ki-67 cells were enhanced in the treated skin sections of the transgenic mice subjected to to the long-term treatment. This showed that combining *Hnrnpk* deletion and long-term OXA treatment increased cell proliferation.

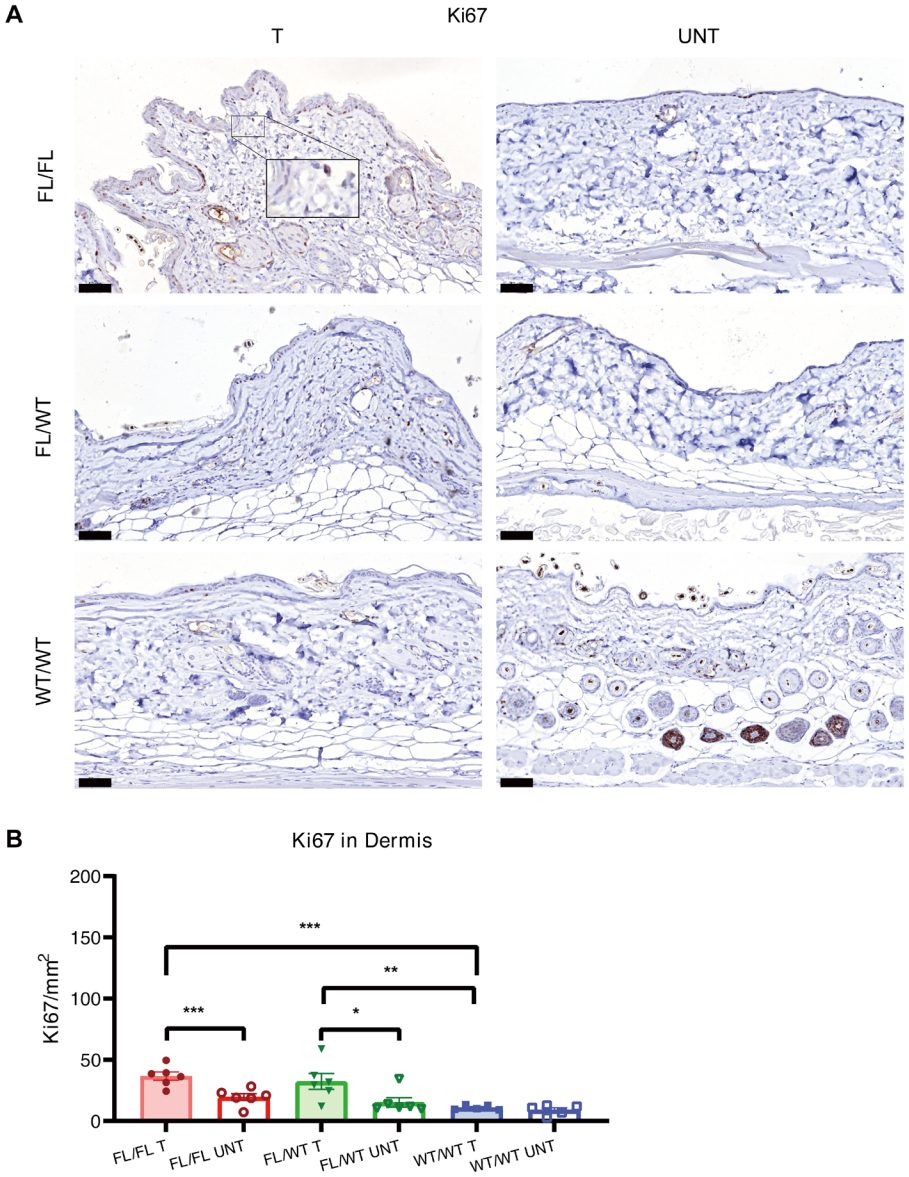

Figure 5. Histological analysis of treated and untreated skins from *Hnrnpk fl/fl Cd4CreER*^{T2}+/-, *Hnrnpk fl/wt Cd4CreER*^{T2}+/- and *Hnrnpk wt/wt Cd4CreER*^{T2}+/- mice of the long-term treatment group revealed increased number of Ki-67 positive cells in dermis. (A). Skin sections from the treated and untreated flanks of mice in the long-term treatment group, stained with Ki67. Magnification is 20x and scale bar is 50 µm. (B). Quantification of the positive stained p-STAT3 cells in dermis of treated and untreated skins of the mice from long-term treatment group. Paired *t*-test and two-way ANOVA with a Tukey's post hoc test were used for statistical analysis. Error bars represent SEM and *

indicates a significant difference (*$P < 0.05$, ***$P < 0.001$, ****$P < 0.0001$). n is 5 or 6 per genotype. Abbreviations: FL/FL is *Hnrnpk fl/fl Cd4CreER^{T2}+/-*. FL/WT is *Hnrnpk fl/wt Cd4CreER^{T2}+/-*. WT/WT is *Hnrnpk wt/wt Cd4CreER^{T2}+/-*. T is treated flank. UNT is untreated flank.

2.6.Loss *Hnrnpk* in autonomous skin inflammation affected the JAK-STAT signaling pathway

IHC staining was performed to analyze the number of p-STAT3 positive cells in the dermis of the long-term and short-term treatment groups to see if the *Hnrnpk* deletion in CD4+ T-cells with persistent skin inflammation affected the JAK-STAT signaling pathway (**Figure 6; Supplementary Figure 8**). In the long-term OXA group, the treated flanks of FL/FL and FL/WT mice had a significantly higher number of p-STAT3 positive cells than those of WT/WT mice (**Figures 6A, & 6B**). Furthermore, p-STAT3 activation was significantly higher in the treated flanks' dermis than in the untreated flanks of FL/FL and FL/WT mice (**Figures 6A**, **& 6B**). There were no significant changes among or between genotypes in the short-term OXA group (**Supplementary Figures 8**). These data revealed that p-STAT3 cells were more numerous in the treated flanks of transgenic mice in the long-term OXA group, implying that *Hnrnpk* deletion combined with long-term OXA boosted Stat3 activation, enhancing the JAK-STAT signaling pathway.

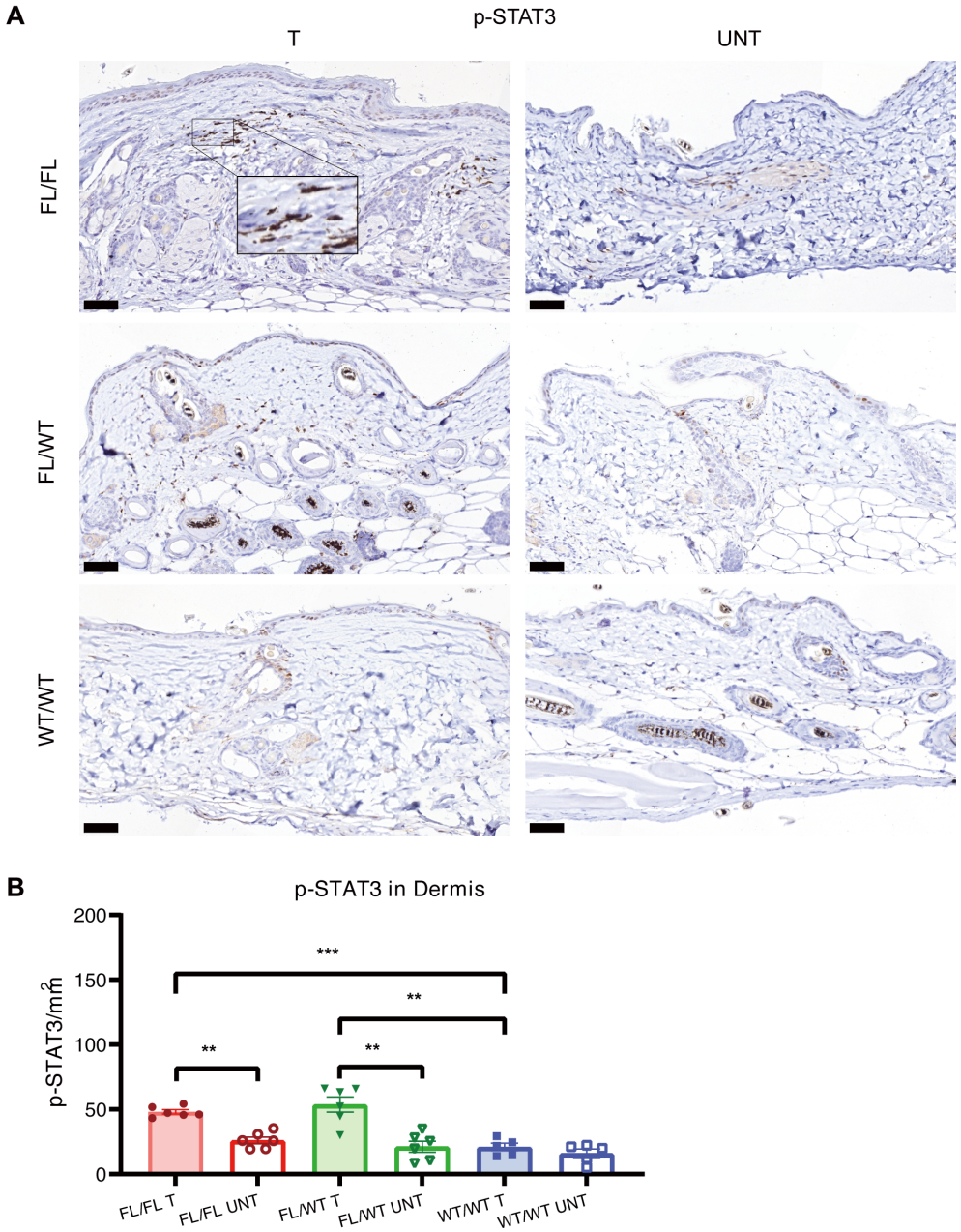

Figure 6. Histological analysis of treated and untreated skins of *Hnrnpk fl/fl Cd4CreER*^{T2}+/-, *Hnrnpk fl/wt Cd4CreER*^{T2}+/- and *Hnrnpk wt/wt Cd4CreER*^{T2}+/- mice from the long-term treatment group revealed increased number of p-STAT3 positive cells in dermis. (A). Skin sections from the treated and untreated flanks of mice in the long-term treatment group, stained with p-STAT3. Magnification is 20x and scale bar is 50 µm. (B). Quantification of the positive stained p-STAT3 cells in dermis of treated and untreated flanks of mice from the long-term treatment group. Paired *t*-test and two-way

ANOVA with a Tukey's post hoc test were used for statistical analysis. Error bars represent SEM and * indicates a significant difference (*$P < 0.05$, ***$P < 0.001$, ****$P < 0.0001$). n is 5 or 6 per genotype. Abbreviations: FL/FL is *Hnrnpk fl/fl Cd4CreER^{T2}*+/-. FL/WT is *Hnrnpk fl/wt Cd4CreER^{T2}*+/-. WT/WT is *Hnrnpk wt/wt Cd4CreER^{T2}*+/-. T is treated flank. UNT is untreated flank.

3.Discussion

This study showed that transgenic mice with *Hnrnpk* deletion in CD4 skin-infiltrating cells and subsequent repeated OXA applications resulted in features of early-stage cutaneous T cell lymphoma. These included autonomous skin inflammation, CD3+ CD4+ lymphocytic infiltration, increased Stat3 signaling, and enhanced lymphocyte proliferation index. Our findings supported prior studies by demonstrating the CTCL-like features associated with both biallelic and monoallelic *Hnrnpk* deletions, shedding light on their significant impact and likely underlying pathways in CTCL formation.

Our previous experience with OXA application revealed that applying modest doses to the skin surface three times a week could reduce skin inflammation without any discomfort. (11) Nevertheless, in the present study, we observed an increase in epidermal layer thickness and dermal infiltration by inflammatory cells in the treated flanks of Hnrnpk knockout mice in the long-term OXA group.

While previous research has indicated *HNRNPK*'s involvement in regulating T-cell activation and cytokine production, the precise role of *HNRNPK* in influencing the infiltration of inflammatory cells in the dermis remains inconclusive. (12) This study added to the body of evidence by revealing the various impacts of *HNRNPK* on T-cell activity.

An earlier research has shown that reduced *Hnrnpk* expression in mice resulted in the development of malignant T-cell lymphoma, marked by the expansion of abnormal lymphocytes and an increase in pro-inflammatory cytokines such as IL-2 and TNF-a. (7) The dual role of *HNRNPK* in tumor suppression and inflammation promotion is also evident in acute myeloid leukemia and lung cancer. (13, 14) Given the inconsistent results of earlier investigations, the mechanisms by which *HNRNPK* deficiency increases inflammation and cancer remain unknown. Some studies have even proposed that *HNRNPK* acts as an oncogene due to its elevated levels in various inflammation-related malignancies, including melanoma, colorectal, and prostate cancer. (15-17) These divergent findings underscore the importance of maintaining the homeostatic balance of *HNRNPK* expression in preventing disease mechanisms and tumor formation. Our study further supports *HNRNPK* deletion increased cell proliferation (Ki-67 expression) and JAK-STAT pathway activation.

In the context of cancer, *HNRNPK* has been suggested to have a dual role, acting as both a

tumor suppressor and an oncogene. (7) A role as oncogene is supported by the notion that elevated *HNRNPK* expression is associated with increased Ki-67 expression in breast cancer (18), down-regulation led to impaired proliferation in head and neck squamous carcinoma with reduced Ki-67 expression. Overexpression of *HNRNPK* in a mouse model increased tumor size and Ki-67 expression, while *HNRNPK* knockdown reduced tumor size and Ki-67 expression. (19). For AML and CTCL a tumor suppressor function for *HNRNPK* is more likely. Our mouse model shows that the proliferation marker Ki-67, which increases with disease progression and has been identified as a prognostic marker in MF, particularly in tumor-stage (20, 21) is increased after knockout of *Hnrnpk* in CD4+ T cells. (22, 23)

The JAK-STAT3 signaling pathway has been confirmed to play a significant role in CTCL pathogenesis. Persistent activation of STAT3 has been observed in CTCL and identified as a driving force behind this malignant condition. (24) Aberrantly active STAT3 promotes tumor cell survival, proliferation, upregulation of immune suppressive factors, and inhibition of Th1 mediators, among other oncogenic properties. (25) Constitutive activation of STAT3 is associated with malignant T-cell proliferation, resistance to apoptosis, and inflammation in CTCL. The expression of phosphorylated STAT3 and its critical role in the survival of CTCL cell lines have been documented. (26) Moreover, STAT3 is expressed in early-stage CTCL but not elevated in healthy skin dermis. (27) Sustained activation of Stat3 in T cells drives disease progression in a CTCL mouse model, although this model exhibited changes in STAT3 in all T cells rather than specifically in CD4+ T cells. (28) *HNRNPK* also inhibits cancer cell proliferation through the p53 signaling pathway, with p53, p21, and CCND1 playing pivotal roles. *HNRNPK*'s involvement in regulating the cancer proteome, including the STAT signaling pathway, also reinforces its influence on tumor growth. (29) (30) We observed enhanced JAK-STAT signaling in heterozygous and homozygous *Hnrnpk* knockout mice. These findings align with previous research suggesting lymphoma development is mediated through *Hnrnpk*-mediated Stat3 activation. (7)

Deletion of a single allele of the *Hnrnpk* gene is sufficient to influence the phenotype of the mouse model, with no significant differences observed between the phenotypes resulting from biallelic and monoallelic gene deletions. Our study included homozygous *Hnrnpk* knockout, heterozygous *Hnrnpk* knockout, and wild-type *Hnrnpk* mice, facilitating comprehensive genotype comparisons to enhance our understanding of the gene's function and its impact on the biological processes studied. (31) All experimental mice were subjected to identical environmental conditions, mitigating potential confounding factors and enhancing the reliability of the results. Considering the possible variability, the incorporation of various genotypes and the increase in the number of mice were crucial for obtaining more reliable and reproducible results. (32)

In conclusion, this extensive research underscores the pivotal role of *Hnrnpk* in CD4+ skin-homing T cells within chronically inflamed skin, exacerbating skin inflammation reminiscent of the early stages of MF. These findings suggest that *HNRNPK* may play an initiating role in the development of MF.

4.Methods and Materials

4.1.Mice

All mouse experiments were supervised by the animal welfare committee (IvD) of the Leiden University Medical Center and approved by the national central committee of animal experiments (CCD) under the permit number AVD116002015271, in accordance with the Dutch Act on Animal Experimentation and EU Directive 2020/63/EU.

Hnrnpk flox (*Hnrnpkem1*Lumc; MGI:99894) mice where loxP sites were introduced in *Hnrnpk* intron 2 and intron 6 were generated at LUMC. *Hnrnpk* flox mice using CrisprCas9 RNP and 200 bp single-stranded oligodeoxynucleotides (ssODN). *Cd4CreER^{T2}* mice (Tg (*Cd4-cre/ER^{T2}*)11Gnri/J; MGI:5493114; JAX:022356) expressing *CreER^{T2}* recombinase under the control of the *Cd4* promoter were purchased from The Jackson Laboratory (JAX). *Hnrnpk* flox mice were mated with *Cd4CreER^{T2}* mice to generate *Hnrnpk flox Cd4CreER^{T2}* mice. The offspring inherited both the targeted *Hnrnpk* flox allele and the *Cre* transgene.

Inducible homozygous (FL/FL) and heterozygous (WT/FL) *Hnrnpk* knockout mice were obtained by crossing conditional *Hnrnpk* knock-out mice (LUMC) with 4OHT inducible *Cd4-CreER^{T2}*-knock-in mice (Jackson's Laboratories) in the C57BL6/6J background. Resulted offspring was characterized by exon 3 to exon 6 deletion in *Hnrnpk* in *Cre*-expressing CD4+ T cells upon 4OHT administration. Wild type littermates (WT/WT) with *Cd4CreER^{T2}* in the C57BL6/6J background were used as a control group throughout the experiment. All mice were assigned to experimental or control groups based on their genotype. Treatments were assigned randomly. Mice were housed in a temperature-controlled room with a 12-hour light-dark cycle. Throughout the experiment, food and tap water were available ad libitum.

4.2.Oxazolone preparation and administration

Sensitization and inflammation of mouse skins were described as before.(33) The skin inflammation was induced by oxazolone (4-Ethoxymethylene-2-phenyl-2-oxazolin-5-one, OXA, Sigma-Aldrich) dissolved in acetone (Macron) to a concentration of 1.5% or 0.5% for each experiment. 1.5% OXA was used to sensitize shaved abdomen skins. After 1 week, 0.5% OXA was applied on shaved left flanks to induce skin inflammation. To maintain skin

inflammation, 0.5% OXA was administrated on shaved left flanks. As control, acetone was administrated on right shaved flanks. Before shaving and OXA treatment, mice were placed in isoflurane box and anesthetized with 2 - 4% isoflurane (Karizoo). Anesthesia was put on 0.25 - 2% isoflurane during shaving and OXA application.

4.3.4-hydroxy-tamoxifen preparation and administration

Cre-mediated deletion of *Hnrnpk* was performed in 6 to 20 weeks old mice with 4OHT (Sigma-Aldrich). 4OHT was dissolved in ethanol (J. T. Baker) and peanut oil (Sigma-Aldrich) to a concentration of 20 mg/ml. Dissolved 4OHT was placed in ultrasound sonicator (Branson 2510) for 2 minutes at room temperature and stored at 4 °C. Before each experiment, 4OHT was warmed to room temperature and administrated once on left shaved skins with 1 mg per mouse. As control, ethanol was administrated on right shaved flanks.

4.4.Flow cytometry

Skin cells were isolated by taking a 4 mm^2 skin biopsy post mortem, which was then digested using the whole skin dissociation Kit (Miltenyi Biotec, NL) following the manufacturer's instructions. Blood samples of mice (50 µL) were obtained from tail vein every week 24 hours after OXA treatment. Samples were transferred to tubes with lysis buffer (Hospital Pharmacy LUMC) and incubated for 10 minutes at 37 °C. After incubation, phosphate-buffered saline (PBS; Orphi Farma) was added to tubes and centrifuged for 5 minutes at 1600 rpm at room temperature. Lysates were transferred to FACS plates and centrifuged for 3 minutes at 1400 rpm at room temperature. Plates were washed with FACS buffer (Thermo Fisher Scientific). Fluorescence-labeled antibodies, anti-mouse CD3 (clone 145-2C11, BD Biosciences), anti-mouse CD19 (clone 1D3, Thermo Fisher Scientific), anti-mouse CD4 (clone RM4-5, Thermo Fisher Scientific) and anti-mouse CD8 (clone 53-6.7, Biolegend), were added to the cells and incubated for 30 minutes on ice. After incubation, cells were washed 2 times with FACS buffer and transferred to tubes with paraformaldehyde (PFA, Sigma-Aldrich). BD Fortessa flow cytometer was used for measurements and samples were analyzed with FlowJo software. For compensation, labeled beads (Thermo Fisher Scientific) were made by the same procedure and used shortly before the measurements.

4.5.Histological and immunohistochemical staining

Mice skin samples were obtained after CO2-mediated sacrifice and fixed with 4% PFA (Added Pharma). Skin tissues were dehydrated with increasing grade of ethanol (50%, 70%, 100%), cleared in xylene (J.T. Baker) and embedded in paraffin (Klinipath) using

Leica HistoCore Arcadia H machine. Embedded skins were placed in microtome (Leica 149MULTI0C1) and sliced at thickness of 4 µm. Skin sections were dewaxed with xylene and rehydrated with decreasing grade of ethanol (100%, 70%, 50%). Slides were stained with haematoxylin and eosin (HE) staining and dehydrated with increasing grade of ethanol (95% and 100%) followed by xylene. Skin sections were mounted on glass lids using Depex (Sigma-Aldrich).

For immunohistochemical (IHC) stainings, paraffin-embedded skin sections were dewaxed with xylene and rehydrated in 100% ethanol. Afterwards, skin sections were blocked with 0.3% hydrogen peroxidase (H202, Sigma-Aldrich) and rehydrated with decreasing grade of ethanol (95%, 85%, 70%). Antigen retrieval was performed in 0.01M sodium citrate solution (Merck; pH 6) for 10 minutes at low-medium in the microwave (Etna). Skin slices were washed 3 times with PBS/0.05% Tween (Sigma-Aldrich). Sections were blocked with SuperBlock (Thermo Fisher Scientific) for 30 minutes at room temperature and incubated with primary antibodies, anti-mouse CD3 (D7A6E, Cell Signaling Technology, dilution 1:200), anti-mouse CD4 (D7D2Z, Cell Signaling Technology, dilution 1:100), anti-mouse CD8 (4SM15, eBioscienceTM, dilution 1:1600) and anti-mouse p-STAT3 (D3A7, Cell Signaling Technology, dilution 1:150), at 4 °C overnight. All primary antibodies were dissolved in PBS with 1% bovine serum albumin (BSA, Thermo Fischer Scientific).

Next day, skin slices were washed 3 times with PBS/0.05% Tween and incubated with secondary antibody goat-anti-rabbit (IgG biotinylated, Sigma-Aldrich, dilution 1:200) or rabbit-anti-rat (IgG biotinylated, Sigma-Aldrich, dilution 1:200) dissolved in PBS/1% BSA for 30 minutes at room temperature. Sections were washed 3 times with PBS/0.05% Tween. Slides were incubated with Vectastain Elite Kit (Vector Labs, dilution 1:200) for 30 minutes at room temperature and washed 3 times with PBS. Skin sections were visualized with diaminobenzidine (DAB, Dako Omnis, dilution 1:100) for 5 minutes at room temperature and washed with MilliQ water. Nuclei were counterstained with filtered haematoxylin (dilution 1:5) for 3 seconds at room temperature. Skin slides were washed in tap and MilliQ water and dehydrated with increasing grade of ethanol (70%, 85%, 95%, 100%). Skin sections were mounted on glass lids using Entellan (Sigma-aldrich).

All slices were photographed and examined with bright field microscope scanner (3D HISTECH, Pannoramic 250). For HE analysis, epidermal layers of each skin section were counted at 20x magnification. Means were estimated and used for statistical analysis. For IHC analysis, CD3, CD4, CD8, Ki-67 and p-STAT3 positive cells were counted in each slide at 20x magnification. Normalization was performed at number of positive cells per mm^2 and means were estimated for statistical analysis.

4.6.Statistical analyses

All data was statistically analyzed and graphed in GraphPad Prism (version 9.3.1). For flow cytometry analysis, mixed-effect analysis with Tukey's post hoc test was performed. For histological and immunohistochemical analysis, paired *t*-test was used to compare treated skin with untreated skin within same genotype. In addition, two-way ANOVA test with Tukey's post hoc comparison was used to compare skin samples between genotypes. *P* values less than 0.05 were considered as significant.

References

1. Tensen CP, Quit KD, Vermeer MH. Genetic and epigenetic insights into cutaneous T-cell lymphoma. Blood. 2022;139(1):15-33. doi: 10.1182/blood.2019004256.
2. Bastidas Torres AN, Cats D, Mei H, Szuhai K, Willemze R, Vermeer MH, et al. Genomic analysis reveals recurrent deletion of JAK-STAT signaling inhibitors HNRNPK and SOCS1 in mycosis fungoides. Genes Chromosomes Cancer. 2018;57(12):653-64. doi: 10.1002/gcc.22679.
3. Park J, Daniels J, Wartewig T, Ringbloom KG, Martinez-Escala ME, Choi S, et al. Integrated genomic analyses of cutaneous T-cell lymphomas reveal the molecular bases for disease heterogeneity. Blood. 2021;138(14):1225-1236. doi: 10.1182/blood.2020009655.
4. Wang Z, Qiu H, He J, Liu L, Xue W, Fox A, et al. The emerging roles of hnRNPK. J Cell Physiol. 2020;235(3):1995-2008. doi: 10.1002/jcp.29186.
5. Mucha B, Qie S, Bajpai S, Tarallo V, Diehl JN, Tedeschi F, et al. Tumor suppressor mediated ubiquitylation of hnRNPK is a barrier to oncogenic translation. Nat Commun. 2022;13(1):6614. doi: 10.1038/s41467-022-34402-6.
6. Chen Y, Zeng Y, Xiao Z, Chen S, Li Y, Zou J, et al. Role of heterogeneous nuclear ribonucleoprotein K in tumor development. J Cell Biochem. 2019;120(9):14296-305. doi: 10.1002/jcb.28867.
7. Gallardo M, Lee HJ, Zhang X, Bueso-Ramos C, Pageon LR, McArthur M, et al. hnRNP K Is a Haploinsufficient Tumor Suppressor that Regulates Proliferation and Differentiation Programs in Hematologic Malignancies. Cancer Cell. 2015;28(4):486-99. doi: 10.1016/j.ccell.2015.09.001.
8. Inoue K, Fry EA. Haploinsufficient tumor suppressor. Adv Med Biol. 2017;118:83-122. PMID: 28680740.
9. Kwabi-Addo B, Giri D, Schmidt K, Podsypanina K, Parsons R, Greenberg N, et al. Haploinsufficiency of the Pten tumor suppressor gene promotes prostate cancer progression. PNAS. 2001;98(20):11563-11568. doi: 10.1073/pnas.201167798.
10. Davoli T, Xu AW, Mengwasser KE, Sack LM, Yoon JC, Park PJ, et al. Cumulative haploinsufficiency and triplosensitivity drive aneuploidy patterns and shape the cancer genome. Cell. 2013;155(4):948-962. doi: 10.1016/j.cell.2013.10.011.
11. Luo Y, Vermmer M, de Haan S, Kinderman P, de Gruijl FR, van Hall T, et al. Socs1-knockout in skin-resident CD4(+) T cells in a protracted contact-allergic reaction results in an autonomous skin inflammation with features of early-stage mycosis fungoides. Biochem Biophys Rep. 2023;35:101535. doi: 10.1016/j.bbrep.2023.101535.
12. Popović B, Nicolet BP, Guislain A, Engels S, Jurgens AP, Paravinja N, et al. Time-dependent regulation of cytokine production by RNA binding proteins defines T cell effector function. Cell Rep. 2023;42(5):112419. doi: 10.1016/j.celrep.2023.112419.
13. Kerstin Rahn, Isabel Naarmann-de Vrie, Yvonne Sackmann, Felicitas Klein, Antje Ostareck-Lederer, Dirk Ostareck, et al. Role of hnRNP K and Interacting mRNAs in Pathogenesis of AML with 9q Deletion. Blood. 2018;132(Supplement 1):1531. doi: 10.1182/blood-2018-99-114699
14. Li M, Yang X, Zhang G, Wang L, Zhu Z, Zhang W, et al. Heterogeneous nuclear ribonucleoprotein K promotes the progression of lung cancer by inhibiting the p53-dependent signaling pathway. Thorac Cancer. 2022;13(9):1311-1321. doi: 10.1111/1759-7714.14387.

15. Carpenter B, McKay M, Dundas SR, Lawrie LC, Telfer C, Murray GI. Heterogeneous nuclear ribonucleoprotein K is over expressed, aberrantly localised and is associated with poor prognosis in colorectal cancer. Br J Cancer. 2006;95(7):921-7. doi: 10.1038/sj.bjc.6603349.

16. Ciarlo M, Benelli R, Barbieri O, Minghelli S, Barboro P, Balbi C, et al. Regulation of neuroendocrine differentiation by AKT/hnRNPK/AR/b-catenin signaling in prostate cancer cells. Int J Cancer. 2011;131(3):582-90. doi: 10.1002/ijc.26402.

17. Wen F, Shen A, Shanas R, Bhattacharyya A, Lian F, Hostetter G, et al. Higher Expression of the Heterogeneous Nuclear Ribonucleoprotein K in Melanoma. Ann Surg Oncol. 2010;17(10):2619-27. doi: 10.1245/s10434-010-1121-1.

18. Iwabuchi E, Miki Y, Suzuki T, Hirakawa H, Ishida T, Sasano H. Heterogeneous Nuclear Ribonucleoprotein K Is Involved in the Estrogen-Signaling Pathway in Breast Cancer. Int J Mol Sci. 2021;22(5).2581. doi: 10.3390/ijms22052581.

19. Zhou W, Jie Q, Pan T, Shi J, Jiang T, Zhang Y, et al. Single-cell RNA binding protein regulatory network analyses reveal oncogenic HNRNPK-MYC signalling pathway in cancer. Commun Biol. 2023;6(1):82. doi: 10.1038/s42003-023-04457-2.

20. Zohdy M, Abd El Hafez A, Abd Allah MYY, Bessar H, Refat S. Ki67 and CD31 Differential Expression in Cutaneous T-Cell Lymphoma and Its Mimickers: Association with Clinicopathological Criteria and Disease Advancement. Clin Cosmet Investig Dermatol. 2020;13:431-42. doi:10.2147/CCID.S256269

21. Shen X, Wang B, Li K, Wang L, Zhao X, Xue F, et al. MicroRNA Signatures in Diagnosis and Prognosis of Cutaneous T-Cell Lymphoma. J Invest Dermatol. 2018;138(9):2024-32. doi: 10.1016/j.jid.2018.03.1500.

22. Chang JW, Koike T, Iwashima M. hnRNP-K is a nuclear target of TCR-activated ERK and required for T-cell late activation. Int Immunol. 2009;21(12):1351-1361. doi: 10.1093/intimm/dxp106.

23. Sengupta S, West K, Sanghvi S, Laliotis G, Agosto LM, Lynch KW, et al. PRMT5 Promotes Symmetric Dimethylation of RNA Processing Proteins and Modulates Activated T Cell Alternative Splicing and Ca(2+)/NFAT Signaling. Immunohorizons. 2021;5(10):884-97. doi: 10.4049/immunohorizons.2100076.

24. Sommer VH, Clemmensen OJ, Nielsen O, Wasik M, Lovato P, Brender C, et al. In vivo activation of STAT3 in cutaneous T-cell lymphoma. Evidence for an antiapoptotic function of STAT3. Leukemia. 2004;18(7):1288-95. doi: 10.1038/sj.leu.2403385.

25 Yu H, Kortylewski M, Pardoll D. Crosstalk between cancer and immune cells: role of STAT3 in the tumour microenvironment. Nat Rev Immunol. 2007;7(1):41-51. doi: 10.1038/nri1995.

26. Gluud M, Pallesen EMH, Buus TB, Gjerdrum LMR, Lindahl LM, Kamstrup MR, et al. Malignant T cells induce skin barrier defects through cytokine-mediated JAK/STAT signaling in cutaneous T-cell lymphoma. Blood. 2023;141(2):180-93. doi: 10.1182/blood.2022016690.

27. Olszewska B, Zawrocki A, Lakomy J, Karczewska J, Glen J, Zablotna M, et al. Mapping signal transducer and activator of transcription (STAT) activity in different stages of mycosis fungoides and Sezary syndrome. Int J Dermatol. 2020;59(9):1106-12. doi: 10.1111/ijd.15036.

28. Fanok MH, Sun A, Fogli LK, Narendran V, Eckstein M, Kannan K, et al. Role of Dysregulated Cytokine Signaling and Bacterial Triggers in the Pathogenesis of Cutaneous T-Cell Lymphoma. J Invest

Dermatol. 2018;138(5):1116-25. doi: 10.1016/j.jid.2017.10.028.
29. Huang H, Han Y, Yang X, Li M, Zhu R, Hu J, et al. HNRNPK inhibits gastric cancer cell proliferation through p53/ p21/CCND1 pathway. Oncotarget. 2017;8(61):103364-103374. doi: 10.18632/oncotarget.
30. Sudhakaran M, Doseff A. Role of Heterogeneous Nuclear Ribonucleoproteins in the Cancer-Immune Landscape. Int J Mol Sci. 2023;24(6):5086. doi: 10.3390/ijms24065086.
31. Lu ZY, Chen P, Xu QY, Li B, Jiang SD, Jiang LS, et al. Constitutive and conditional gene knockout mice for the study of intervertebral disc degeneration: Current status, decision considerations, and future possibilities. JOR Spine. 2023;6(1): e1242. doi: 10.1002/jsp2.1242.
32. Lampreht Tratar U, Horvat S, Cemazar M. Transgenic Mouse Models in Cancer Research. Front Oncol. 2018;8:268. doi: 10.3389/fonc.2018.00268.
33. Luo Y, Vermeer MH, de Gruijl FR, Zoutman WH, Sluijter M, van Hall T, et al. In vivo modelling of cutaneous T-cell lymphoma: The role of SOCS1. Front Oncol. 2022;12:1031052. doi: 10.3389/fonc.2022.1031052.

Supplementary Information

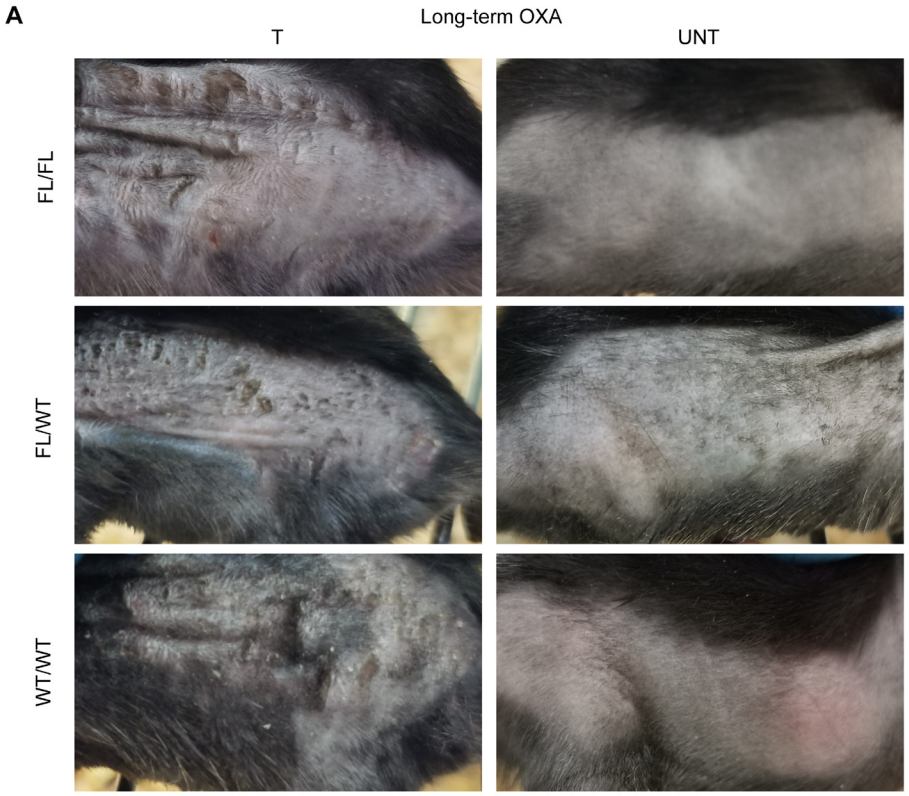

Supplementary Figure 1. Macroscopic analysis of treated and untreated skin from *Hnrnpk fl/fl Cd4CreER^{T2}+/-*, *Hnrnpk fl/wt Cd4CreER^{T2}+/-* and *Hnrnpk wt/wt Cd4CreER^{T2}+/-* mice shows presence of inflammation symptoms in treated skins in the long-term group.

Representative clinical photos of treated and untreated skin images of *Hnrnpk fl/fl Cd4CreER^{T2}+/-*, *Hnrnpk fl/wt Cd4CreER^{T2}+/-* and *Hnrnpk wt/wt Cd4CreER^{T2}+/-* mice of the long-term treatment group.

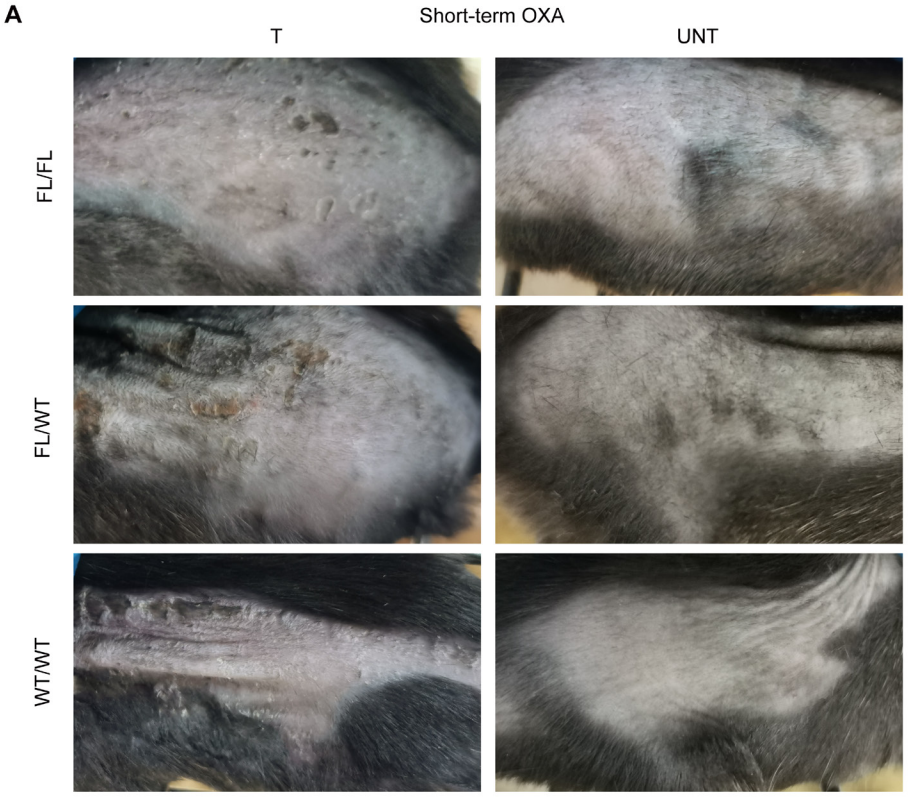

Supplementary Figure 2. Macroscopic analysis of treated and untreated skin from *Hnrnpk fl/fl Cd4CreER^{T2}+/-*, *Hnrnpk fl/wt Cd4CreER^{T2}+/-* and *Hnrnpk wt/wt Cd4CreER^{T2}+/-* mice shows presence of inflammation symptoms in treated skins in the short-term treatment group.

Representative clinical photos of treated and untreated skin images of *Hnrnpk fl/fl Cd4CreER^{T2}+/-*, *Hnrnpk fl/wt Cd4CreER^{T2}+/-* and *Hnrnpk wt/wt Cd4CreER^{T2}+/-* mice of the short-term treatment group.

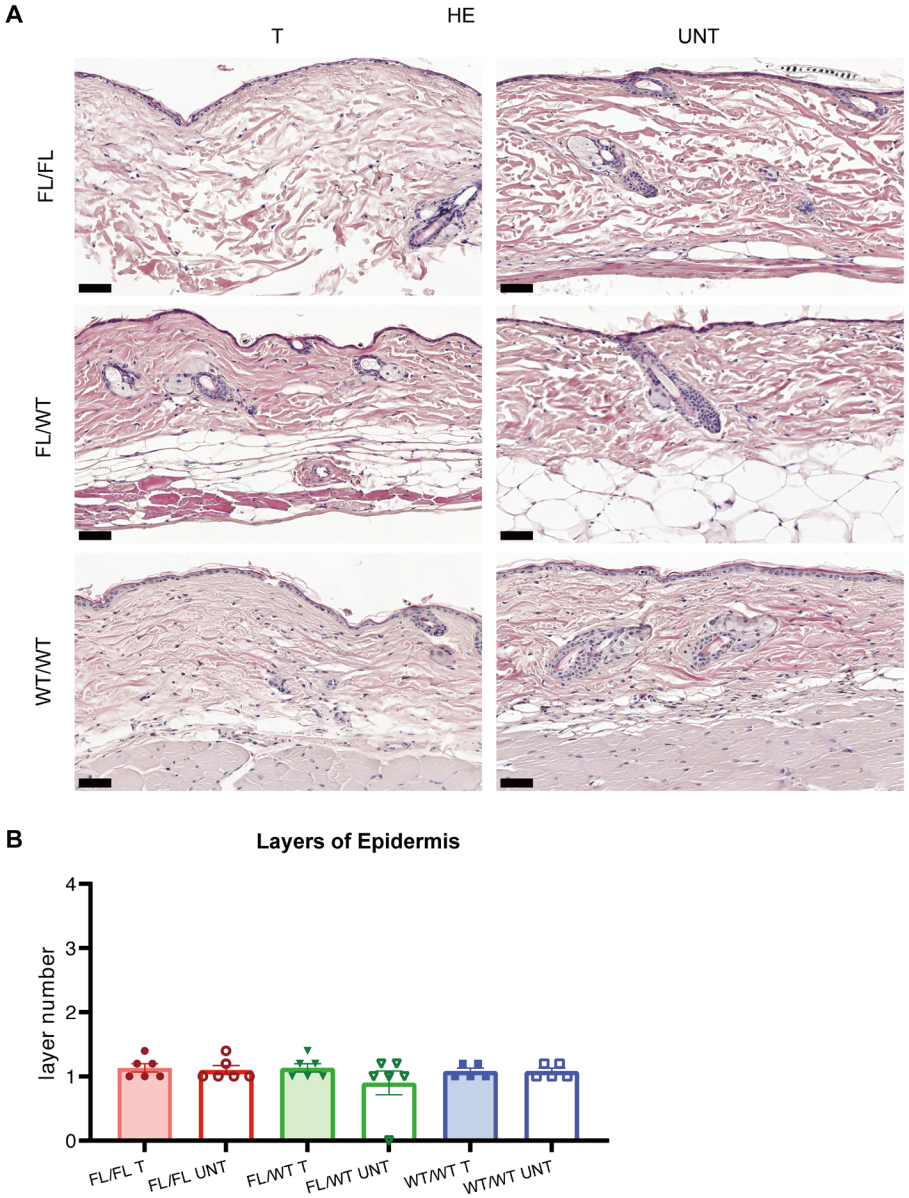

Supplementary Figure 3. Histological analysis of treated and untreated skin from *Hnrnpk fl/fl Cd4CreER^{T2}+/-*, *Hnrnpk fl/wt Cd4CreER^{T2}+/-* and *Hnrnpk wt/wt Cd4CreER^{T2}+/-* mice of the short-term treatment group demonstrates no changes in number of epidermal layers. (A) Treated and untreated skin sections of *Hnrnpk fl/fl Cd4CreER^{T2}+/-*, *Hnrnpk fl/wt Cd4CreER^{T2}+/-* and *Hnrnpk wt/wt Cd4CreER^{T2}+/-* mice stained with the HE staining. Magnification is 20x and scale bar is 50 µm. B) Quantification of the number of epidermal layers of treated and untreated skin from *Hnrnpk fl/*

fl Cd4CreER^{T2}+/-, *Hnrnpk fl/wt Cd4CreER*^{T2}+/- and *Hnrnpk wt/wt Cd4CreER*^{T2}+/- mice. A paired t-test and two-way ANOVA with a Tukey's post hoc test were used for statistical analysis and error bars representing standard errors of the mean (SEM). n is 5 or 6 per genotype.

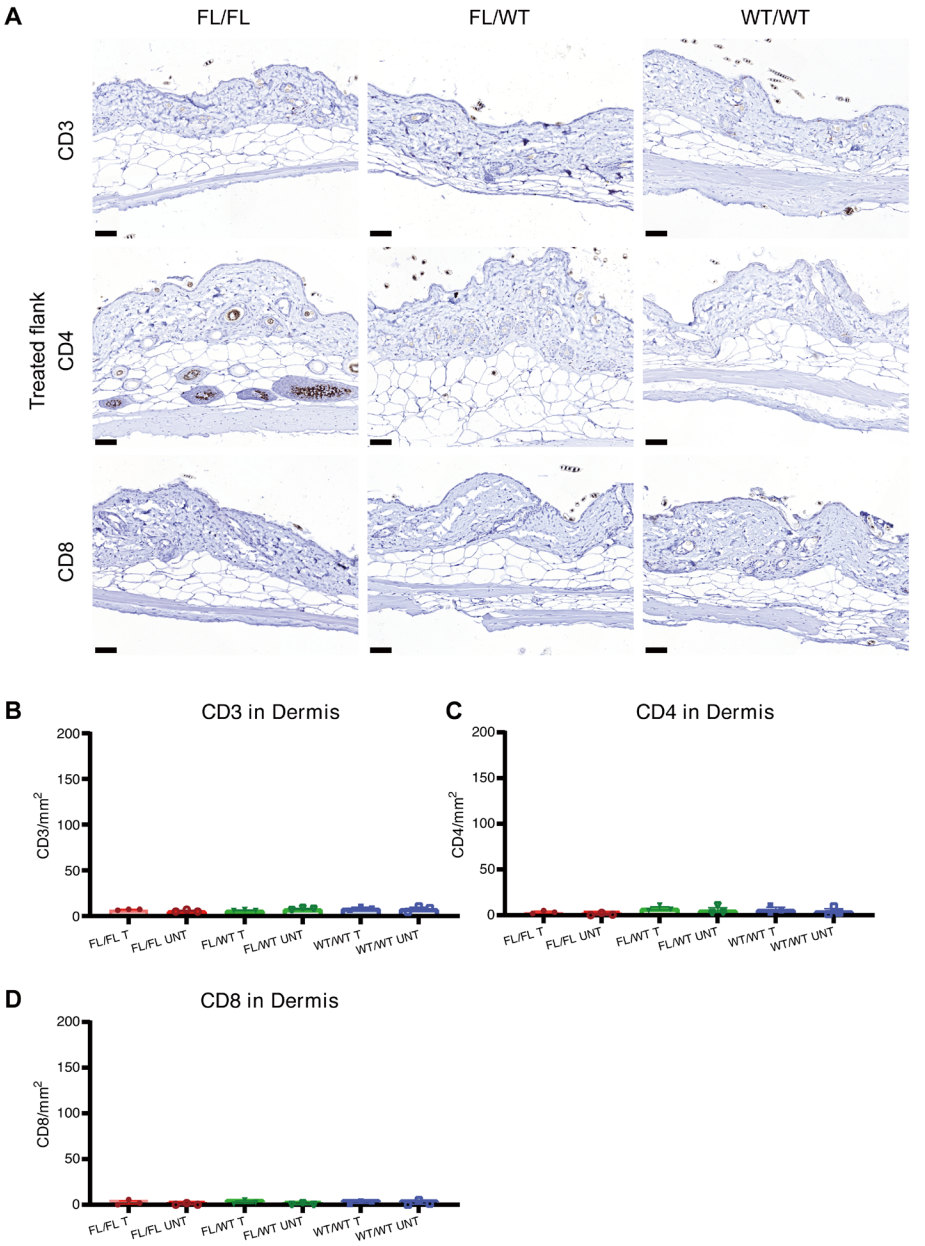

Supplementary Figure 4. Histological analysis of treated skin from *Hnrnpk fl/fl Cd4CreER*^{T2}+/-, *Hnrnpk*

fl/wt Cd4CreER^{T2}+/- and *Hnrnpk wt/wt Cd4CreER*^{T2}+/- mice of the short-term treatment group demonstrates no differences in number of CD3, CD4 and CD8 cells in the dermis. (A) Treated skin sections of *Hnrnpk fl/fl Cd4CreER*^{T2}+/-, *Hnrnpk fl/wt Cd4CreER*^{T2}+/- and *Hnrnpk wt/wt Cd4CreER*^{T2}+/- mice stained with CD3, CD4 and CD8 IHC staining. Magnification is 20x and scale bar is 50 µm. Black arrows indicate stained cells. B, C, D) Quantification of the positive stained CD3 (B), CD4 (C) and CD8 (D) cells in the dermis of treated and untreated skin from *Hnrnpk fl/fl Cd4CreER*^{T2}+/-, *Hnrnpk fl/wt Cd4CreER*^{T2}+/- and *Hnrnpk wt/wt Cd4CreER*^{T2}+/- mice. A paired t-test and two-way ANOVA with a Tukey's post hoc test were used for statistical analysis. Error bars represent SEM and n is 3 per genotype.

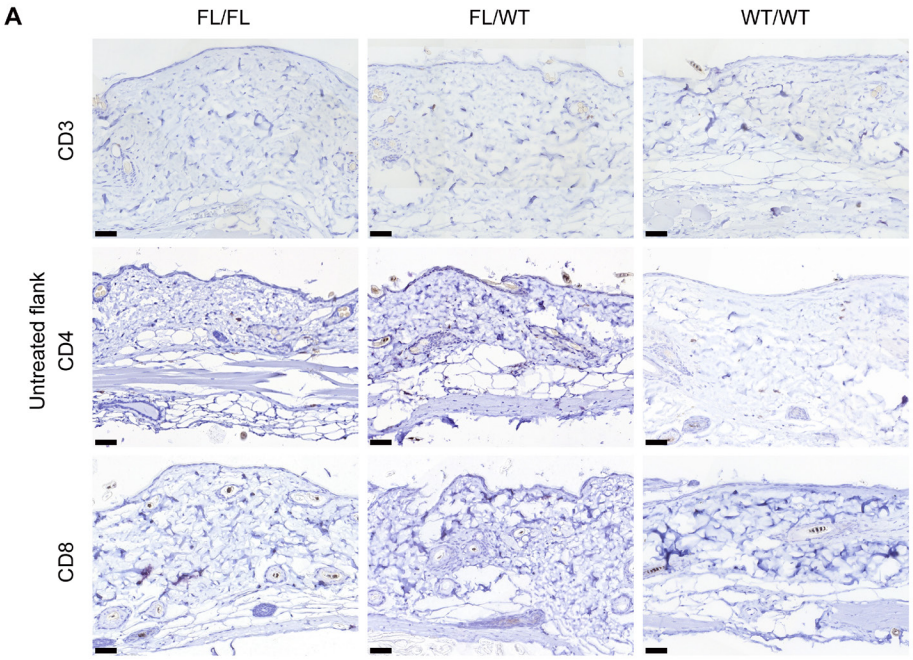

Supplementary Figure 5. Histological analysis of untreated skin from *Hnrnpk fl/fl Cd4CreER*^{T2}+/-, *Hnrnpk fl/wt Cd4CreER*^{T2}+/- and *Hnrnpk wt/wt Cd4CreER*^{T2}+/- mice of the long-term treatment group reveals unchanged number of CD3, CD4 and CD8 cells in the dermis. Untreated skin sections of *Hnrnpk fl/fl Cd4CreER*^{T2}+/-, *Hnrnpk fl/wt Cd4CreER*^{T2}+/- and *Hnrnpk wt/wt Cd4CreER*^{T2}+/- mice stained with CD3, CD4 and CD8. Magnification is 20x and scale bar is 50 µm. Black arrows indicate positive stained cells. n is 5 or 6 per genotype.

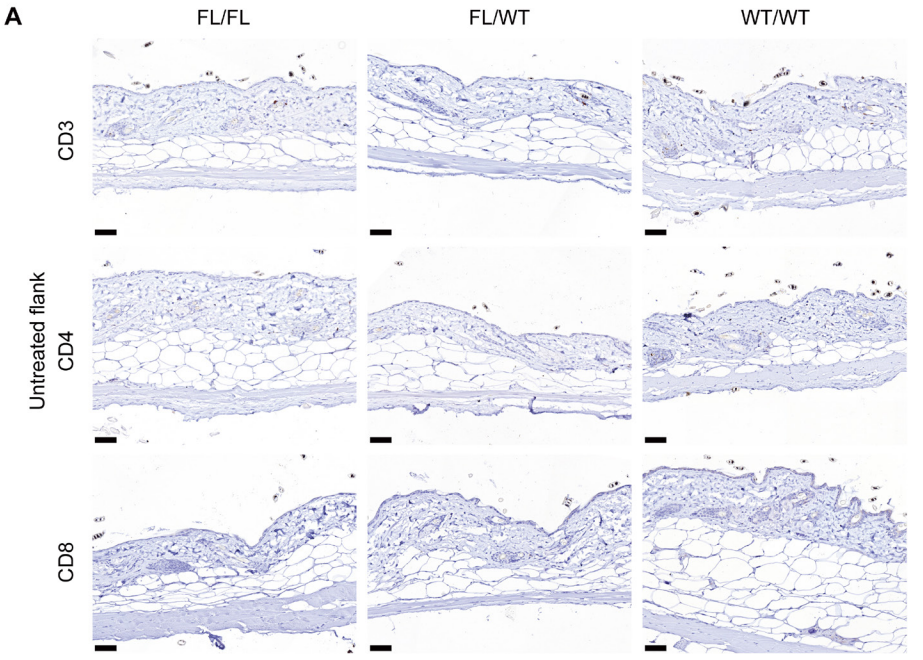

Supplementary Figure 6. Histological analysis of untreated skin from *Hnrnpk fl/fl Cd4CreER^{T2}+/-*, *Hnrnpk fl/wt Cd4CreER^{T2}+/-* and *Hnrnpk wt/wt Cd4CreER^{T2}+/-* mice of the short-term treatment group demonstrates no differences in number of CD3, CD4 and CD8 cells in the dermis. Untreated skin sections of *Hnrnpk fl/fl Cd4CreER^{T2}+/-*, *Hnrnpk fl/wt Cd4CreER^{T2}+/-* and *Hnrnpk wt/wt Cd4CreER^{T2}+/-* mice stained with CD3, CD4 and CD8. Magnification is 20x and scale bar is 50 µm. Black arrows indicate positive stained cells. n is 3 per genotype.

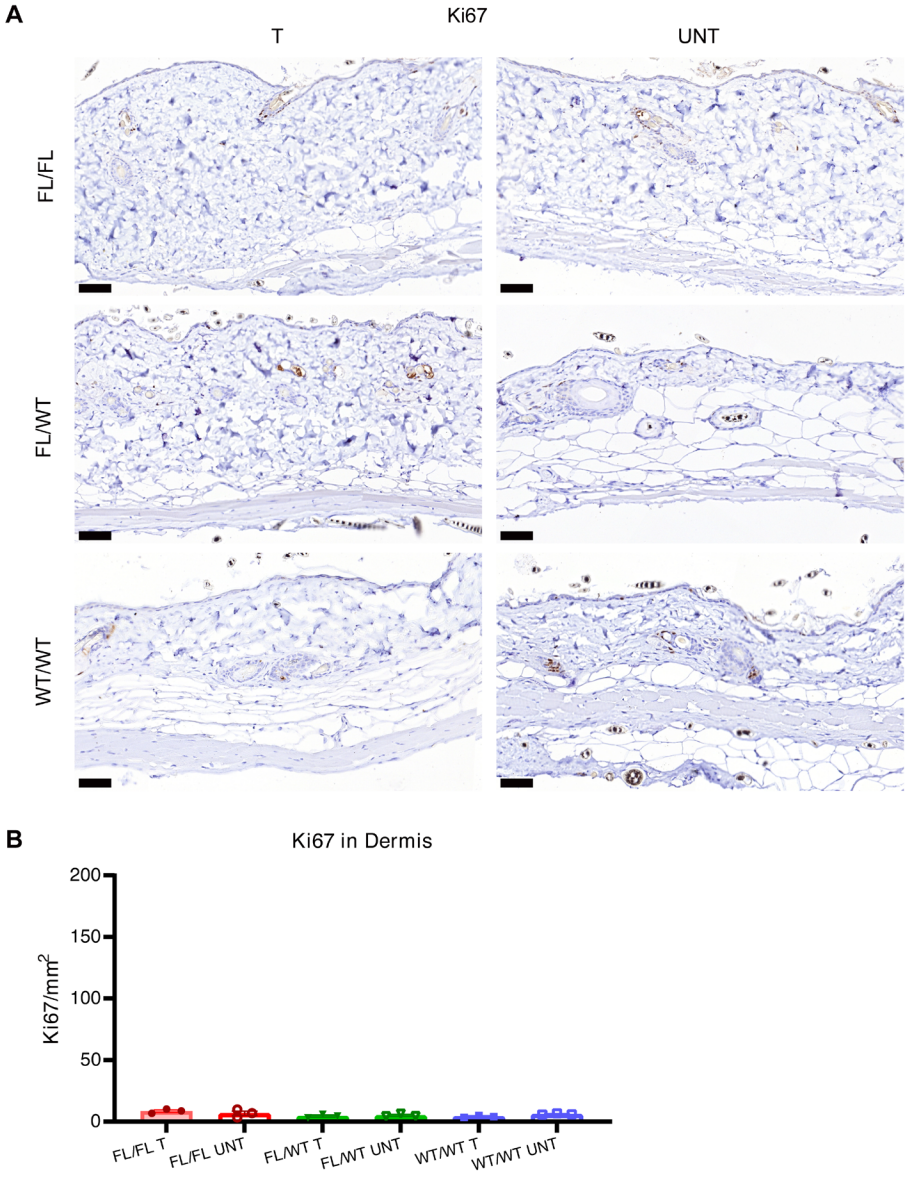

Supplementary Figure 7. Histological analysis of treated and untreated skins from *Hnrnpk fl/fl Cd4CreER^{T2}+/-*, *Hnrnpk fl/wt Cd4CreER^{T2}+/-* and *Hnrnpk wt/wt Cd4CreER^{T2}+/-* mice of the short-term treatment group shows no changes in number of Ki-67 positive cells in the dermis.

A) Treated and untreated skin sections of *Hnrnpk fl/fl Cd4CreER^{T2}+/-*, *Hnrnpk fl/wt Cd4CreER^{T2}+/-* and *Hnrnpk wt/wt Cd4CreER^{T2}+/-* mice stained with Ki-67. Magnification is 20x and scale bar is 50 µm. Black arrows indicate stained cells. B) Quantification of the positive Ki-67 cells in the dermis of

treated and untreated skin from *Hnrnpk fl/fl Cd4CreER^{T2}+/-*, *Hnrnpk fl/wt Cd4CreER^{T2}+/-* and *Hnrnpk wt/wt Cd4CreER^{T2}+/-* mice. Paired t-test and two-way ANOVA with a Tukey's post hoc test were used for statistical analysis. Error bars represent SEM and n is 5 or 6 per genotype.

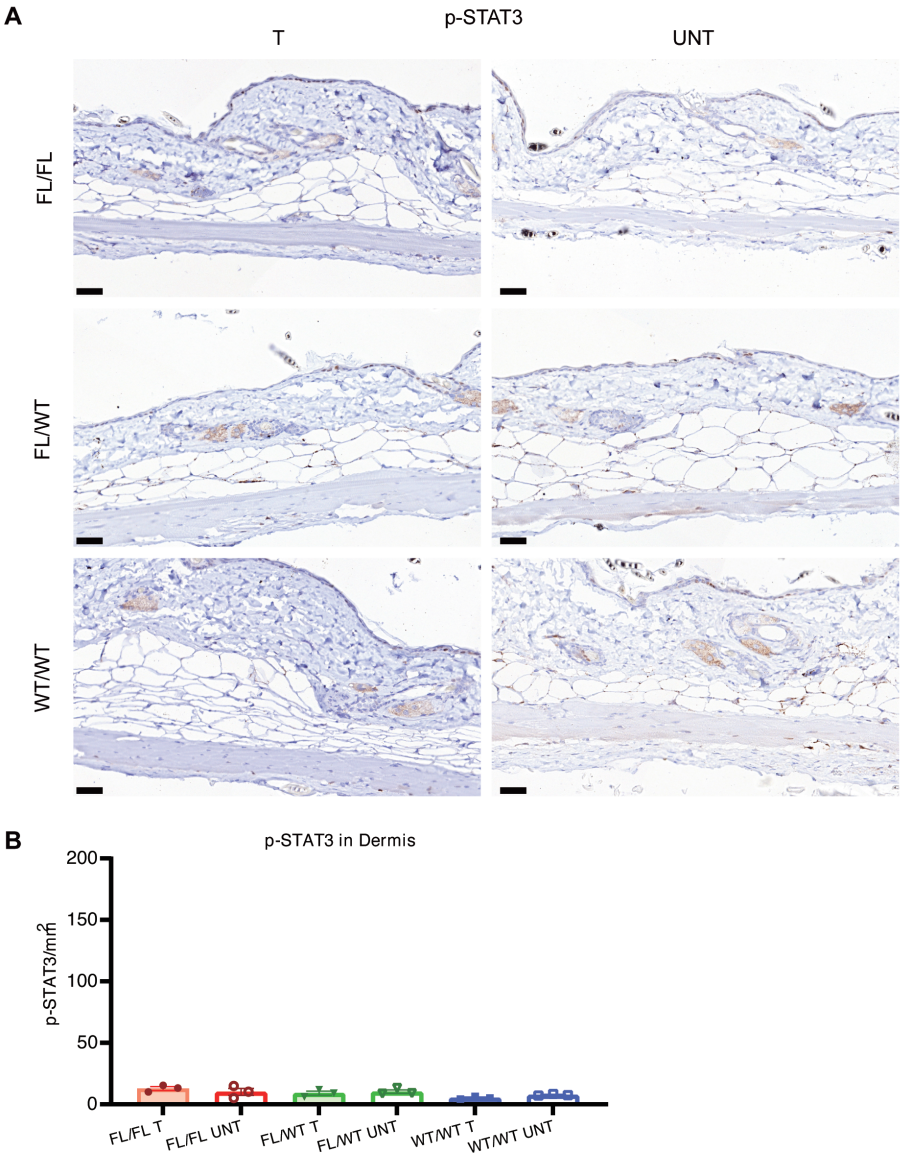

Supplementary Figure 8. Histological analysis of treated and untreated skins from *Hnrnpk fl/fl Cd4CreER^{T2}+/-*, *Hnrnpk fl/wt Cd4CreER^{T2}+/-* and *Hnrnpk wt/wt Cd4CreER^{T2}+/-* mice of the short-term treatment group shows no changes in number of p-STAT3 positive cells in the dermis.

A) Treated and untreated skin sections of *Hnrnpk fl/fl Cd4CreER^{T2}+/-*, *Hnrnpk fl/wt Cd4CreER^{T2}+/-* and *Hnrnpk wt/wt Cd4CreER^{T2}+/-* mice stained with p-STAT3. Magnification is 20x and scale bar is 50 µm. Black arrows indicate stained cells. B) Quantification of the positive stained p-STAT3 cells in the dermis of treated and untreated skin from *Hnrnpk fl/fl Cd4CreER^{T2}+/-*, *Hnrnpk fl/wt Cd4CreER^{T2}+/-* and *Hnrnpk wt/wt Cd4CreER^{T2}+/-* mice. Paired t-test and two-way ANOVA with a Tukey's post hoc test were used for statistical analysis. Error bars represent SEM and n is 5 or 6 per genotype.

6

General discussion

General discussion and future perspective

The work presented in this thesis focused on developing advanced genetically engineered mouse models (GEMMs) to enhance research on Cutaneous T-cell Lymphoma (CTCL). By specifically targeting skin-homing CD4+ T cells and incorporating an inflammatory skin reaction, these models replicate the natural progression of CTCL, significantly improving our understanding of its early-stage genesis. They also offer promising avenues for the development of early interventions. This final chapter summarizes and discusses the findings of **Chapters 2, 3, 4, and 5**, culminating in conclusions and future perspectives.

Cd4CreER^{T2} System and Inducible Conditional Knockout Mouse Generation

In **Chapter 1**, we provided an overview of mouse models utilized in CTCL research, with a particular emphasis on the importance of the development of GEMMs. In the realm of CTCL studies, GEMMs are categorized into non-skin targeted and skin-targeted CD4+ T cell GEMMs. The latter category, which is the main content in this thesis and characterized by skin-target CD4+ T cells, offers a more faithful representation of the natural origin of CTCL pathogenesis.

The most commonly used tool for targeting gene knockout in (skin-homing) CD4+ T cells is the *Cd4CreER^{T2}* system. (1) This innovative system combines the versatility of the Cre-loxP recombination strategy with the precision of inducible gene targeting, making it an useful tool in the study of gene function in a temporally controlled manner. (2) Fundamentally, the *Cd4CreER^{T2}* system relies on Cre recombinase, derived from the P1 bacteriophage, renowned for its ability to catalyze site-specific recombination between loxP sites. These loxP sites are short DNA sequences strategically inserted into the genome, flanking the target gene. (3) Cre recombinase efficiently excises or inverts the DNA between these loxP sites, leading to the deletion or modification of the gene of interest. (4)

The unique aspect of the *Cd4CreER^{T2}* variant lies in the fusion of *Cre* recombinase with a mutated estrogen receptor (ERT2), which renders the enzyme inactive at physiological estrogen levels. (5) This inactivity persists until the administration of Tamoxifen, a selective estrogen receptor modulator. Tamoxifen binds to the ERT2 portion, causing a conformational change that activates the *Cre* recombinase. (6) This inducible system provides a high degree of control over the timing of gene recombination, allowing researchers to study gene function in various developmental stages or disease states. In addition, topical administration of tamoxifen (e. g. painting on the skin) offers the possibility to restrict recombination in discerning regions of the body.

This *Cd4CreER*^{T2} system is crucial to our thesis's main experiments. In **Chapters 2** and **Chapter 3**, we crossed *Cd4CreER*^{T2} mice with *Socs1* flox mice, while in **Chapters 4** and **Chapter 5**, the crossbreeding involved *Cd4CreER*^{T2} and *Hnrnpk* flox mice. The *Cre* recombinase in this context is under the control of the *Cd4* promoter, enabling its specific activation in CD4+ T cells. The knockout of *Socs1* in CD4+ T cells of these crossbred mice could be detected using flow cytometry, thanks to a reporter. (7) For *Hnrnpk*, which lacks a reporter, the knockout was verified by extracting DNA from enriched CD4+ T cells and using PCR techniques. These procedures have confirmed the effectiveness of the *Cd4CreER*^{T2} tool.

In the Cre-lox system, there are various methods to activate *Cre* with Tamoxifen, especially in *in vivo* models. These methods include intraperitoneal injection, gavage (oral administration), and intravenous injection, depending on the experimental purpose and the target cells. (1) (8) (9) To verify the effectiveness of the *Cd4CreER*^{T2}-LoxP system in our mouse model, we initially used intraperitoneal injection of Tamoxifen for validation (**Chapter 2**). Our research focuses on primary cutaneous T-cell lymphoma, targeting skin-homing CD4+ T cells. Hence, we employed a topical application method. Additionally, since Tamoxifen needs to be metabolized in the liver to form 4OH Tamoxifen, and topical Tamoxifen cannot undergo this metabolism, we used the active form, 4OH Tamoxifen, directly. There is no standard protocol for the topical application of 4OH Tamoxifen, so we compared the effects of 3 and 5 topical applications on the genes in systemic CD4+ T cells. We determined that three topical applications of 4OH Tamoxifen were sufficient to knock out the target gene in skin-homing CD4+ T cells (**Chapter 2**). In further research, we optimized the use of 4OH Tamoxifen. Our study data show that even a single topical application of Tamoxifen is enough to activate the *Cd4CreER*^{T2}-LoxP system and can do so with minimal systemic disturbance (**Chapters 3, 4, and 5**).

Initial Effects of Genome Alteration in the Pathogenesis of CTCL

Genetic alteration in the Janus kinase-signal transducers and activators of transcription (JAK-STAT) pathway is a critical chain of interactions between proteins within a cell. Genetic alterations in the JAK-STAT pathway, including deletions and mutations, play a significant role in the pathogenesis of CTCL. (10) Activating mutations in JAK kinases have been reported in CTCL. (11) These mutations frequently occur in the JAK-STAT signaling pathway and may serve as indicators for targeted therapy. (12) For instance, recurrent mutations in genes of the JAK-STAT signaling pathway, including *STAT3*, *JAK1*, and others have been identified. (11) (13) In addition to mutations, deletions of tumor suppressors *HNRNPK* and *SOCS1* were found to be the most frequent genetic alterations in MF after deletion of *CDKN2A*. (14) Notably, *SOCS1* deletion could be detected even in early-stage MF. These

deletions, resulting from genomic rearrangements, lead to up-regulation of the JAK-STAT pathway, among others.

Biallalic knockout and Haploinsufficient of tumor suppressor genes in CTCL

Biallelic knockout, which involves the complete loss of both alleles of a gene, can result in the complete absence of gene function. In the context of CTCL, this can be particularly relevant when studying TSGs (Tumor Suppressor Genes) that are implicated in the regulation of T-cell proliferation and survival. (15)

Understanding the consequences of biallelic knockout of specific TSGs can provide insights into whether their loss contributes to the uncontrolled proliferation of CD4+ T cells seen in CTCL. On the other hand, haploinsufficiency arises when an organism possesses only one functional copy of a gene due to the loss of function of a single allele. (16) In the context of CTCL, haploinsufficiency of certain TSGs may lead to reduced protein levels in CD4+ T cells, potentially impairing their normal regulatory functions. This can create an environment conducive to the development and progression of CTCL. (17)

Exploring the interplay between biallelic knockout, haploinsufficiency, and specific TSGs in the context of CTCL offers a deeper understanding of the molecular mechanisms underlying this lymphoma. (18) By elucidating how genetic alterations in TSGs affect T-cell behavior, researchers can uncover novel therapeutic targets and potential interventions for CTCL.

Specific Insights into Biallalic knockout and Haploinsufficiency of *Socs1* and *Hnrnpk* Genes

Haploinsufficiency of *SOCS1* is a recognized cause of early-onset autoimmune diseases. (19) Human studies align with findings in mice, notably that *Socs1*-/- mice experience neonatal lethality attributed to excessive IFN-γ signaling and extensive inflammatory infiltration. (7) Lineage mutations in *SOCS1* leading to haploinsufficiency result in heightened activation of the JAK-STAT pathway in response to various cytokines. (20) Mice with a haploinsufficient dose of *Socs1* can survive to adulthood, but with age, they develop systemic autoimmune diseases. Given the widespread expression of *SOCS1* and the coordinating role of cytokines in the immune system, multiple cell types may contribute to autoimmunity under conditions of *SOCS1* haploinsufficiency.

While *SOCS1* haploinsufficiency is a recognized cause of early-onset autoimmunity, our study is the first to demonstrate data specifically focused on *Socs1* haploinsufficiency in skin-resident CD4+ T cells. In **Chapter 2**, although the experiments conducted over only

8 weeks showed that *Socs1* monoallelic knockout in skin-homing CD4+ T cells was not sufficient to induce CTCL, we were able to observe differences between experimental mice and wild-type mice, confirming the impact of *Socs1* haploinsufficiency even when restricted to CD4+ T cells.

Additionally, despite insufficient numbers of mice with bi-allelic knockout of *Socs1* for statistical analysis, all these mice exhibited visibly thicker epidermis, increased inflammatory cell presence (CD3, CD4, CD8), and a greater number of cells positive for p-STAT3 in the lymphocytes. Even without quantitative statistical data, the distinctions between mice with homozygous *Socs1* knockout and heterozygous *Socs1* knockout in CD4+ T cells were evident, suggesting that homozygous *Socs1* knockout in CD4+ T cells could lead to more pronounced phenotypic changes.

In **Chapter 3**, with an extended experimental period, the differences in phenotype between mice with monoallelic knockout of *Socs1* in skin-homing CD4+ T cells and wild-type mice were more pronounced, likely indicating systemic pathological lymphocyte proliferation. This further confirmed the effects of *Socs1* haploinsufficiency, highlighting the role of *Socs1* as a tumor suppressor gene.

The knockout of both alleles of *Hnrnpk* (*Hnrnpk*-/-) is generally incompatible with embryonic survival; complete loss of *Hnrnpk* is lethal in early developmental stages. (21) (22) Such loss also severely impairs the function and development of functional CD4+ T cells. (23) This underlines the significance of our development of *Hnrnpk* flox mice in **Chapter 4**, where, through crossing with *Cd4CreER*^{T2} mice, we obtained a model that allows controlled timing of specific *Hnrnpk* knockouts in skin-homing CD4+ T cells.

Hnrnpk functions as a haploinsufficient tumor suppressor. *Hnrnpk* haploinsufficiency can lead to reduced survival, increased tumor formation, genomic instability, and the development of transplantable hematologic malignancies. (24) In **Chapter 4**, we present, for the first time, data on the effects of single-gene knockout of *Hnrnpk* in skin-homing CD4+ T cells combined with chronic skin allergies. Coupled with the homozygous knockout mice of *Hnrnpk* in **Chapter 5**, our research encompasses homozygous and heterozygous *Hnrnpk* knockouts, as well as wild-type *Hnrnpk* mice, allowing for comprehensive comparison. We confirmed that the loss of a single allele of the *Hnrnpk* gene is sufficient to affect the phenotype of the mouse model, and no significant differences were observed between the phenotypes resulting from bi-allelic and mono-allelic knockouts.

The Role of *SOCS1* in the Pathogenesis of Early-Stage CTCL

SOCS1, a key regulator of cytokine signaling, when knocked out in skin-resident CD4+ T

cells, leads to a state of autonomous skin inflammation. (**Chapter 2 and Chapter3**) The *Socs1* knockout mouse model mimics the features of early-stage mycosis fungoides, the most common form of CTCL. The loss of *Socs1* results in uncontrolled JAK-STAT signaling, leading to the initiation of skin inflammation that does not resolve on its own, along with sustained activation of STAT3 within the skin.

Within these *Socs1* knockout mice, we observe a significant increase in T-cell infiltration in the skin, along with heightened and sustained expression of activated STAT3. These changes are indicative of the disrupted immune surveillance and control mechanisms typically seen in CTCL. The prolonged contact-allergic reaction in these mice further demonstrates the potential for chronic inflammation to progress into a malignant state, emphasizing the critical role of *Socs1* in maintaining normal immune homeostasis and preventing the onset of CTCL.

The *Socs1* flox *Cd4CreER*^{T2} mouse model discussed in **Chapter 2** and **Chapter 3** is of importance in CTCL research, especially for understanding the role of *SOCS1* in the progression of the disease. *SOCS1* has been found to be deficient in patients with CTCL, particularly in those with early-stage MF. (14) By selectively deleting the *Socs1* gene in the CD4+ T cells of mice—which is accomplished by the cross breeding of *Cre* transgenic and *Socs1* floxed mice - researchers can observe the effects of the absence of this gene in skin-resident T cells involved in inflammation of the skin (activation of *Cre* by topical application of tamoxifen on the inflamed skin). This model has revealed that isolated loss of the *Socs1* gene does not lead to pronounced malignant changes, even when coupled with short term inflammatory challenges.

However, with protracted challenges - specifically, over a period of 20 weeks— the skin inflammation becomes autonomous and mirrors early-stage MF, offering a more profound understanding of the disease's early development and potential intervention.

***Hnrnpk* Knockout Mouse Model and Its Implications in Early-Stage CTCL**

Hnrnpk flox *Cd4CreER*^{T2} mouse model can be utilized to examine the impact of *Hnrnpk* gene haplodeficiency or its complete absence in CD4+ T cells, aiming to elucidate its role in CTCL pathogenesis. (14, 25) This aproach is informed by prior studies highlighting significant deletions of *Hnrnpk* in the JAK-STAT pathway among CTCL patients. (25) It builds on the foundational research conducted using the *Socs1* flox *Cd4CreER*^{T2} mouse model, which has paved the way for exploring the effects of these genes related to CTCL.

The *Hnrnpk* knockout model has provided significant insights into the pathogenesis of early- stage CTCL. The loss of one copy of *Hnrnpk* in CD4+ T cells leads to a cascade of

molecular events that simulate the early stages of CTCL. (**Chapter 4 and Chapter 5**) This model has shed light on the intricate role of *Hnrnpk* in maintaining genomic stability and regulating gene expression. The *Hnrnpk* knockout mice exhibit characteristics such as increased cellular proliferation, impaired apoptosis, and dysregulated cytokine signaling, all of which are hallmarks of early-stage CTCL.

The induction of chronic skin inflammation in these mice parallels the inflammatory environment seen in CTCL patients. Notably, the persistent activation of the JAK-STAT pathway, a consequence of *Hnrnpk* loss, mirrors the cytokine dysregulation observed in CTCL. These findings underscore the importance of *HNRNPK* as a regulatory factor in T-cell homeostasis and its potential role in the initiation of lymphomagenesis.

Comparing the *Socs1* knockout model with *Hnrnpk* knockout model reveals both overlapping and unique features pertinent to CTCL pathogenesis. Although, the function of *Hnrnpk* emphasizes the role of genetic stability and gene regulation in the disease's progression (26), whereas the function of *Socs1* gene related the impact of disrupted cytokine signaling control. Both models show dysregulated JAK-STAT signaling, an important pathway in CTCL, the similar inflammatory environment seen in CTCL patients and the pathological proliferation of immune cells. (14) Together, these models significantly contribute to our understanding of early-stage CTCL. The insights gained from these models are crucial for the development of targeted therapies and offer a more detailed understanding of the molecular mechanisms underlying CTCL.

Future Perspectives and Concluding Remarks

In this thesis, the work has provided a viable model and practical methods for the targeted knockout of skin-homing CD4+ T cells in the mouse skin, along with an optimized approach applying Tamoxifen topically. Our data indicates that under current experimental conditions, although the mice exhibit early-stage CTCL-like characteristics, they are not yet satisfactory as a fully developed, ready-to-use tumor model.

As a next step from **Chapter 2** and **Chapter 3**, which explored the role of *Socs1* following its knockout in mouse skin-homing CD4+ T cells, our goal is to further validate our results by expanding the sample size of mice with *Socs1* bi-allelic knockout. We aim to assess whether bi-allelic and mono-allelic knockouts of *Socs1* have different impacts on the onset and progression of CTCL.

Our subsequent steps for *Hnrnpk* gene research in **Chapter 4** and **Chapter 5** are similar to those for *Socs1*. Additionally, transcriptome analysis of skin-homing CD4+ T cells isolated from *Hnrnpk* knockout mice can be used to characterize the imbalance of affected target

genes and transcripts. This approach helps identify cellular processes impacted by the loss of the *Hnrnpk* gene, ultimately elucidating the mechanisms behind the exacerbated skin inflammation observed in our transgenic mice. Moreover, this method can be employed to validate the enhanced JAK-STAT signaling pathways observed in our *Hnrnpk* gene heterozygous and homozygous knockout mice treated and challenged with OXA. By extending the experimental period and utilizing skin-homing CD4+ T cell bi-allelic knockout GEMM mice, along with constructing large-sample experiments, we can further determine and optimize early-stage CTCL mouse models.

Continuously refining our model-building approach for gene knockout in skin CD4+ T cells is a key focus. Our next step is to explore genetic alterations relevant to CTCL pathogenesis, using our knockout models to investigate potential gene changes. In future model construction, we plan to cross with other GEMMs harboring genetic alterations, such as loss of *Cdkn2A* often observed in CTCL(10) or, which hold potential for tumorigenesis. These endeavors will enhance our understanding of CTCL's genetic underpinnings and might contribute to more efficient model development.

In conclusion, our research focuses on establishing autochthonous mouse models closely resembling CTCL, allowing selective gene knockouts in skin-homing CD4+ T-cells. While our skin-target GEMMs may not capture all malignant aspects, they closely mimic CTCL's origin and early changes. Future research will leverage emerging technologies like *CRISPR-Cas9* gene editing to enhance model accuracy and relevance, enabling exploration of gene effects and understanding the genesis of early-stage CTCL. This work can contribute to a better understanding of CTCL pathogenesis, validates the driving role of relevant genes in its early stages, and creates research platforms for (precision) medicine in early-stage CTCL treatment.

References

1. Aghajani K, Keerthivasan S, Yu Y, Gounari F. Generation of CD4CreER(T^2) transgenic mice to study development of peripheral CD4-T-cells. Genesis. 2012;50(12):908-913. doi:10.1002/dvg.22052
2. Kim H, Kim M, Im SK, Fang S. Mouse Cre-LoxP system: general principles to determine tissue-specific roles of target genes. Lab Anim Res. 2018;34(4):147-159. doi:10.5625/lar.2018.34.4.147
3. Sauer B. Inducible gene targeting in mice using the Cre/lox system. Methods. 1998;14(4):381-392. doi:10.1006/meth.1998.0593
4. Donocoff RS, Teteloshvili N, Chung H, Shoulson R, Creusot RJ. Optimization of tamoxifen-induced Cre activity and its effect on immune cell populations. Sci Rep. 2020;10(1):15244. Published 2020 Sep 17. doi:10.1038/s41598-020-72179-0
5. Hirrlinger PG, Scheller A, Braun C, Hirrlinger J, Kirchhoff F. Temporal control of gene recombination in astrocytes by transgenic expression of the tamoxifen-inducible DNA recombinase variant CreERT2. Glia. 2006;54(1):11-20. doi:10.1002/glia.20342
6. Indra AK, Warot X, Brocard J, et al. Temporally-controlled site-specific mutagenesis in the basal layer of the epidermis: comparison of the recombinase activity of the tamoxifen-inducible Cre-ER(T) and Cre-ER(T2) recombinases. Nucleic Acids Res. 1999;27(22):4324-4327. doi:10.1093/nar/27.22.4324
7. Chong MM, Cornish AL, Darwiche R, et al. Suppressor of cytokine signaling-1 is a critical regulator of interleukin-7-dependent CD8+ T cell differentiation. Immunity. 2003;18(4):475-487. doi:10.1016/s1074-7613(03)00078-5
8. Feil S, Valtcheva N, Feil R. Inducible Cre mice. Methods Mol Biol. 2009;530:343-363. doi:10.1007/978-1-59745-471-1_18
9. Madisen L, Zwingman TA, Sunkin SM, et al. A robust and high-throughput Cre reporting and characterization system for the whole mouse brain. Nat Neurosci. 2010;13(1):133-140. doi:10.1038/nn.2467
10. Tensen CP, Quint KD, Vermeer MH. Genetic and epigenetic insights into cutaneous T-cell lymphoma. Blood. 2022;139(1):15-33. doi:10.1182/blood.2019004256
11. Pérez C, González-Rincón J, Onaindia A, et al. Mutated JAK kinases and deregulated STAT activity are potential therapeutic targets in cutaneous T-cell lymphoma. Haematologica. 2015;100(11):e450-e453. doi:10.3324/haematol.2015.132837
12. Cortes JR, Patrone CC, Quinn SA, et al. Jak-STAT Inhibition Mediates Romidepsin and Mechlorethamine Synergism in Cutaneous T-Cell Lymphoma. J Invest Dermatol. 2021;141(12):2908-2920.e7. doi:10.1016/j.jid.2021.04.023
13. Vadivel CK, Gluud M, Torres-Rusillo S, et al. JAK3 Is Expressed in the Nucleus of Malignant T Cells in Cutaneous T Cell Lymphoma (CTCL). Cancers (Basel). 2021;13(2):280. Published 2021 Jan 14. doi:10.3390/cancers13020280
14. Bastidas Torres AN, Cats D, Mei H, et al. Genomic analysis reveals recurrent deletion of JAK-STAT signaling inhibitors HNRNPK and SOCS1 in mycosis fungoides. Genes Chromosomes Cancer. 2018;57(12):653-664. doi:10.1002/gcc.22679

15. Yumeen S, Girardi M. Insights Into the Molecular and Cellular Underpinnings of Cutaneous T Cell Lymphoma. Yale J Biol Med. 2020;93(1):111-121. Published 2020 Mar 27
16. Inoue K, Fry EA. Haploinsufficient tumor suppressor genes. Adv Med Biol. 2017;118:83-122
17. Morris LG, Chan TA. Therapeutic targeting of tumor suppressor genes. Cancer. 2015;121(9):1357-1368. doi:10.1002/cncr.29140
18. Lai P, Wang Y. Epigenetics of cutaneous T-cell lymphoma: biomarkers and therapeutic potentials. Cancer Biol Med. 2021;18(1):34-51. doi:10.20892/j.issn.2095-3941.2020.0216
19. Hadjadj J, Castro CN, Tusseau M, et al. Early-onset autoimmunity associated with SOCS1 haploinsufficiency. Nat Commun. 2020;11(1):5341. Published 2020 Oct 21. doi:10.1038/s41467-020-18925-4
20. Körholz J, Gabrielyan A, Sowerby JM, et al. One Gene, Many Facets: Multiple Immune Pathway Dysregulation in SOCS1 Haploinsufficiency. Front Immunol. 2021;12:680334. Published 2021 Aug 5. doi:10.3389/fimmu.2021.680334
21. Xu H, Guo J, Wu W, et al. Deletion of Hnrnpk Gene Causes Infertility in Male Mice by Disrupting Spermatogenesis. Cells. 2022;11(8):1277. Published 2022 Apr 9. doi:10.3390/cells11081277
22. Chen Y, Zhou T, Liao Z, et al. Hnrnpk is essential for embryonic limb bud development as a transcription activator and a collaborator of insulator protein Ctcf. Cell Death Differ. 2023;30(10):2293-2308. doi:10.1038/s41418-023-01207-z
23. Chang JW, Koike T, Iwashima M. hnRNP-K is a nuclear target of TCR-activated ERK and required for T-cell late activation. Int Immunol. 2009;21(12):1351-1361. doi:10.1093/intimm/dxp106
24. Gallardo M, Lee HJ, Zhang X, et al. hnRNP K Is a Haploinsufficient Tumor Suppressor that Regulates Proliferation and Differentiation Programs in Hematologic Malignancies. Cancer Cell. 2015;28(4):486-499. doi:10.1016/j.ccell.2015.09.001
25. Park J, Daniels J, Wartewig T, et al. Integrated genomic analyses of cutaneous T-cell lymphomas reveal the molecular bases for disease heterogeneity. Blood. 2021;138(14):1225-1236. doi:10.1182/blood.2020009655
26. Mikula M, Bomsztyk K, Goryca K, Chojnowski K, Ostrowski J. Heterogeneous nuclear ribonucleoprotein (HnRNP) K genome-wide binding survey reveals its role in regulating 3'-end RNA processing and transcription termination at the early growth response 1 (EGR1) gene through XRN2 exonuclease. J Biol Chem. 2013;288(34):24788-24798. doi:10.1074/jbc.M113.496679

Appendix

Nederlandse Samenvatting

List of publications

Curriculum vitae

Portfolio

Acknowledgements

Nederlandse Samenvatting

Deze PhD-thesis, getiteld “Validatie van de Genetische Veranderingen bij Cutaan T-cel Lymfoom: Het Ontrafelen van de Rol van *SOCS1* en *HNRNPK* door Middel van Genetisch Gemodificeerde Muismodellen”, presenteert een uitgebreide studie naar CTCL, een zeldzame vorm van non-Hodgkin lymfoom. Het onderzoek richt zich op het verkennen van de genetische factoren die van invloed zijn op CTCL en maakt gebruik van geavanceerde in vivo muismodellen om ons begrip van de ziekte te verdiepen. Het eerste hoofdstuk introduceert de toepassing van *in vivo* muismodellen in CTCL-onderzoek, waarbij de nadruk ligt op hun cruciale rol bij het ontrafelen van de pathogenese van de ziekte en het testen van mogelijke behandelingsmethoden. Het doel van dit proefschrift is het opzetten van Huid-Gerichte Genetisch Gemodificeerde Muismodellen door gebruik te maken van genveranderingen gevonden in tumoren van patiënten, die mogelijk een sleutelrol spelen in het ontstaan van CTCL. Deze modellen zijn ontworpen om de pathogene rol van deze genen in de vroege stadia van CTCL te onderzoeken.

In **Hoofdstuk 2** wordt de rol van het *SOCS1*-gen in CTCL onderzocht. Er werd gebruik gemaakt van GEMM-muizen die in staat zijn tot specifieke *Socs1*-uitschakeling in huidgerichte CD4+ T-cellen. Deze muizen toonden aan dat een enkelvoudig verlies van *Socs1*, gecombineerd met aanhoudende ontsteking, niet voldoende is om een vroeg-stadium mycosis fungoides-achtig fenotype te induceren binnen acht weken.

Hoofdstuk 3 bevestigt de causale rol van *Socs1*-allelverlies in de ontwikkeling van MF. Een grotere groep muizen werd gebruikt voor een betere statistische onderbouwing en de duur van het experiment werd verlengd tot 20 weken. Lokaal *Socs1* mono-allelisch verlies in CD4+ T-cellen in chronisch ontstoken huid leidt tot autonome huidontsteking met vroege MF-kenmerken.

In **Hoofdstuk 4** wordt een nieuw conditioneel knockout-muismodel met *Hnrnpk* mono-allelische deletie in CD4+ T-cellen geïntroduceerd. Dit model bootst belangrijke kenmerken van vroege CTCL na, waaronder chronische huidontsteking, CD4+ T-celinfiltratie en minimale verstoring in perifeer bloed. Het biedt een experimenteel traject om de complexe micro-omgevingen en immuunreacties te bestuderen.

Het onderzoek beschreven in **Hoofdstuk 5** gebruikt de nieuwe stam van homozygote en heterozygote muizen die ontwikkeld zijn in Hoofdstuk 4 om de rol van *Hnrnpk* als een initiërende factor bij de pathogenese van CTCL in huidgerichte CD4+ T-cellen te verduidelijken.

Hoofdstuk 6 presenteert een uitgebreid overzicht van de verzamelde gegevens, samen met een verkenning van zowel de klinische als onderzoeksimplicaties die samenhangen met deze thesis.

Ter afsluiting, deze PhD-thesis draagt significant bij aan het begrijpen van de genetische grondslagen van CTCL en draagt bij aan de ontwikkeling van gerichte therapieën voor de vroege behandeling van deze complexe ziekte. Het onderzoek legt een fundament voor toekomstige studies die opkomende technologieën zoals CRISPR-Cas9-genbewerking gebruiken om modelnauwkeurigheid en relevantie in CTCL-onderzoek te verbeteren.

List of publications

Luo, Y., de Gruijl, F. R., Vermeer, M. H., & Tensen, C. P. (2024). “Next top” mouse models advancing CTCL research. *Frontiers in cell and developmental biology,* 12, 1372881. https://doi.org/10.3389/fcell.2024.1372881

Luo, Y., Vermeer, M. H., de Gruijl, F. R., Zoutman, W. H., Sluijter, M., van Hall, T., & Tensen, C. P. (2022). In vivo modelling of cutaneous T-cell lymphoma: The role of SOCS1. *Frontiers in oncology,* 12, 1031052. https://doi.org/10.3389/fonc.2022.1031052

Luo, Y., Vermeer, M. H., de Haan, S., Kinderman, P., de Gruijl, F. R., van Hall, T., & Tensen, C. P. (2023). Socs1-knockout in skin-resident CD4+ T cells in a protracted contact-allergic reaction results in an autonomous skin inflammation with features of early-stage mycosis fungoides. *Biochemistry and biophysics reports*, 35, 101535. https://doi.org/10.1016/j.bbrep.2023.101535

Curriculum vitae

Yixin Luo was born on July 3rd, 1990, in Zhengzhou, Henan Province, China. She completed her Bachelor's degree in Clinical Medicine at Zhengzhou University, Zhengzhou City. During her undergraduate studies, she interned at The First Affiliated Hospital of Zhengzhou University, gaining comprehensive clinical and research experience across multiple departments.

In 2014, Yixin pursued her Master of Medicine at Peking Union Medical College and Tsinghua University in Beijing, specializing in dermatology and venereology. Under the supervision of Prof. Dr. Jie Liu, her master's research focused on cutaneous T-cell lymphoma, specifically establishing dermoscopic criteria for the early detection of mycosis fungoides, enhancing diagnostic processes.

In 2017, Yixin began her PhD studies at Leiden University Medical Center in the Netherlands. Guided by Prof. Maarten Vermeer and Dr. Cornelis P. Tensen, her doctoral research explores the pathogenesis of cutaneous T-cell lymphoma using innovative in vivo models. A significant focus of her study is the role of SOCS1 and HNRNPK as initiating factors in the development of CTCL. This research is presented in her thesis titled "Validating the Genetic Alterations in Cutaneous T-cell Lymphoma: Unraveling the Role of SOCS1 and HNRNPK through Genetically Engineered Mouse Models."

Portfolio

PhD Training

Hightlight Courses

- Introduction to Flow Cytometry (Dec 2017)
- Animal Handling Course (May 2018)
- Big Data Analysis on SHARK Cluster (June 2018)
- Next Generation Sequencing Data Analysis (Aug 2019)
- Using R for Data Analysis (Sep 2019)
- eBROK certification (2019 - 2023) & eBROK re-registration (2023 - 2026)

Teaching Experience

- **Supervising 9-Month Master Biomedical Science Internship**
  Julia van der Bie: *HNRNPK* deletion in skin-homing mCD4+ T-cells resembles early-stage Mycosis Fungoides characterized by persistent skin inflammation.
- **Supervising 9-Month University of Applied Science Internships**
  Amelia G Maduro Rodriguez: The role of *SOCS1* deletion in CD4+ T cells of oxazolone-induced dermatitis on transgenic mice.
  Jamie Dawson: Examination of the functional role of Suppressor Of Cytokine Signaling 1 in Mycosis Fungoides.
  Roos Gaarkeuken: The oncogenesis function of *Hnrnpk* deletion in transgenic mice.

Peer Reviews for International Journals

- *Biochemistry and Biophysics Reports*

Symposia and Presentations

- ***EORTC Cutaneous Lymphoma Group Meetings, Athens (Sep 2019)***
  Mycosis fungoides and variants of mycosis fungoides: A retrospective study of 93 patients in a Chinese population at a single center.
- ***Dutch Society for Experimental Dermatology Annual Meetings, Lunteren (Jun 2022)***
  Assessment of *SOCS1* deletion in CD4+ T cells of chronically inflamed mouse skin to develop a pathogenic model of Mycosis Fungoides.
- ***EORTC Cutaneous Lymphoma Group Meetings, Madrid (Sep 2022)***
  In vivo modelling of Cutaneous T-cell lymphoma: The role of *SOCS1*.
- ***Dutch Society for Experimental Dermatology Annual Meetings, Lunteren (Jun 2023)***
  Knockout of JAK/STAT signaling inhibitors in skin-resident CD4+ T cells results in an autonomous skin inflammation, with features of early-stage Mycosis Fungoides.
- ***EORTC Cutaneous Lymphoma Group Meetings, Leiden (Sep 2023)***
  A novel inducible knockout mouse strain to study the impact of one-copy loss of *HNRNPK* in CD4+ T cells as an experimental model of cutaneous lymphoma.
- ***Medical Genetics Center Symposium, Rotterdam (Sep 2023)***
  Genetically engineered mouse models of cutaneous lymphomas: From pathogenesis to therapeutic intervention.

Acknowledgement

First and foremost, I wish to express my profound gratitude to my esteemed promoter, Prof. Dr. Maarten H. Vermeer, and my dedicated co-promotors, Dr. Cornelis (Kees) P. Tensen and Dr. Frank de Gruijl. Maarten, your support and the opportunities provided by our research group have been instrumental in fostering my strength and independence. Kees, your meticulous guidance, generous spirit, and unyielding optimism have not only shaped my research but have also set a lifelong example for me to follow. Beyond the knowledge and research skills you've imparted, it was your trust that kept me from wavering during this challenging Ph.D. journey. Frank, I extend my heartfelt thanks for your expertise in mouse experiments, invaluable discussions, and constructive input on my manuscripts. Your continuous support has been immensely beneficial to my work.

To my close colleagues, Wim and Sanne, your consistent support in practical techniques and in our daily lives has been invaluable. Safa, Nicolas, Marion, Abdoel, Shidi, Fenna, Alesha, Alita, Koen, Erno, Peter, Mieke, Nelleka, Amelia, Jaime, Roos, Julia, Yang Liu and all the wonderful colleagues, your helpfulness and kindness have made this journey more enjoyable. I will forever cherish the laughter-filled moments we shared together.

I am grateful to Thorbald, Prisilla, Marjolein and Camelia from Department of Oncology, and Sophie from Department of Anatomy for their assistance in launching the mouse project and providing access to essential research reagents for my experiments.

To my dear friends who have enriched my days during my time in Leiden—Zhenfeng and Guoping, Yuanyuan and Zhihang, Meiru and Shixiong, Zhenyang, Jing and Bart, Melanie, Zhuoyi and Ouyang, Yang Ge, Zhihan and Wei Chen, Di Wang, Xvhan, Xueying, Wei Wang, Licheng and Dajia, Xuezi, Xiangyu, Jinqiu, Tzu-Yi Hsu, Sephideh, and many others—thank you for your friendship, your companionship, and for making my days in Leiden vibrant and memorable.

I would also like to express my heartfelt appreciation to my partner, Yi-Ching Hsu. With you, I can truly be myself—playful, carefree, and at peace. You are my emotional sanctuary, my greatest support, and my best friend. Thank you for your unwavering companionship and for turning Leiden into a place that truly feels like home. A special thank you to our feline companions, Meean and Gina, for bringing joy and warmth into our Dutch home.

My deepest gratitude goes to my parents for their unwavering support throughout my Ph.D. journey. They have always stood by my side, embracing my unconventional choices with unconditional love, tenderness, and strength. In moments of hardship, their simple yet reassuring words, "*You are our treasure. We will always support you. We only want you to be happy,*" have been a constant source of comfort and inspiration. I love you both more than words can express, and you remain my greatest source of motivation.

May our lives continue to shine brightly, free from regret, as the best is still ahead for all of us.